ASSESING THE SAFETY OF FOOD PROTEIN NANOFIBRILS: CROSS-SEEDING OF HEN AND HUMAN LYSOZYME AMYLOID POLYMORPHS.

by

LIDA RAHIMI ARAGHI

(Under the Direction of Derek R. Dee)

ABSTRACT

Food protein amyloid-like nanofibrils are gaining interest as new food ingredients. Nanofibrils can self-propagate by 'seeding' and can 'cross-seed' the fibrillation of similar proteins from other species. Nanofibrils can potentially survive digestion and spread to other parts of the body. Currently, there is limited knowledge on the propensity for food protein nanofibrils to cross-seed fibril formation of similar human proteins. Thus, it is prudent to examine their impact on human health before employing nanofibrils in food. This study used lysozyme as a model to examine the seeding and cross-seeding reactions between two unique fibril polymorphs (formed at pH 2, and pH 6.3) of lysozymes from human and hen. Both polymorphs of HEWL could cross-seed aggregation of HLZ, but this reaction was markedly reduced under simulated gastric conditions. Surprisingly, the 6.3 fibril polymorph was dominant even at pH 2, indicating, distinct polymorphs of the same protein have unique abilities to self-propagate.

INDEX WORDS: Food protein nanofibrils, Hen Egg-white Lysozyme (HEWL), Human Lysozyme (HLZ), seeding, cross-seeding, polymorphism.

# ASSESING THE SAFETY OF FOOD PROTEIN NANOFIBRILS: CROSS-SEEDING OF HEN AND HUMAN LYSOZYME AMYLOID POLYMORPHS.

by

LIDA RAHIMI ARAGHI

B.S., The Islamic Azad University of Tabriz, Iran, 2012

A Thesis Submitted to the Graduate Faculty of The University of Georgia in Partial Fulfillment of the Requirements for the Degree

MASTER OF SCIENCE

ATHENS, GEORGIA

2018

ASSESING THE SAFETY OF FOOD PROTEIN NANOFIBRILS: CROSS-SEEDING OF HEN AND HUMAN LYSOZYME AMYLOID POLYMORPHS

by

LIDA RAHIMI ARAGHI

| | |
|---|---|
| Major Professor: | Derek R. Dee |
| Committee: | Bingqian Xu |
| | Chad M. Paton |

Electronic Version Approved:

Suzanne Barbour
Dean of the Graduate School
The University of Georgia
December 2018

# DEDICATION

This study is wholeheartedly dedicated to my beloved family, who have been a constant source of inspiration, support and encouragement throughout my life.

ACKNOWLEDGEMENTS

I would like to express my special appreciation and gratitude to my advisor Dr. Derek R. Dee. I wouldn't be here without your constant support and guidance, thank you for giving me this opportunity, and it was an honor to work under your supervision. I would also like to thank my committee members, Dr. Chad M. Paton, and Dr. Bingqian Xu for serving as my committee members, their time, and knowledge.

To my collaborators, Thong Zhang, and Keren Zhang, thank you for all the time and effort you put into getting AFM images for my project. Taryn Kormanik, Ana Jaworsky, Alyssa Robertson, John Woody, and Clare Hill, it was great knowing and working with you all and thank you for sharing these unforgettable two years with me in the lab.

Special thanks to Emine Ozen for her support and friendship, and Carl Ruiz for all the good advice. I couldn't finish my project without your help. Thank you and Rommel Ortiz for fixing our plate-reader. Thanks to Dr. John Shields, Mary Ard, and Dr. Eric Formo for sharing their knowledge on TEM with me. I couldn't have taken these great images without your continuous support. Thanks to Dennis Phillips for the MALDI results. To my dear friend, Alyxandra Reed, thank you for editing my thesis.

To my dear family, maman, baba, Zhila, and Kamal, I couldn't do it without your tremendous emotional and financial support. My dear aunts and uncles, it wouldn't be possible for me to live here without your continuous generosity.

TABLE OF CONTENTS

Page

LIST OF TABLES

Page

LIST OF FIGURES

Page

## ABBREVIATIONS

| | |
|---|---|
| HEWL | Hen egg-white lysozyme |
| HLZ | Human lysozyme |
| ThT | Thioflavin-T |
| GdnHCl | Guanidine Hydrochloride |
| A-BETA | Amyloid beta peptides |
| AA | Amyloid A |
| vCJD | Variant Creutzfeldt-Jakob disease |
| SGF | Simulated Gastric Fluid |
| TEM | Transmission Electron Microscopy |
| AFM | Atomic Force Microscopy |
| MALDI | Matrix Assisted Laser Desorption/Ionization |
| TOF | Time of Flight |
| SDS | Sodium Dodecyl Sulfate |
| PAGE | Polyacrylamide Gel Electrophoresis |
| PI | Isoelectric Point |
| RPM | Revolutions per Minute |
| A.U. | Arbitrary Unit |
| UV-Vis | Ultraviolet-Visible |

# CHAPTER 1

# 1 INTRODUCTION

## 1.1 Protein folding and aggregation

Amino acids are the building blocks of the polymeric sequences of proteins. The function of a protein depends largely on its folded structure. Upon synthesis, a polypeptide chain undergoes spontaneous folding reactions to reach its final three-dimensional structure, resulting in a functioning and active protein (C.M. Dobson, 2004; Shamsi, Athar, Parveen, & Fatima, 2017). The folded protein is stabilized by hydrophobic interactions, covalent interactions, and weak forces (Zaidi, Hassan, Islam, & Ahmad, 2014). The process of folding and unfolding is driven thermodynamically through a complex and intricate process, in which there are alternative three-dimensional structures, and folding intermediates that a polypeptide can adopt. Sometimes a proteins can misfold, resulting in the improper final three-dimensional protein structure. Since the final three-dimensional structure ultimately determines the protein's functionality, the misfolded protein will not have the same initial function, therefore potentially leading to an inactive protein. Usually, protein aggregation occurs because of misfolding or improper folding of an unfolded or partially folded protein (Alam, Siddiqi, Chturvedi, & Khan, 2017; E. K. Kumar, Haque, & Prabhu, 2017; Siddiqi, Alam, Chaturvedi, Shahein, & Khan, 2017).

Proteins may aggregate in two general ways, either clumping together to form amorphous aggregates, or they form β-strands and stack perpendicular to the fibril axis in a highly-ordered manner and form amyloid fibrils. Amyloid fibrils are the most thermodynamically stable structure that a protein can adopt (Nelson & Eisenberg, 2006). (see Figure 1.1).

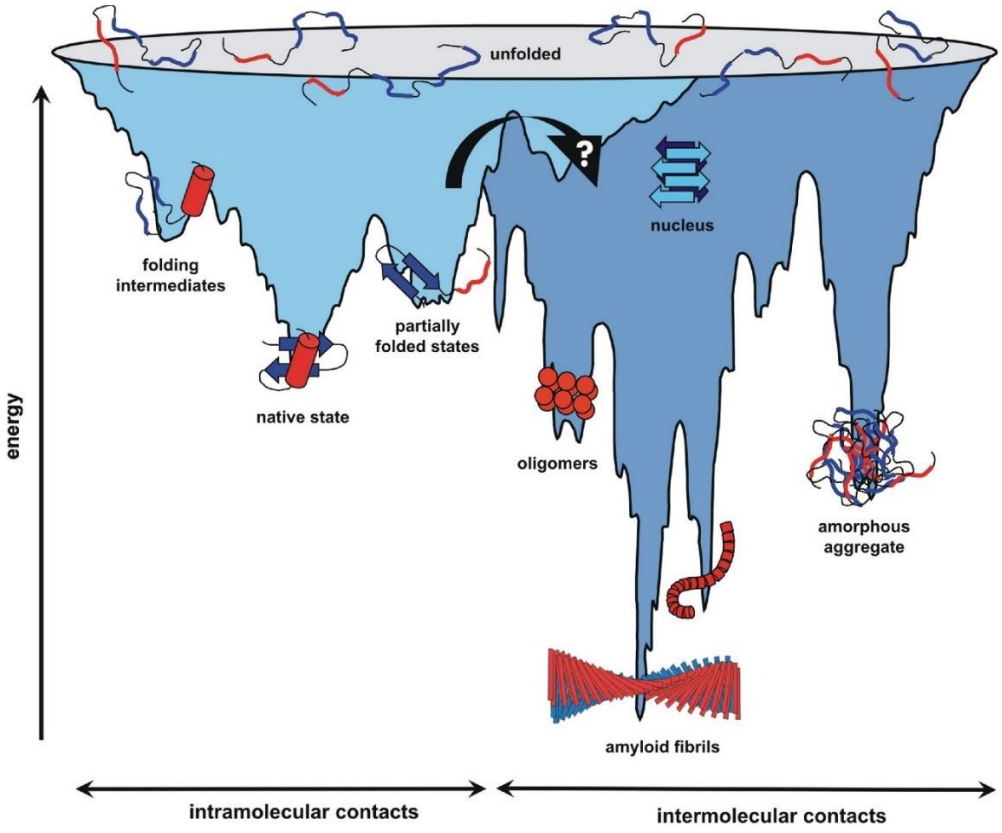


Figure 1.1 Schematic energy landscape of protein folding and aggregation. Figure is adapted from the FEBS Journal (Jahn & Radford, 2005) with permission from John Wiley and Sons publisher.

## 1.2 Amyloid fibrils

The word amyloid is derived from the Latin (amylum) and Greek (amylom) words for starch, so-named in 1854 by Virchow when he thought deposits observed in brain sections upon staining with iodine resembled cellulose (Tjernberg, Rising, Johansson, Jaudzems, & Westermark, 2016). Amyloid fibrils are aggregates formed both *in vivo* and *in vitro* by a soluble polypeptide chain or a protein monomer, which assembles into a shape that allows many copies of the identical polypeptide chain or monomer units to stack together, called homotypic polymerization (Dovidchenko & Galzitskaya, 2015). These units stack together form insoluble fibrils that are resistant to degradation (Dovidchenko & Galzitskaya, 2015). A remarkable aspect of amyloid fibrils is that, regardless of their native conformations, different proteins form similar fibrillar structures (Chiti & Dobson, 2006; Makin & Serpell, 2005). Amyloid aggregates have a cross-β-sheet structural core, in which β-sheets are formed by stacking β-strands on top of one another perpendicular to the fibril axis via hydrogen bonds (Nelson et al., 2006; Sunde et al., 1997). On a molecular level, the peptides are lined up straight and stacked on top of each other in a highly ordered manner, allowing them to line up their electrostatic dipoles on their backbone so that they can form hydrogen bonds.

Amyloid fibrils are usually unbranched, are about 5-10 nm in diameter and can grow to be several microns in length. A single isolated beta sheet is not stable in solution, so normally two to six sheets laminate together forming protofilaments, which allows the side chains from the proteins to interdigitate with each other, thus providing additional binding energy to stabilize the sheets. The fibrils are composed of several protofilaments

that are twisted with one another (Chiti & Dobson, 2006; E. K. Kumar et al., 2017; Toyama & Weissman, 2011). Amyloid fibrils can bind to fluorescent dyes such as Congo red (Antimonova et al., 2016) and thioflavin-T (Sebastiao, Quittot, & Bourgault, 2017), which allow them to be identified using histological staining techniques, polarized light microscopy, and ThT kinetic assays. ThT fluorescence increases upon binding of the dye to the amyloid fibrils, and although the interaction between the dye and amyloid is still not fully understood, it is believed that the ThT binds parallel to the fibril axis between adjacent β-sheets or protofilaments (Biancalana & Koide, 2010; Groenning, 2010; Groenning et al., 2007).

Amyloids formation is usually associated with diseases, but proteins that are not correlated with diseases can also form amyloid-like aggregates *in vitro* conditions under partially denaturing conditions (Litvinovich et al., 1998). It appears that amyloid formation is a generic and intrinsic property of the chemical structure of polypeptide chains, and most or all proteins can form such structures under correct solution conditions (Chiti et al., 1999; Sawaya et al., 2007)

### 1.3 Mechanism of fibril formation

The mechanism of fibril assembly is important to understanding several human diseases, for nanotechnology applications, and some biological processes (S. Kumar & Udgaonkar, 2010). Generally, a folded protein needs to at least partially unfold to form a state that is prone to aggregate (Kelly, 1998), and partially-unfolded and fully-unfolded states can lead to different aggregate end-state (Morozova-Roche et al., 2000). Describing the fibrillation process is challenging due to the multitude of possible pathways that the

protein monomers can take to reach their final fibril structure (Chiti & Dobson, 2006; Invernizzi, Papaleo, Sabate, & Ventura, 2012). Aggregation may occur in which the nucleation is in one step (directly from the monomer protein to fibrils) or two steps (step one being the formation of oligomers and step two being the conversion of oligomers to fibrils). Many aggregation reactions go through a nucleation-dependent polymerization process; however, some can go through linear polymerization which does not involve nucleation. Where protein monomers act as fibril nuclei, with no nucleation barrier (Kashchiev, 2015).

Nucleation is a set of necessary but unfavorable steps in the reaction that bottleneck the formation of large aggregates, where the nucleation step is a conformational change in the monomeric protein (Marcon, Plakoutsi, & Chiti, 2006). Three rules that must be met in order to classify the aggregation mechanism as the nucleation-dependent polymerization are: 1) a critical protein concentration required to start the polymerization reaction, 2) the observation of a lag phase, and 3) the ability of seeds to abolish the lag phase. If only two of the three parameters is met, the aggregation may follow linear polymerization rather than nucleated polymerization (Schmit, Ghosh, & Dill, 2011). Initially, nuclei must be formed by monomers (primary nucleation), and after a certain amount of aggregates are formed (Auer, Ricchiuto, & Kashchiev, 2012), the secondary pathway takes control of the growth (secondary nucleation).

In the early steps of aggregation, soluble aggregates are formed, then continue to form longer protofibrils and eventually fibrils. Prefibrillar aggregates are toxic because they are soluble and can form pores on the membranes (Adamcik & Mezzenga, 2011).

Nucleation time can vary from hours to days, however, after the nucleation step, aggregation starts, and the reaction takes off very quickly, then saturates. Overall, nucleation time depends on the nuclei concentration. The fibril can also induce the formation of other fibrils by the following three mechanisms: fragmentation, branching, and nucleation on the fibril surface, with all three mechanisms together leading to exponential growth (Eichner & Radford, 2011; Tipping et al., 2015).

The two generally accepted models for amyloid formation are the nucleation-elongation and the unfolding-fragmentation-fibrillation models (see Figure 1.2). In the nucleation-elongation model, the formation of a nucleus from an at least partially-unfolded monomeric form of the protein is necessary, followed by the accelerated growth through the addition of monomeric structures to the nucleus leads to the formation of protofilaments and oligomers. Later upon prolonged incubation, the mature fibrils form, and the reaction plateaus. In the unfolding-fragmentation-fibrillation model, the protein unfolds and hydrolyzes into smaller fragments, followed by formation of protofilaments and oligomers, where finally mature fibrils are formed upon incubation (Adamcik & Mezzenga, 2011a). Hydrolysis usually occurs as the consequence of elevated temperature and low pH during incubation.

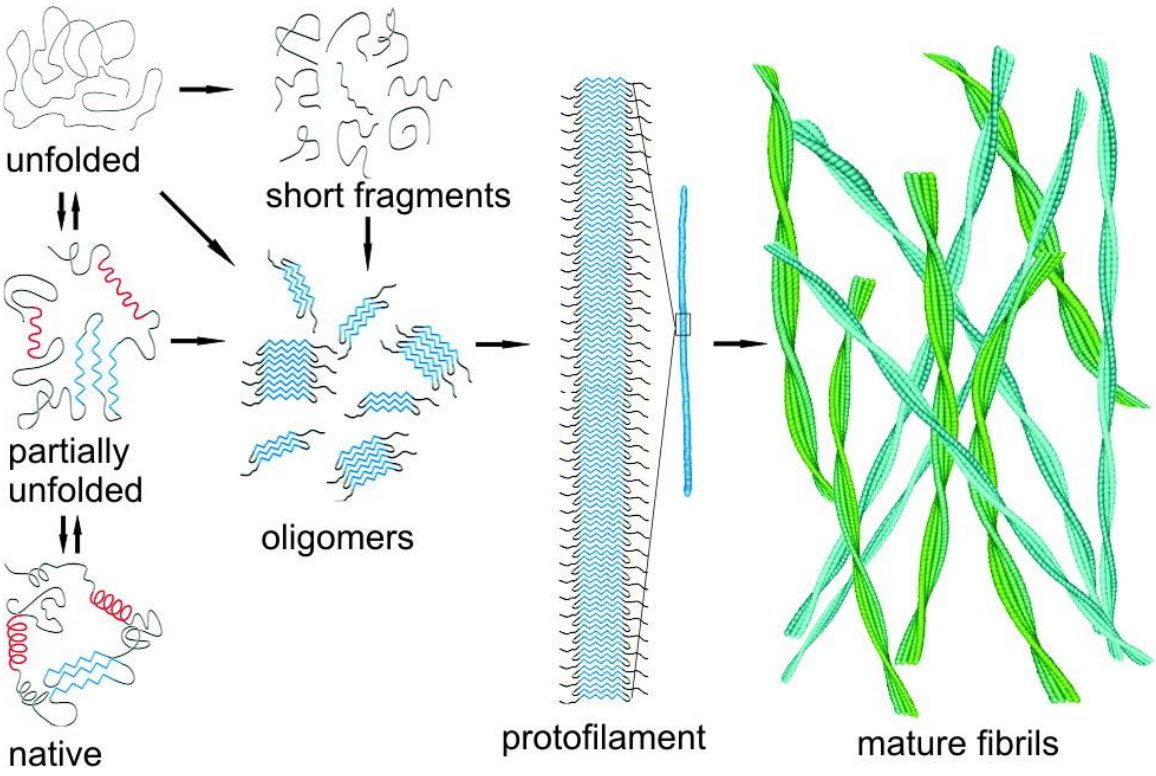


Figure 1.2 Mechanism of amyloid fibril formation from globular proteins. Figure is adapted with permission from (Adamcik & Mezzenga, 2012). Copyright (2012) American Chemical Society.

Interactions between surfaces and proteins combined with mechanical agitation, can often induce the amyloid aggregation by promoting the primary nucleation rate. This favors mass transport to promote fragmentation (through more nucleation sites) and fibril formation (Grigolato, Colombo, Ferrari, Rezabkova, & Arosio, 2017). Abdolvahabi et al. reported that different gyrating beads can accelerate and promote the amyloid formation and that there is a linear correlation between bead mass and fibril formation rate, that is likely due to the generation of more nucleation sites (fibril ends) by fibril fragmentation

(Abdolvahabi et al., 2017). It was reported that shear flow enhances the rate of fibril formation through unfolding and causes aggregation (Bekard & Dunstan, 2014).

Another study found that shear flow enhances the rate of fibril formation only when applied during nucleation, by breaking the filaments and inducing secondary nucleation (van den Akker, Schleeger, Bonn, & Koenderink, 2014).

### 1.4 Functional amyloid fibrils

Aside from disease-related amyloid, many non-pathogenic amyloid fibrils exist in nature, called "functional amyloid", that contain useful biological activities without incurring toxicity (Chapman et al., 2002; Shewmaker, McGlinchey, & Wickner, 2011). Functional amyloids are found in an extensive range of organisms, such as humans, insects, invertebrates (Fowler, Koulov, Balch, & Kelly, 2007), bacteria (Romero, Vlamakis, Losick, & Kolter, 2014), and fungi (Erskine et al., 2018). Some of these naturally occurring amyloids are utilized by different organisms for their functional characteristics, including biofilm formation in *E. coli* and *Salmonella* (Barnhart & Chapman, 2006; Cherny et al., 2005; Taglialegna, Lasa, & Valle, 2016; Van Gerven, Van der Verren, Reiter, & Remaut, 2018), chaplins in *Steptomyces coelicolor* (Claessen et al., 2003; Gebbink, Claessen, Bouma, Dijkhuizen, & Wösten, 2005), hydrophobins in *Pseudomonas* for spore coating (Dueholm et al., 2010; Rouse et al., 2017), and biofilm formation (Zeng et al., 2015), memory formation in fruit flies (Majumdar et al., 2012), insect immune response (Falabella et al., 2012), adhesive formation in marine invertebrates (Mostaert et al., 2009), protection of fish embryos and eggshells (Iconomidou, Vriend, & Hamodrakas, 2000; Podrabsky, Carpenter, & Hand, 2001),

HET-s (Balguerie et al., 2003), Sup35p for translational regulation in wild-type yeast (Chernoff et al., 2000), URE2p in regulation of nitrogen catabolism in yeast (Lian, Jiang, Zhang, Jones, & Perrett, 2006), spidroins in spider silk (Kenney, Knight, Wise, & Vollrath, 2002), Pmel17 in humans that is involved in melanin biosynthesis for skin pigmentation (Fowler et al., 2007; McGlinchey & Lee, 2018), and as storage hormones (insulin, glucagon, and calcitonin) in humans (Berchowitz et al., 2015).

### 1.5 Food protein amyloid fibrils

Food-derived proteins can be induced to form amyloid-like fibrils, also termed 'protein nanofibrils'. Nanofibrils made from food proteins (*e.g.*, from milk, eggs, cereals, and legumes) are gaining interest as new food ingredients and attractive nanomaterials, due to their unique structural and biological properties, highly functional surface chemistry, aspect ratio, and rheological behavior in solutions, as stabilizers, and gelling agents (S M Loveday, Wang, Rao, Anema, & Singh, 2011). Nanofibrils are insoluble, highly-stable aggregates that are heat resistant, and likely to contribute to the structural characteristics of the final food product (Moayedzadeh, Madadlou, & Khosrowshahi asl, 2015; Riek & Eisenberg, 2016). Pearce et al. found that protein aggregates formed during food processing may be amyloid-like in nature, resembling either rigid, long, straight fibrils, or semiflexible worm-like fibrils (Pearce, Mackintosh, & Gerrard, 2007). Many food proteins, such as pea protein isolate (Munialo, Martin, van der Linden, & de Jongh, 2014), soy glycinin and soy protein isolate (Akkermans et al., 2007), the egg-ovalbumin (Cecile Lara, Gourdin-Bertin, Adamcik, Bolisetty, & Mezzenga, 2012; Veerman, de Schiffart, Sagis, & van der Linden, 2003) and lysozyme (Arnaudov & De Vries, 2005;

Ow & Dunstan, 2013; Sugimoto et al., 2011), milk proteins including whey proteins (Simon M. Loveday, Su, Rao, Anema, & Singh, 2012), β-lactoglobulin (Kavanagh, Clark, Gosal, & Ross-Murphy, 2000; Serfert et al., 2014) α-lactalbumin (Otte, Ipsen, Bauer, Bjerrum, & Waninge, 2005), serum albumin (Veerman, Sagis, & Van der Linden, 2003; Vetri et al., 2011) lactoferrin (Nilsson & Dobson, 2003), and κ-casein (Thorn et al., 2005), cotton seed 7S storage protein (Zhou, Zhang, Yang, Wang, & Qian, 2014), and rice bran protein (Y.-H. H. Zhang & Huang, 2014), have been formed into amyloid fibrils (see Table 1.1).

Food protein nanofibrils are attractive ingredients and edible nanomaterials due to their improved functional characteristics in food systems and nanotechnology applications. Food protein nanofibrils can be utilized as an emulsion stabilizer (Gao et al., 2017), foam stabilizer (Oboroceanu, Wang, Magner, & Auty, 2014), gelling agent (Foegeding, 2007; Foegeding & Davis, 2011; Munialo et al., 2014), forming cold-set gels (Farjami, Madadlou, & Labbafi, 2016), forming aerogels (Nyström, Fernández-Ronco, Bolisetty, Mazzotti, & Mezzenga, 2016), for encapsulation, as a texturizer in food systems, as a cellular scaffold for enzyme immobilization (Pilkington, Roberts, Meade, & Gerrard, 2010; Shen et al., 2017; Taglialegna et al., 2016), for forming films, nanowires (Elfwing, Bäcklund, Musumeci, Inganäs, & Solin, 2015), design of graphene-based biosensors and biomaterials (Gras, 2007), biomimetic artificial bones (X. Li et al., 2013), binding to antibodies (Schmuck, Sandgren, & Härd, 2017), underwater adhesives, organic photovoltaics, water purification membranes (Bolisetty & Mezzenga, 2016) and nanotubes (Fuciños et al., 2017; Graveland-Bikker & de Kruif, 2006) in nanotechnology

applications (Knowles & Mezzenga, 2016). The ability of food protein nanofibrils to increase viscosity at relatively low concentrations makes them very economic texturizers. The emulsifying activity of proteins increases during fibrillation. Food protein fibrils can stabilize different type of emulsions including water-in-water (Gonzalez-Jordan, Nicolai, & Benyahia, 2016) and oil-in-water (Ng, Lee, Chuah, & Cheng, 2017). Gelation is one the most central properties of the proteins, and fibrillated food proteins are considered as efficient gelation agents because they can form gels at much lower concentrations compared to native proteins (Veerman, Sagis, et al., 2003).

Forming films, composites and silk fibers is another intrinsic property of food nanofibrils since they are stiff, strong and thermodynamically stable (C. Li, Adamcik, & Mezzenga, 2012). They make polymer composites (Byrne et al., 2011), and protein-based films (Knowles, Oppenheim, Buell, Chirgadze, & Welland, 2010) from hen egg white lysozyme (HEWL). Use of edible nanofibrils as encapsulating agents for drug delivery and food industries are promising since they are biocompatible, and have emulsification and film forming abilities (Schleeger et al., 2013). Scientists have made microcapsules from lysozyme, ovalbumin, soy, and whey proteins with different properties and indicates that food proteins can make microcapsules with tunable properties (Farjami, Madadlou, & Labbafi, 2015). Nanofibrils from whey proteins, bovine insulin, hen lysozyme, and β-lactoglobulin were used as biosensors to detect different materials such as the β-lactamases bacterial enzyme, metal ions, water, and glucose (Viguier et al., 2011). Food protein fibrils have a high metal binding activity, and they can be used for water purification (Bolisetty & Mezzenga, 2016).

Table 1.1 Examples of food protein nanofibrils. Table is taken from Trends in Food Science & Technology (Mohammadian & Madadlou, 2018) with permission from Elsevier publisher.

| Source of protein | Fibril forming protein | Fibrillation conditions | Fibrils morphology | Reference |
|---|---|---|---|---|
| Milk | Whey protein isolate (WPI) | pH 2.0, 90 °C, 20–22 h | Length of 1–10 μm and diameter of 2–10 nm | Sasso et al. (2014) |
| | Whey protein concentrate (WPC) | pH 2.0, 90 °C, 10 h | Micrometric length with nanometric diameter | Gao et al. (2013) |
| | Whey protein hydrolysate (WPH) | pH 2.0, 85 °C, 5 h | Micrometric length with diameters less than 10 nm | Mohammadian and Madadlou (2016a) |
| | β-Lactoglobulin (β-lg) | pH 2.0, 80 °C, 20 h | Long fibrils with diameter of 8.2 nm | Bateman et al. (2011) |
| | α-Lactalbumin | pH 2.0, 55 °C, 0–40 h | Fibrils with ~ 10 nm in diameter and ~ μm in length | Wang, Liu, Wen, and Wang (2011) |
| | Bovine serum albumin | pH 2.0, 90 °C, up to 145 h | Micrometric length with diameters of 2–6 nm | Usov, Adamcik, and Mezzenga (2013) |
| | Caseins | pH 2.0, 90 °C, 48 h | Fibrils with a length greater than 1 μm and nanometric diameter | Pan and Zhong (2015) |
| | κ-Casein | pH 6.0, 37 °C, 18 h | Micrometric length with thicknesses about 5–7 nm | Leonil et al. (2008) |
| Egg | Lysozyme | pH 2.0, 57–65 °C, 60–70 h | Average length of 600 nm and thickness of 15 nm | Song et al. (2016) |
| | Ovalbumin | pH 2.0, 85 °C, 3 h | Semi-flexible fibrils with a contour length of a few hundred nanometer and effective diameters of a few nanometer | Humblet-Hua et al. (2011) |
| Soy | Glycinin | pH 2.0, 80 °C, 0–16 h | Fibrils with heights of 1.4–2.2 nm and contour length of around 600–800 nm | Tang and Wang (2010) |
| | β-Conglycinin | | | |
| | Soy protein isolate (SPI) | pH 1.6, 80 °C, 22 h | Curly fibrils with diameter of 8 nm and 250–300 nm in length | Lassé et al., 2016 |
| Pea | Pea protein isolate | pH 2.0, 85 °C, 20 h | Highly flexible, branched and, curly fibrils with micrometric length and nanometric thickness (these authors reported that soy protein fibrils were more flexible and more branched then whey protein fibrils) | Munialo et al. (2014) |
| Kidney bean | Vicilin | pH 2.0, 85 °C, 0–24 h | Fibrils with nanometric diameter and heterogeneous length | Liu and Tang (2013) |
| | Phaseolin | pH 2.0, 85 °C, 0–24 h | Fibrils with diameter of about 10 nm and average contour length of about 52–950 nm (increase with the increasing of heating time) | Tang, Zhang, Wen, and Huang (2010) |
| | Kidney bean protein isolate (KPI) | pH 1.6, 80 °C, 22 h | Curly fibrils with diameter of 8 nm and 250–300 nm in length | Lassé et al., 2016 |
| Mung bean and red bean | Vicilin | pH 2.0, 85 °C, 0–24 h | Fibrils with nanometric diameter and heterogeneous length | Liu and Tang (2013) |
| Rice | Rice bran protein | pH 2.0, 90 °C, 2 h | Fibrils with contour length of 650 nm and width of ~ 10 nm | Zhang and Huang (2014) |
| | Rice bran globulin | pH 2.0, 90 °C, 2 h | Fibrils with contour length of about 100–500 nm (increasing with increasing the ionic strength) and width around 20 nm | Huang, Zhang, and Li (2014) |
| Meat | Hemoglobin | pH 2.8, 80 °C, 24 h | Diameter of 5 ± 3 nm and peak-to-peak distance of 54 ± 19 nm | Jayawardena et al. (2017) |

#### 1.5.1.1 Protease resistance (digestibility)

Digestibility of food nanofibrils is an important property for food applications. A fibril digestibility study by Bateman et al. on β-lactoglobulin fibrils reported complete digestion of fibrils within 2 minutes of incubation in a simulated gastric fluid with pepsin, followed by reformation of new thinner fibrils. These came from hydrolysates (>2000-8000 Da) of original fibrils digested by pepsin under gastric conditions during prolonged incubation (Bateman, Ye, & Singh, 2010, 2011). This finding suggests that there could be an equilibrium between fibrils and hydrolysates. However, another study reported that β-lactoglobulin fibrils were not fully digested when exposed to gastric and ileum juice containing pepsin, trypsin, and chymotrypsin (Oboroceanu, 2011). Therefore, more studies are needed to investigate the fate of the amyloid fibrils after consumption.

Lassé et al. investigated *in vitro* digestibility of amyloid fibrils made from whey, kidney bean, soy bean, and ovalbumin. They found that fibrils showed some degree of resistance to *in vitro* digestion by proteinase K, pepsin, and pancreatin after three hours, which could be related to variations in morphology of different fibrils. The fibrils could persist in whole or in part and may have time to interact with the cells of the gastrointestinal tract (Lassé et al., 2016). Fibrils are mainly insoluble under physiological conditions and show resistance to proteolysis by trypsin and proteinase K (Conway, Harper, & Lansbury, 2000; Legname et al., 2004).

#### 1.5.1.2 Toxicity and safety of food nanofibrils

Protein nanofibrils may find use in food applications because of their appealing functional and biophysical properties, however, there are some concerns about their

safety and toxicity if particular protein aggregates accumulate upon oral consumption (Raynes, Carver, Gras, & Gerrard, 2014; Solomon et al., 2007). Some proteins have been known to associate with disease-related amyloid fibrils (Lassé et al., 2016). The evidence of oral transmissibility of disease upon consumption of amyloid fibrils such as prions (Acheson, 2002), murine amyloid-A (Cui, Kawano, Hoshii, Liu, & Ishihara, 2008), and serum amyloid-A (Solomon et al., 2007) amyloids has raised food safety concerns about the consumption of amyloidotic or purified amyloid fibrils. Amyloid fibrils can be found in edible avian and mammalian food-animal tissue, where recommended cooking temperatures are unable to eliminate them before consumption. The evidence of cross-seeding in prion proteins (Stępkowski & Bieniaś, 2012) and mice studies showed that injection or feeding amyloid fibrils (serum amyloid-A) caused systemic amyloidosis in transgenic mice (Solomon et al., 2007). These amyloid fibrils were extracted from duck or goose-derived pâté de foie gras (fatty liver produced by force-feeding). These studies indicate that amyloid disease may be transmissible by oral consumption of amyloid fibrils in a susceptible population under certain conditions (Tjernberg et al., 2016). Like prions (Cobb & Surewicz, 2009; J. Zhang et al., 2006), amyloid-A fibrils can cross the gut barrier and cause disease (Greger, 2008). Cooking, freezing/thawing, using disinfectants, and autoclaving for three hours could not eliminate the amyloids. Landmark et al. (2002) performed a similar foie gras experiment on healthy mice, and healthy mice did not develop amyloidosis within days as the transgenic mice did; however, they did develop amyloidosis later in their lifespan with an extended interval between consumption or injection and inflammation of 180 days (Lundmark et al., 2002).

Bovine prions fed to mice trigger murine spongiform encephalopathy, while bovine amyloid-A fed to mice triggers amyloid-A amyloidosis (Cui et al., 2002). Amyloid-A (AA) amyloidosis occurs in many animals, including cattle, chickens, goats, dogs, horses, sheep, cats, and pigs (Ménsua et al., 2003). AA amyloidosis can be transmitted through contaminated fecal matter among captive cheetahs (B. Zhang et al., 2008). Prions can spread from human to human, as in kuru disease, where people from New Guinea who practiced cannibalism, ate brains of the dead as part of their funeral ritual (Glasse, 1967; Steadman & Merbs, 1982). Prions also spread from animal to human in variant Creutzfeldt-Jakob disease, caused by eating contaminated beef products such as brain and spinal cord, and from animal to animal by feeding the contaminated meat and bone powders as animal feed (Westermark, Lundmark, & Westermark, 2009). There is also some evidence that fibrils made from synthetic peptides designed for nanotechnology can induce amyloidosis in susceptible animals (Westermark et al., 2009).

Mocanu et al. reported that hen egg white lysozyme (HEWL) fibrils formed at pH 2.7 affected renal cell growth in a dose-dependent manner (Mocanu et al., 2014). Lassé et al. investigated the *in vitro* toxicity of amyloid fibrils made at acidic pH from whey, kidney bean, soy bean, and ovalbumin. They evaluated the toxicity of mature fibrils, early-stage oligomeric forms, and sonicated fibrils in two different human cell lines (Caco-2, and Hec-1a), and found no toxicity at a fibril concentration up to 0.25 mg/mL (Lassé et al., 2016). A separate study on whey protein fibrils, also formed at acidic pH, also showed no toxicity towards Hec-1a cells (Kaur et al., 2014). With only these few

studies, there is not enough information to establish the safe use of nanofibrils in food (Krebs et al., 2004).

### 1.6 Disease related amyloid fibrils

There are numerous diseases affecting millions globally (Chiti & Dobson, 2006; Harrison, Sharpe, Singh, & Fairlie, 2007) that are associated with amyloid aggregates (see Table 1.2). Each disease is associated with a specific precursor protein that misfolds to form amyloid fibrils. These protein aggregates can form plaques and tangles when misfolded inside or outside of organs and cause eventual cell death and disease (Stefani & Dobson, 2003).

Many studies report that the soluble precursor forms (*e.g.*, pre-fibrillar oligomers or protofilaments) are more toxic than the mature fibrils (Glabe, 2008; Glabe & Kayed, 2006; Haass & Selkoe, 2007; Stroud, Liu, Teng, & Eisenberg, 2012). However, some studies report amyloid toxicity is caused by mature fibrils, not fibrillar oligomers (Gharibyan et al., 2007; Stefani, 2010; Xue, Homans, & Radford, 2009). It is believed that soluble aggregates can disrupt the cell membrane by making a pore causing $Ca^{2+}$ release and oxidative damage (Stefani & Dobson, 2003). Since membrane disruption may be linked to the hydrophobicity of the aggregates, different cell lines can act differently in the presence of the same amyloid aggregate (Stefani, 2010). Bovine insulin can form either toxic fibrils with a parallel β-sheet conformation, or non-toxic filaments that have an anti-parallel β-sheet structure (Zako, Sakono, Hashimoto, Ihara, & Maeda, 2009).

Table 1.2 Some amyloidosis and their respective precursors and amyloidogenic proteins. Table is adapted from (Rambaran & Serpell, 2008).

| Disease | Precursor Protein | Amyloid Protein |
|---|---|---|
| Alzheimer's disease | Amyloid precursor protein | Ab peptides |
| Artial amyloidosis | Artial natriuretic factor (ANF) | Amyloid ANF |
| Spongiform encephalopathies | Prion protein (PrPc) | PrPsc |
| Primary systemic amyloidosis | Immunoglobulin light & heavy chains | AL and AH |
| Senile systemic amyloidosis | Wild-type transthyretin | ATTR |
| Hemodialysis-related amyloidosis | B2-microglobulin | Ab2M |
| Hereditary non-neuropathic systemic amyloidosis | Lysozyme | ALys |
| Type 2 diabetes mellitus (T2DM) | Pro-IAPP | IAPP or amylin |
| Injection-localized amyloidosis | Insulin | AIns |
| Secondary systemic amyloidosis | (Apo) serum amyloid A | Serum amyloid A |
| British familial dementia | Amyloid Bri Precursor Protein | ABri |

### 1.7 Polymorphism

Amyloid fibrils share a common core of β-sheet structure regardless of the source of the protein (Glabe & Kayed, 2006; Kayed et al., 2003), however, later studies reported that despite the tremendous structural similarities between individual amyloid aggregates, amyloid fibrils formed from different proteins are not identical (C.M. Dobson, 2004). Even a single amino acid difference in the protein sequence leads to different fibrils, for

instance, wild-type alpha-synuclein versus its disease mutant (Celej, Caarls, Demchenko, & Jovin, 2009; Nielsen et al., 2013).

A given protein can be induced to form different amyloid fibrils that have unique structural properties—termed *polymorphs*. It is important to study amyloid fibril polymorphism since it may be relevant to understanding disease-causing amyloids such as prions and amyloid beta-peptide (A-BETA) (Sneideris, Milto, & Smirnovas, 2015). Recent studies have reported environment-induced polymorphism of amyloid fibrils made from human lysozyme(HLZ) (Mossuto et al., 2010), hen egg white lysozyme (HEWL) (Adamcik & Mezzenga, 2011), insulin (Sneideris, Darguzis, et al., 2015), alpha-synuclein (Bousset et al., 2013), serum albumin (Usov, Adamcik, & Mezzenga, 2013), amyloid beta-peptide (A-BETA) (Jeong, Ansaloni, Mezzenga, Lashuel, & Dietler, 2013; X. Li et al., 2013), prion protein (Cobb, Apostol, Chen, Smirnovas, & Surewicz, 2014; Šneideris, Kulicka, & Smirnovas, 2018).

Mossuto et al. characterized two types of human lysozyme amyloid fibrils with distinct morphology, molecular structure, stability and size of the cross-β core formed at two different pH conditions *in vitro*. Different polymorphs of the same protein can have different toxicity behavior, for instance, human lysozyme amyloid fibrils formed at pH 2 are non-toxic for the human neuroblastoma cells, while amyloid fibrils formed at neutral pH lead to the death of these cells. Interestingly, human lysozyme fibril polymorphs with smaller cores demonstrated substantial cytotoxic effects in human cell lines (Mossuto et al., 2010). Different polymorphs of the same protein can have different properties, for instance, lysozyme fibrils made at pH 7.0, and pH 2.0, demonstrate different

photophysical properties, and different ThT binding parameters (Sulatskaya, Rodina, Povarova, Kuznetsova, & Turoverov, 2017).

A study done by Cheon group reported that polymorphism of amyloid beta peptides (A-BETA) depends on the size of the oligomers that are being formed during oligomerization and fibrillization process (Cheon, Kang, & Chang, 2016). Another study done by Auer reported that the fibril polymorphism is related to fibril nucleation and the nucleation is depended on protein concentration and solubility, which is somewhat in an agreement with Cheong's work (Auer, 2015). Annamalai et al. investigated the *in vivo* fibrils from humans, and animals and they have found *in vivo* fibrils to be polymorphic (Annamalai et al., 2016). Pellarin et al. reported that amyloid polymorphism is kinetically controlled, and nucleation barriers determine the population of the dominant nuclei. Therefore, different conditions can favor the formation of different nuclei, leading into the formation of different fibril polymorphs (Pellarin, Schuetz, Guarnera, & Caflisch, 2010). A study done by Thirumalai et al. reported that the arrangement of the water molecules around the oligomers and protofilaments during fibrillation could result in different fibril polymorphs (Thirumalai, Reddy, & Straub, 2011).

Since the accumulation of lysozyme amyloid fibrils in human organs can lead to the development of systemic amyloidosis, it is prudent to study lysozyme polymorphism and cross-seeding among polymorphs (Sattianayagam et al., 2012). This work aimed to study the polymorphism and cross-seeding of lysozyme amyloid fibrils formed under two different pH conditions. This will be the first to study the polymorph seeding of lysozyme fibrils.

The polymorphism of amyloid fibrils is crucial as it may underlie the natural variability of diseases-related amyloids and could help to better understand the molecular basis of amyloid aggregation (Mocanu et al., 2014). Interestingly, despite the strikingly similar natures of the fibrillar structures, the formed fibrils differ in morphology, stability, and cytotoxicity depending on factors utilized during fibrillization (Alavez, Vantipalli, Zucker, Klang, & Lithgow, 2011). The structure of amyloid fibrils can be affected by many factors such as protein concentration, pH, temperature, denaturing agents, salts (Sulatskaya, Kuznetsova, & Turoverov, 2011). Lara et al. reported that some proteins such as lysozyme and β-lactoglobulin could form multi-stranded amyloid ribbons over time with widths up to 173 nm due to a modular lateral assembly (Cécile Lara, Adamcik, Jordens, & Mezzenga, 2011). Morphologic differences have been reported for different types of shear forces. Fibrils fragment in strong shear forces, leading to the formation of fibril seeds, which can also promote toxicity (Bekard & Dunstan, 2014).

**1.8 Seeding and cross-seeding**

Previously formed fibrils can get fragmented into smaller fibrils via mechanical forces (sonication), or protease digestion, so-called *seeds*. De novo amyloid formation or simply unseeded fibrillation can take from days to weeks. It is known that the polymerization process and rate of fibril formation of a particular protein are enhanced by the addition of the seeds (preformed fibrils that are broken into shorter pieces) of the same protein, providing more fibril ends for elongation, leading to homologous seeding (homoseeding) or simply self-seeding. If the fibril composed of one protein acts as seeds

for the elongation of another protein, the process is called heterologous seeding (heteroseeding) or simply cross-seeding (see Figure 1.3). If the fibril composed of one protein polymorph act as seeds for the elongation of another polymorph of the same protein (seeding between different strains of a protein), the process is called polymorphic seeding. If the fibril composed of one protein polymorph act as seeds for the elongation of another polymorph from another protein, the process is called polymorphic cross-seeding (double cross-seeded; species and polymorphs).

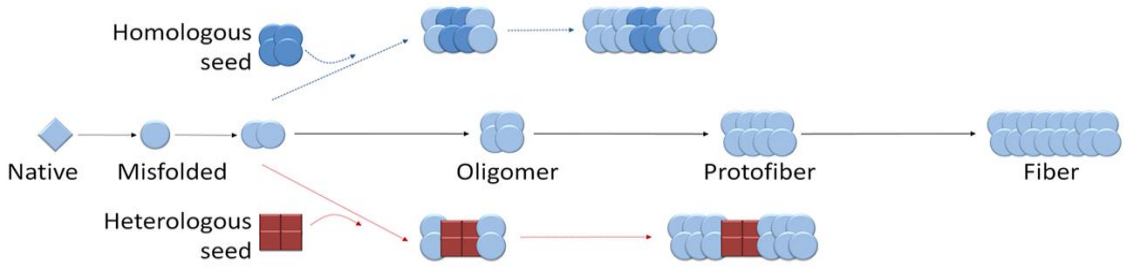


Figure 1.3 Seeding phenomenon. Figure is taken from (Morales, Moreno-Gonzalez, & Soto, 2013). Copyright (2013) PLOS.

Some studies suggest that high sequence identity (>40%) is required for amyloid aggregates to be able to cross-seed one another (Clarke et al., 2005; Krebs et al., 2004). In contrast, some studies do exist that report the evidence of cross-seeding between dissimilar protein sequences, for instance cross-seeding evidence of dissimilar amyloid sequences such as curli protein and prostate acid phosphatase (Hartman et al., 2013), amyloid-β and human islet amyloid polypeptide with 25% sequence identity (M. Zhang et al., 2015). These findings indicate that if the two dissimilar amyloid proteins can adopt highly similar structures, and can cross-seed each other despite the sequence divergence (Wasmer et al., 2010). Prions can cross the species barrier and induce amyloid formation

in another species, for instance, in the variant form of Creutzfeldt-Jakob disease (CJD), the disease can be transmitted upon oral consumption. Mostly, cross-species barrier studies have been done on disease-related proteins, and to our knowledge, only one study has been done by Krebs et al. claimed that they had observed some evidence of cross-seeding between egg-white and human lysozyme, but the data was not shown.

Amyloid fibril formation is followed by seeding/nucleation polymerization model. This aggregation process is composed of two phases, the nucleation/lag phase, and the polymerization/elongation phase. After central nuclei have formed the aggregation process increases exponentially from small oligomers into fibrils. The addition of preformed seeds leads to a shorter lag phase and a faster aggregation, the lag phase is much smaller with homologous seeds than heterologous seeds (see Figure 1.4).

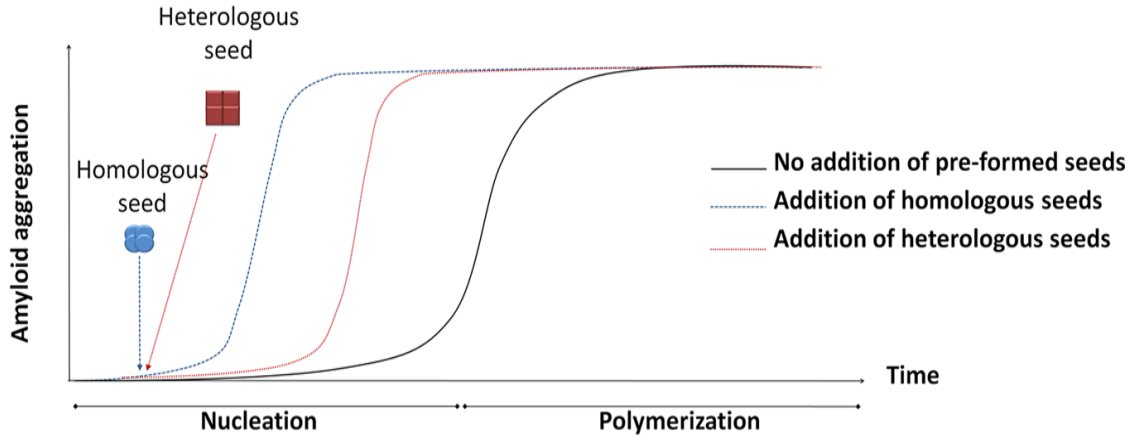


Figure 1.4 ThT binding kinetics of fibril formation. Figure is taken from (Morales et al., 2013). Copyright (2013) PLOS.

To date, polymorphic cross-seeding studies have not been thoroughly investigated. Different polymorphs of a particular protein may have different seeding capability, toxicity, therefore it is prudent to study cross-seeding among different

polymorphs of food nanofibrils with human proteins, to ensure no cross-seeding can occur upon consumption. This study is the first to study the cross-seeding between HEWL and HLZ polymorphs.

### 1.9 Protein sequence alignment

Sequence and structural similarities are generally considered important to understanding the cross-seeding phenomenon between proteins (Sander & Schneider, 1991). Some studies suggest that high sequence identity (>40%) is required for amyloid aggregates to be able to cross-seed one another (Clarke et al., 2005; Krebs et al., 2004). In contrast, some studies reported cross-seeding between dissimilar proteins, for instance, curli protein and prostatic acid phosphatase (PAP248-286) (Hartman et al., 2013), and amyloid-β and human islet amyloid polypeptide with 25% sequence identity (M. Zhang et al., 2015). Homology is when the two sequences or structures share more similarity than would be expected by chance (Chung & Subbiah, 1996). The primary sequence of hen egg-white lysozyme (P00698), and human lysozyme (P61626) are 58% identical, and the three-dimensional crystal structure of HEWL and HLZ are aligned using PyMol software shown below (see Figure 1.5).

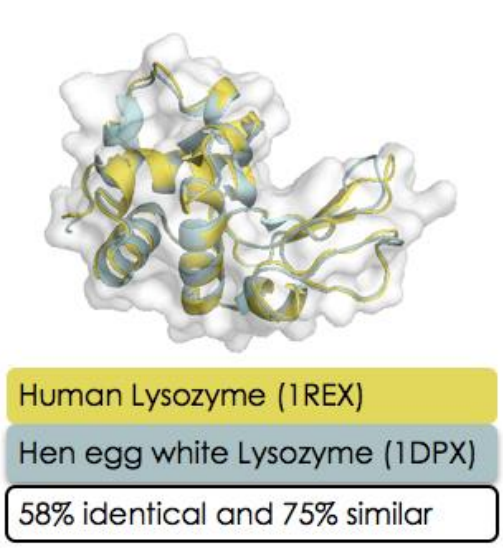


Human Lysozyme [Homo sapiens]

```
MKALIVLGLV LLSVTVQGKV FERCELARTL
KRLGMDGYRG ISLANWMCLA KWESGYNTRA
TNYNAGDRST DYGIFQINSR YWCNDGKTPG
AVNACHLSCS ALLQDNIADA VACAKRVVRD
PQGIRAWVAW RNRCQNRDVR QYVQGCGV
```

Hen Egg White Lysozyme [Gallus gallus]

```
MRSLLILVLC FLPLAALGKV FGRCELAAAM
KRHGLDNYRG YSLGNWVCAA KFESNFNTQA
TNRNTDGSTD YGILQINSRW WCNDGRTPGS
RNLCNIPCSA LLSSDITASV NCAKKIVSDG
NGMNAWVAWR NRCKGTDVQA WIRGCRL
```

Figure 1.5 Sequences and crystal structures of hen egg-white and human lysozyme.

### 1.10 Lysozyme fibrillation

Lysozyme is an antimicrobial protein synthesized by macrophages throughout the body (Melrose, Ghosh, & Taylor, 1989). The largest population of macrophages is in the liver, but lysozyme is also present in high concentration in articular cartilage, milk, saliva, tears and a trace amount in body fluids such as serum and cerebrospinal fluid (Morozova-Roche et al., 2000). Lysozyme has been studied widely as a model for protein folding and aggregation, and mutational variants of human lysozyme are associated with hereditary non-neuropathic systemic amyloidosis (Felice et al., 2004; Pepys et al., 1993). HEWL readily forms amyloid fibrils *in vitro*, including upon exposure to partial denaturation conditions (low pH, high temperature, and low concentration of denaturants), for a prolonged period (Mishra et al., 2007; Sugimoto et al., 2011).

Hen egg white lysozyme (HEWL) is homologous to human lysozyme (HLZ), with 58% sequence identity. HEWL has 129 amino acids (14.3 kDa), and HLZ has 130

amino acids (14.7 kDa). Lysozyme is a positively charged protein with eight cysteine residues which covalently bond together forming four disulfide bridges. The native state of lysozyme is composed of two domains, α-domain and β-domain (Kumita et al., 2006), the β-domain has three β-sheets in its structure which might be essential for the amyloid fibril formation (see Figure 1.6). The α-domain folds faster than the β-domain during lysozyme folding and refolding.

The charge distribution on the protein affects the propensity to form amyloid fibrils. The native state under conditions where hydrogen bonds and other interactions are still favorable is the critical factor for fibril formation (Chiti et al., 1999).

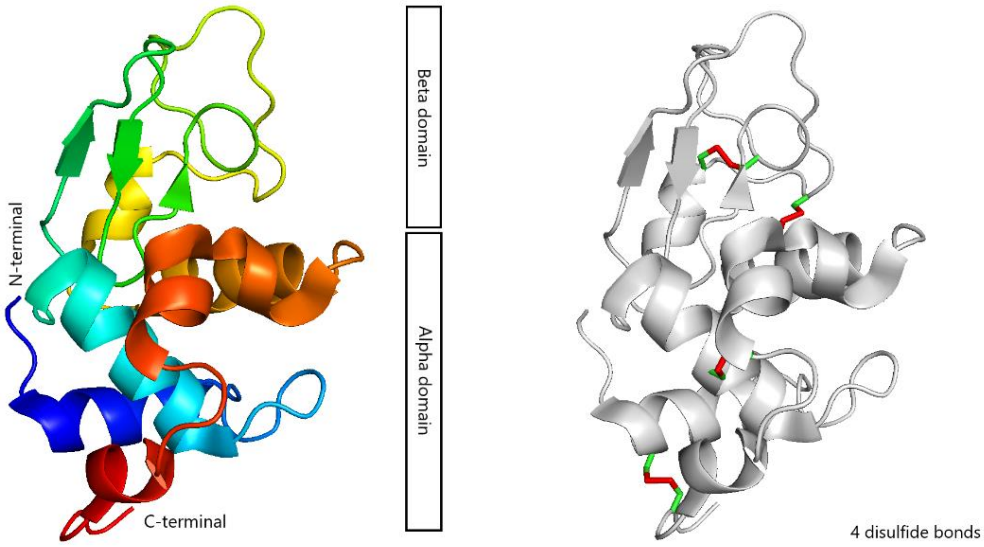


Figure 1.6 Crystal structure of lysozyme (1DPX) presenting different domains and disulfide bonds. Figure is made using PyMol.

Mutations of human lysozyme which can cause amyloidosis (Pepys et al., 1993). The common disease-related lysozyme variants Ile56Thr (1IOC), and Asp67His (1LYY) are also 58% identical and 75% similar in sequence to HEWL (1DPX). I56T and D67H

are structurally very similar in their native state to wild-type human lysozyme. It has been shown that wild-type human lysozyme forms a stable partially folded "molten globule" state at acidic pH (Haezebrouck et al., 1995).

Intracellular compartments such as lysosomes have a low pH, and an acidic environment may promote fibrillation *in vivo*. Normal pH values inside macrophage lysosomes have been found to be around 4.5 to 4.8 (Ohkuma & Poole, 1978). Low pH and high temperature promote amyloid fibril formation and indicate that unfolded and partially folded states are important in such aggregation processes (Morozova-Roche et al., 2000).

### 1.11 Thesis objectives

Nanofibrils made from food proteins (*e.g.*, from milk, eggs, cereals, and legumes) are gaining interest as new food ingredients and nanomaterials, because of their unique structural and biological properties. Before we use nanofibrils directly in food or food-contact surfaces, it would be crucial to investigate their consequences and impact on human health. Studies on cytotoxicity and cell viability assays were done on some nanofibrils made from food proteins, but to our knowledge, few studies, if any, have considered cross-seeding between food protein nanofibrils and similar proteins, endogenous to humans that are structurally related. That is, cross-seeding between protein homologs from different species (*e.g.*, cross-seeding between hen egg-white lysozyme, and human lysozyme) *in vitro.*

Cross-seeding is more likely the more similar in sequence and structure two proteins are, and the milk and egg proteins most commonly used to form nanofibrils are

structurally similar (60-90% similarity) to several human proteins. Amyloid fibrils can survive digestion and spread to other parts of the body, as evidenced by prions (Colby & Prusiner, 2011) and amyloid A (AA) protein from foie gras (Solomon et al., 2007). These findings indicate that protein nanofibrils may induce the amyloid formation of other structurally similar human proteins upon oral consumption, in a susceptible population under certain conditions.

The objective of this research was to examine the cross-seeding ability of food protein nanofibrils and determine if they can induce their homologous human proteins to misfold and aggregate. The key hypothesis of this study is that food protein nanofibrils can induce fibril formation in related human proteins, using human lysozyme (HLZ) and hen egg-white lysozyme (HEWL) as a model system.

To test the central hypothesis, three specific objectives were examined:

(1) Examine the impact of different environmental conditions (*e.g.*, pH, temperature, agitation, chemical denaturant presence) on fibril formation kinetics.
    a. Identify conditions for seeding reactions
    b. Optimize seed formation
(2) Test the cross-seeding ability of HEWL and HLZ
(3) Characterize the polymorphism of the human lysozyme and hen egg-white lysozyme and determine if they can cross-seed the fibrillation of one another under the tested conditions *in vitro*.
(4) Examine the effects of gastric conditions on fibril structure and seeding.

# CHAPTER 2

# 2 MATERIALS AND METHODS

## 2.1 Materials

### 2.1.1 Proteins and chemicals

All proteins were analytical grade. Hen egg white lysozyme (HEWL-L6876) lyophilized powder, human lysozyme (HLZ-L1667) lyophilized recombinant protein expressed in rice, lyophilized pepsin from porcine gastric mucosa (3,200-4,500 units/mg SLBS5133), Thioflavin T (ThT) (T3516), purchased from Sigma-Aldrich (St. Louis, MO 63103 USA), Guanidine hydrochloride (GdnHCl), purchased from Fisher and used without further purification. Uranyl acetate, and 0.5% Formvar solution (15820) purchased from Electron Microscopy. Protein solutions were made by dissolving the appropriate amount of protein in the buffer of choice; then protein concentrations were measured and verified using ThermoScientific NanoDrop One Microvolume UV-Vis Spectrophotometer at 280 nm, using extinction coefficient of 37,970 $M^{-1}cm^{-1}$ and 36,940 $M^{-1}cm^{-1}$ for HEWL and HLZ, respectively. All buffers and solutions were prepared with ultra-pure water (>18 mΩ) obtained from the Purelab Ultra water purification system (ELGA, UK).

### 2.1.2 Buffers and solutions

50 mM Glycine-HCl pH 2.0 ± 0.1, and 20 mM potassium phosphate (K-Phos) pH 6.3 ± 0.1 buffer with 3M Guanidine hydrochloride filtered through 0.45 μm fisher brand/PES filter. Since Guanidine hydrochloride is hygroscopic, preparing stock solutions by mass can lead to errors. Therefore, the GdnHCl stock solutions are prepared using refractive index (RI) measurements using the following equation $M= 57.147(\Delta N) + 38.68(\Delta N)^2 – 91.60(\Delta N)^3$. ΔN is the refractive index of the Guanidine hydrochloride solution and of the buffer solution. (Grimsley et al., 2004- Cold Spring Harb Protoc; 2006; doi:10.1101/pdb.prot4241).

## 2.2 Methods

### 2.2.1 Lysozyme fibril formation - De Novo Nucleation (non-seeded)

The hen egg-white lysozyme (HEWL) was stored at -20°C, while the human lysozyme (HLZ), stored at -70°C, were thawed in an ice bucket (~0°C). HEWL and HLZ were prepared through the incubation of 1 mM protein with constant shaking (300 rpm) (i) in 50 mM Glycine-HCl buffer of pH 2.0, at 65 (HEWL 2.0, HLZ 2.0) and (ii) in 20 mM potassium phosphate (K-Phos) buffer of pH 6.3 containing 3 M GdnHCl, at 50°C (HEWL 6.3, HLZ 6.3). Formation of fibrils was confirmed by ThT fluorescence and morphology characteristics of the fibrils were evaluated with TEM and AFM. Protein concentrations were verified by NanoDrop One at 280 nm, using extinction coefficient of 37,970 $M^{-1}cm^{-1}$ and 36,940 $M^{-1}cm^{-1}$ for HEWL and HLZ, respectively. All four samples were centrifuged at a speed of 9000 rpm for 20 minutes in then filtered through 0.22 μm filters. Centrifugation was done to remove any preformed aggregates potentially formed

during the thawing and dissolving process as reported by DiCostanzo, A. C., et al. (J. Biol. Chem. 2012). The pH 2.0 samples (HEWL 2.0 & HLZ 2.0) were incubated for about a week, and the pH 6.3 samples (HEWL 6.3 & HLZ 6.3) were incubated for 2 or 3 days. Once samples were finished incubating, fibrils were ready to be sonicated for seed formation.

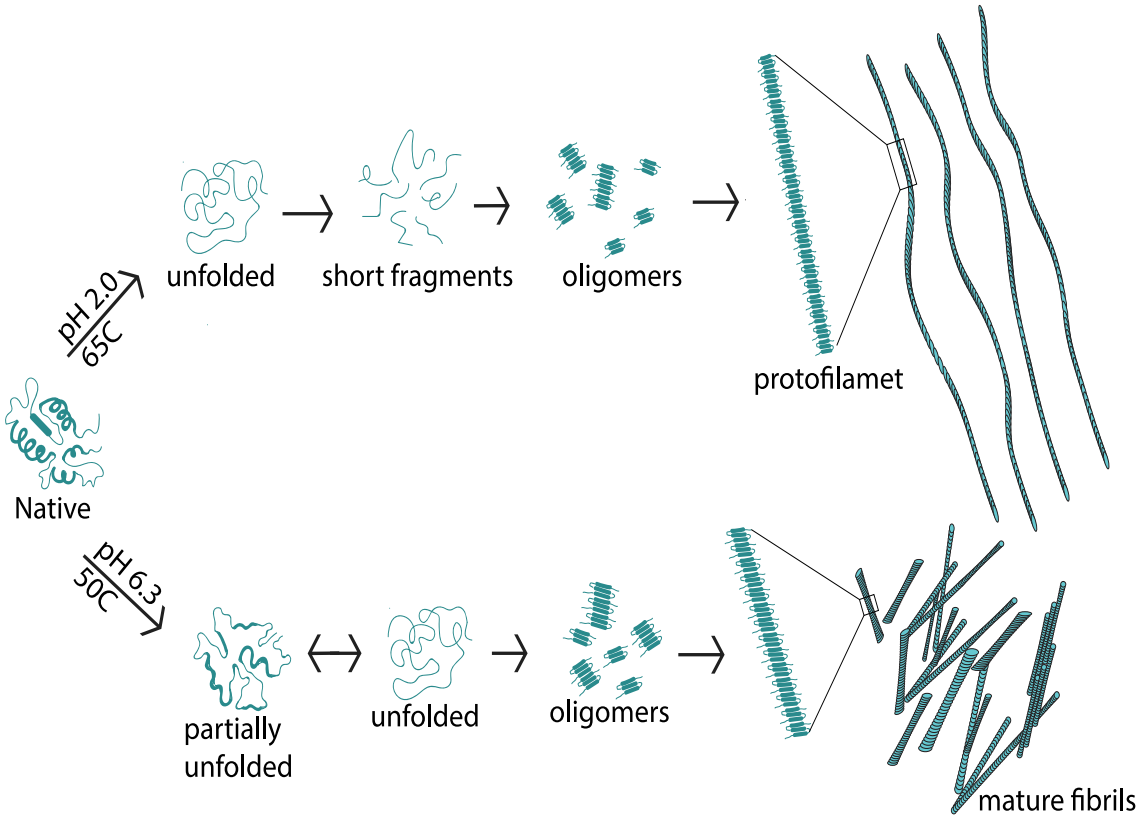


Figure 2.1 Fibril formation mechanism. Figure is adapted from (Adamcik & Mezzenga, 2012) and made by Adobe Illustrator software.

### 2.2.2 Preparation of fibril seeds

It is known that amyloid fibrils are resistant to protease digestion, or they get partially digested (Legname et al., 2004). In order to mimic food processing and body

conditions, sonication and protease treatment were used to form seeds for seeding reactions. Pre-formed fibrils were sonicated at room temperature using a Vibra-Cell VC-50 ultrasonic processor (Sonics & Materials Inc., Danbury CT, USA) with 50 W power, 20 kHz frequency fitted with a flat standard 2mm (5/64") titanium microtip probe. Experiments were performed at 20 kHz (VC50). The instrument power was set to 40% ultrasonic amplitude. Samples were sonicated for three pulses of 10 seconds, each followed by 5 seconds rest before the next pulse, to prevent overheating in a beaker with iced water (45 seconds total sonication time) (Sivalingam, Prasanna, Sharma, Prasad, & Patel, 2016).

### 2.2.3 Seeding and cross-seeding

All the seeding and cross-seeding experiments were conducted in a black Greiner-Bio CELLSTAR 96 Well Microplate, Tissue Culture Treated, with transparent clear bottom. The microplates were sealed with a black plastic film, incubated at 45℃ with 20 seconds of shaking every 10 minutes for ~20 days.

5% (m/v) seed were added to fresh protein solution for each seeded and cross-seeded experiments. The final volume in each 96-well microplate was 200 μL.

### 2.2.4 Thioflavin-T (ThT) assay

Formation of amyloid aggregates was detected by the increase in Thioflavin T (ThT) fluorescence intensity. Thioflavin-T was added to the samples to a final concentration of 20 μM. The measurements of ThT binding kinetics were performed in a 96-well plate using a SpectraMax Gemini EM Microplate Reader with dual monochromator spectrofluorometer. The excitation wavelength was fixed at 440 nm and

the emission recorded at 486 nm. The excitation and emission slits were adjusted to (EX<EM) of 9 nm. The temperature was set to 45℃, and the well plate was agitated for 20 seconds every 10 minutes. ThT gives off a much higher fluorescence intensity upon binding and intercalating with protein β-sheet structures, particularly amyloid-like fibril structures, and this method is widely used to study amyloid fibril formation (Biancalana & Koide, 2010). Multiple samples and conditions can be compared using a well plate-reading fluorescence spectrofluorometer. After visual inspection of the curves, the curves were fitted with OriginLab 2018 software by using the following equation $y = y_0 + A/(1 + \exp(-k(t - t_{0.5})))$. The lag phase, the rate constant, and the plateau determined the difference between the non-seeded, seeded and cross-seeded kinetics (Arosio, Knowles, & Linse, 2015). The lag phase was derived by using the following equation $t_{lag} = t_{0.5} - 1/2k$.

### 2.2.5 Microscopy (TEM, AFM)

Morphology and characteristics of the fibrils were evaluated using *transmission electron microscopy* (*TEM*) and *atomic-force microscopy* (*AFM*). A sequential two-droplet negative-staining method was used for TEM sample preparation. Samples were diluted in the MilliQ water (200 μg/mL protein concentration) to be studied under TEM (Grass, 2011). 5μL of a sample was placed on the 200-mesh copper Formvar/carbon-coated grids (TED PELLA, Inc.). After 5 minutes when the sample has partly dried, the grids were washed three times by 5μL ultra-pure water. Excess water was removed by touching the corner of the grid with filter paper. 5μL of 2% (w/v) Uranyl acetate solution, which is filtered through a 0.22 μm filter, was placed on the grid, after 30 seconds the

excess of Uranyl acetate was removed by retouching the edge of the grid by filter paper. After drying the grids at room temperature, grids were stored in a grid box, ready for TEM analysis with a JEOL JEM1011 transmission electron microscope (JEOL, Inc., Peabody, Massachusetts) at 80 kV with a high contrast 2k x 2k AMT mid-mount digital camera. This was done at the Georgia Electron Microscopy facility at the University of Georgia. Even though electron microscopy is unable to provide quantitative assessments of the fibrils, it is still an important technique to confirm that the aggregates formed are well-defined fibrils rather than amorphous aggregates.

AFM samples prepared at the concentration of 200 μg/mL were placed on a freshly cleaved mica surface, then washed three times with ultra-pure water. The samples were then dried at room temperature and stored inside a small Petri dish to be analyzed under AFM by our collaborators. An Agilent 5500 Controller combined with an Agilent multipurpose AFM scanner in tapping mode in the air was used to obtain the AFM images in Dr. Xu's lab.

### 2.2.6 SDS-PAGE

The Mini-PROTEAN Tetra Cell, Biorad PowerPac 1000 Electrophoresis Power Supply, 16.5% precast polyacrylamide gel (Mini-PROTEAN® Tris-Tricine Gel - 4563060), Tricine Sample Buffer (1610739), 10X Tris/Tricine/SDS Running Buffer (1610744), 2-Mercaptoethanol (1610710), Precision Plus Protein Standards, and Dual Color (1610374), were all purchased from Bio-Rad. The Spectra Multicolor Low Range Protein Ladder (26628) was purchased from ThermoFisher Scientific.

Fibril samples were isolated using 50 kDa spin filter, then diluted with an equivalent volume of tricine sample buffer containing 2% β-mercaptoethanol, and finally heated at 95℃ for 5 minutes. These samples were run through 16.5% Tris-Tricine Precast Gels at 100 V for 100 minutes, or till the dye reached the bottom of the gel. Since peptides are prone to diffuse and get lost during staining, gels were fixed by placing them in a fixative solution (40% methanol, and 10% acetic acid) for 30 minutes. Gels were stained for an hour in a staining solution (0.025% w/v Coomassie Blue G-250, 10% acetic acid). Gels were destained using a destain solution (10% acetic acid) three times for 15 minutes or until the desired background was achieved.

### 2.2.7 Mass Spectroscopy (MALDI-TOF)

Fibril samples were isolated via 50 kDa spin filter sent to PAMS (Proteomics and Mass Spectrometry) Core Facility at the University of Georgia. A Bruker Autoflex time-of-flight (TOF) mass spectrometer (Billerica, Massachusetts) was used to perform matrix-assisted laser desorption/ionization (MALDI). Samples were mixed with DHB matrix for analysis. This method was used to look at the peptide composition of the nanofibrils made under different solution condition.

### 2.2.8 *In vitro* pepsin digestion

The pepsin activity of the pepsin product (Sigma No.: P7000) employed here is rated at 250 U/mg powder. At the chosen concentration (0.05 mg/mL) this corresponds to 12.5 U/mL.

Measured levels of pepsin were found to be between 7-70 U/mL in undiluted stomach juice (without food) from healthy people (Ulleberg et al., 2011). ThT fluorescence during hydrolysis was monitored and compared to buffer controls (see Figure 5.7).

Lyophilized pepsin from porcine gastric mucosa with a nominal activity of 3200-4500 U/mg (SLBS5133) purchased from Sigma. A fresh stock solution of 6.25 mg/mL (25000 U/mL) porcine pepsin was made and 0.4 mL was added to 5 mL Simulated Gastric Fluid (SGF), pH 2.0 (adjusted with HCl), to achieve 2000 units of activity per milliliters (U/mL) in the final digestion mixture. The fresh stock solution was prepared before experiments and kept in ice water. The fibril samples were incubated with pepsin for 3 hours at 37℃, and aliquots were taken every 30 minutes between time 0 and 180 minutes. Pepsin digestion progression of fibrils was monitored by SDS-PAGE and decrease of ThT fluorescence intensity in the plate reader, and resulting samples were observed via TEM.

### 2.2.9 Data analysis

Data analysis was performed using ImageJ (TEM analysis), and OriginLab software (data plotting and fitting).

# CHAPTER 3

# 3 RESULTS

## 3.1 Comparing different conditions to induce HEWL fibril formation

It is reported in the literature that almost all proteins can form fibrils under the correct solution conditions (Chiti et al., 1999), such as protein concentration, presence of chemical denaturants and organic solvents, temperature and heating duration, pH value, agitation, stirring, salt concentration and type (Nicolai, Britten, & Schmitt, 2011; Pearce et al., 2007). Different solution conditions, such as buffers with various pH values, different protein concentration and temperature, gyration beads presence (steel and glass), agitation (shaking, stirring), and different seed concentrations were tested in either batch or well plate to get some preliminary data to find the best possible condition to form lysozyme fibrils for further seeding experiments.

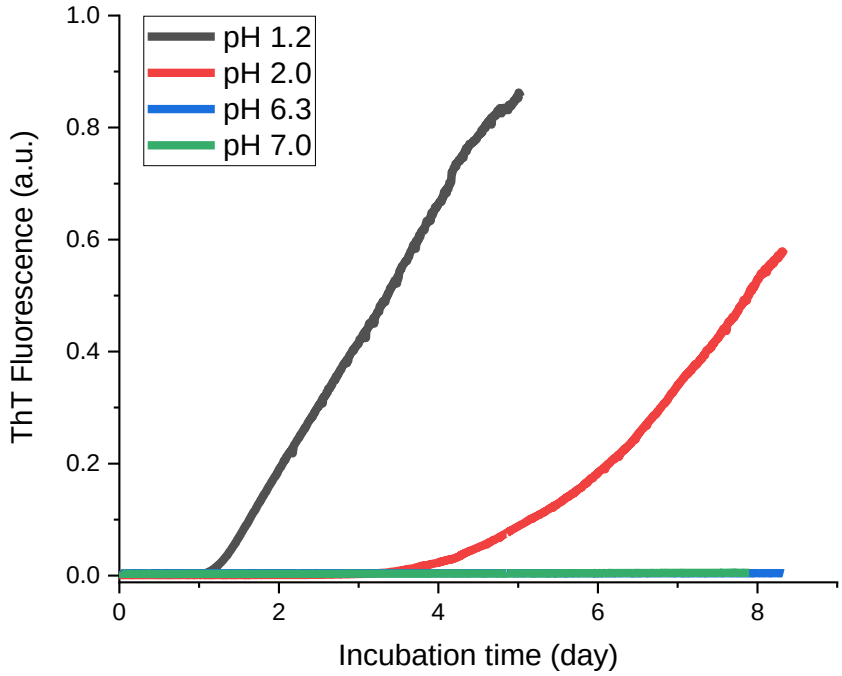


Figure 3.1 Effect of pH on inducing HEWL fibril formation.

In order to understand pH effect on fibrillation of HEWL, samples at 2 mg/mL concentration were incubated with agitation (20 s of shaking every 10 min) in different buffers with different pH values. The solution conditions were SGF at pH 1.2 ( 0.034 M NaCl), 50 mM Glycine-HCl buffer of pH 2.0, 20 mM potassium phosphate of pH 6.3, and 50mM sodium phosphate buffer of pH 7.0 at 45°C. Samples were mixed with 20 µM Thioflavin-T and ThT fluorescence emission intensity was collected every 10 minutes for nine days at 486 nm upon excitation at 440 nm using a Molecular Devices SpectraMax Gemini EM plate reader. Fluorescence was normalized to 0-1. The results suggested that HEWL aggregates faster at pH 1.2 compared to pH 2.0, while the aggregation was delayed significantly at pH 6.3 and 7.0.

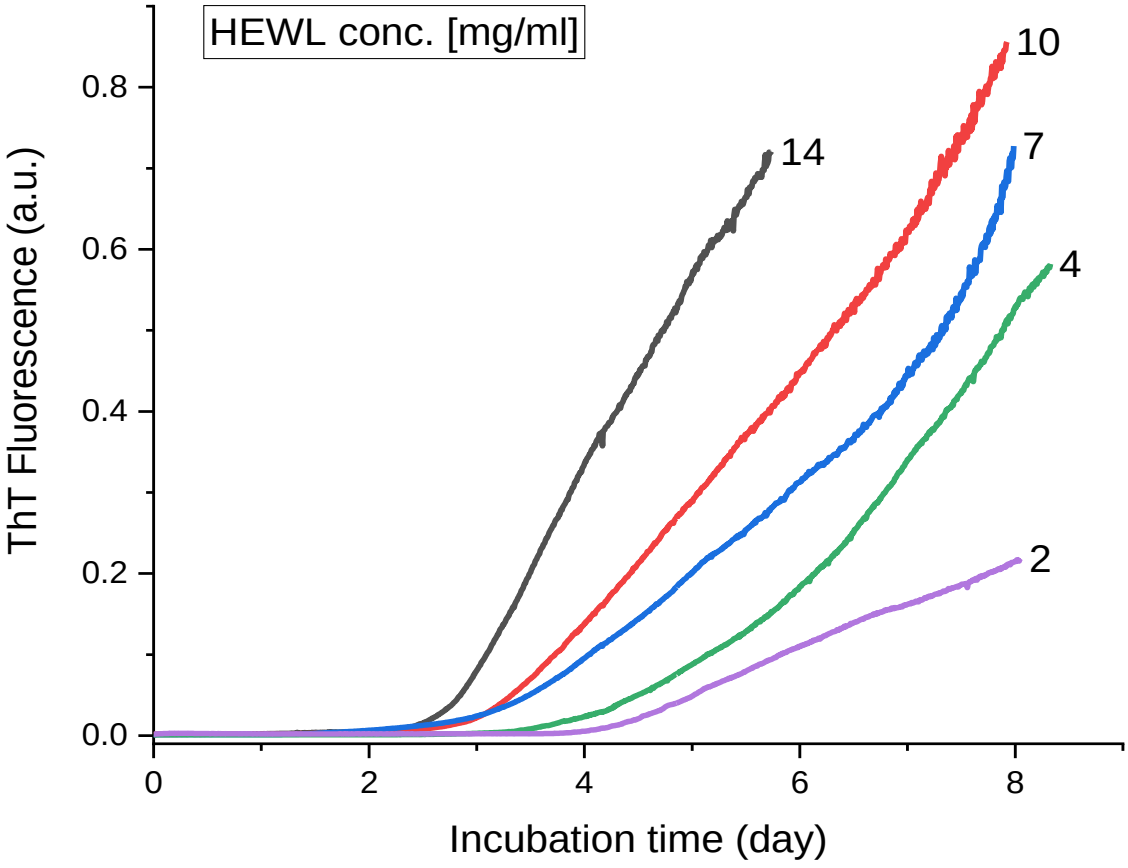


Figure 3.2 Effect of protein concentration on inducing HEWL fibril formation.

In order to study effect of protein concentration on fibril formation of HEWL, samples at different protein concentrations (14, 10, 7, 4, and 2 mg/mL) were incubated at pH 2.0, 45℃. Samples were mixed with 20 µM Thioflavin-T and ThT fluorescence emission intensity were collected every 10 minutes for eight days at 486 nm upon excitation at 440 nm using Molecular Devices SpectraMax Gemini EM plate reader. Fluorescence was normalized to 0-1. The results suggested that a higher protein concentration accelerates the aggregation rate and reduces the lag phase, and HEWL fibrillation was concentration dependent.

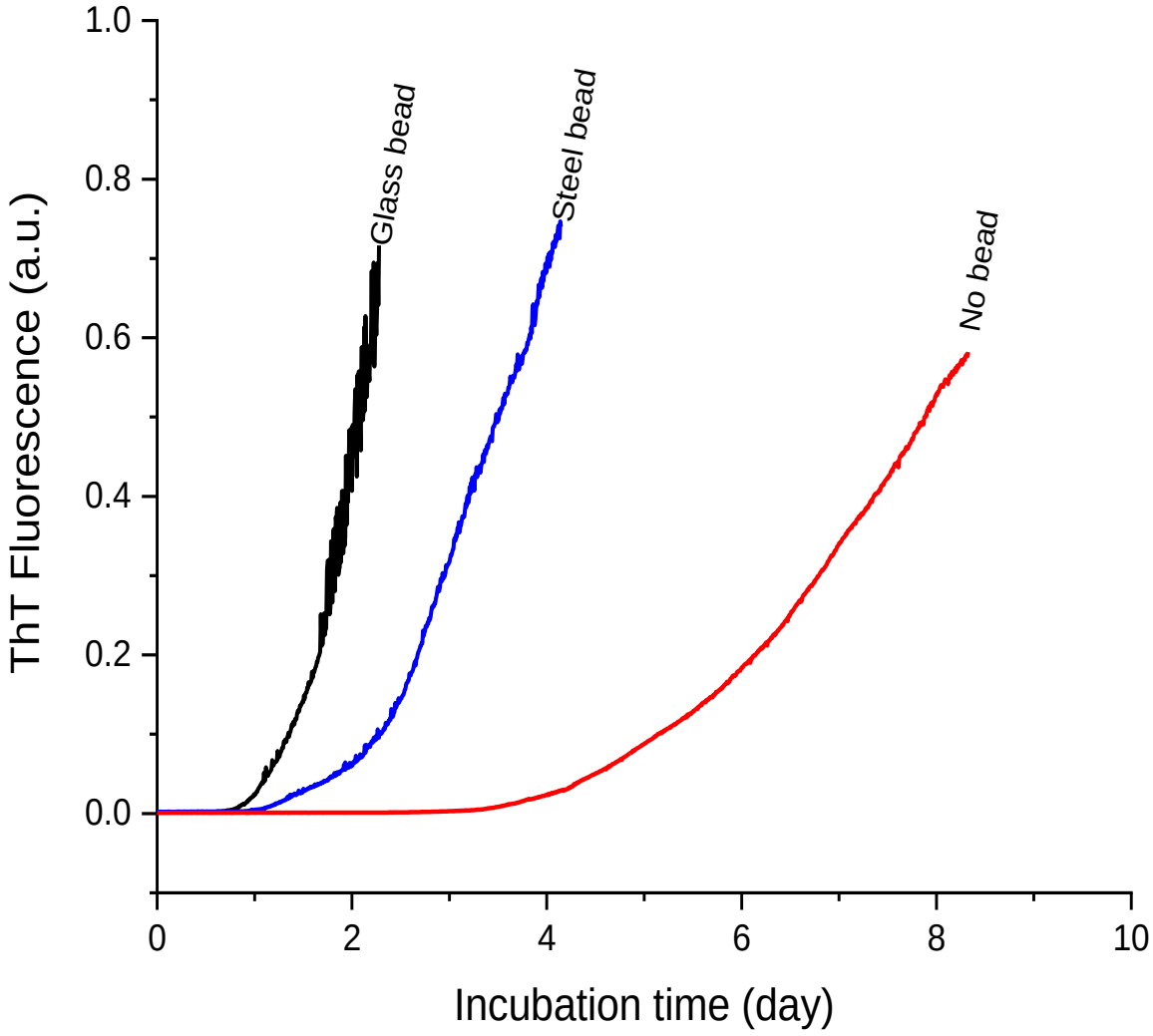


Figure 3.3 Effect of gyration beads on inducing HEWL fibril formation.

In order to understand the effect of gyration beads in the solution, glass and steel beads were added in each well of 2 mg/mL HEWL samples at pH 2.0, 45℃. Samples were mixed with 20 µM Thioflavin-T and ThT fluorescence emission intensity were collected every 10 minutes for eight days at 486 nm upon excitation at 440 nm using Molecular Devices SpectraMax Gemini EM plate reader. Fluorescence was normalized to

0-1. The results suggested that HEWL aggregates faster in the presence of glass beads compared to stainless steel beads.

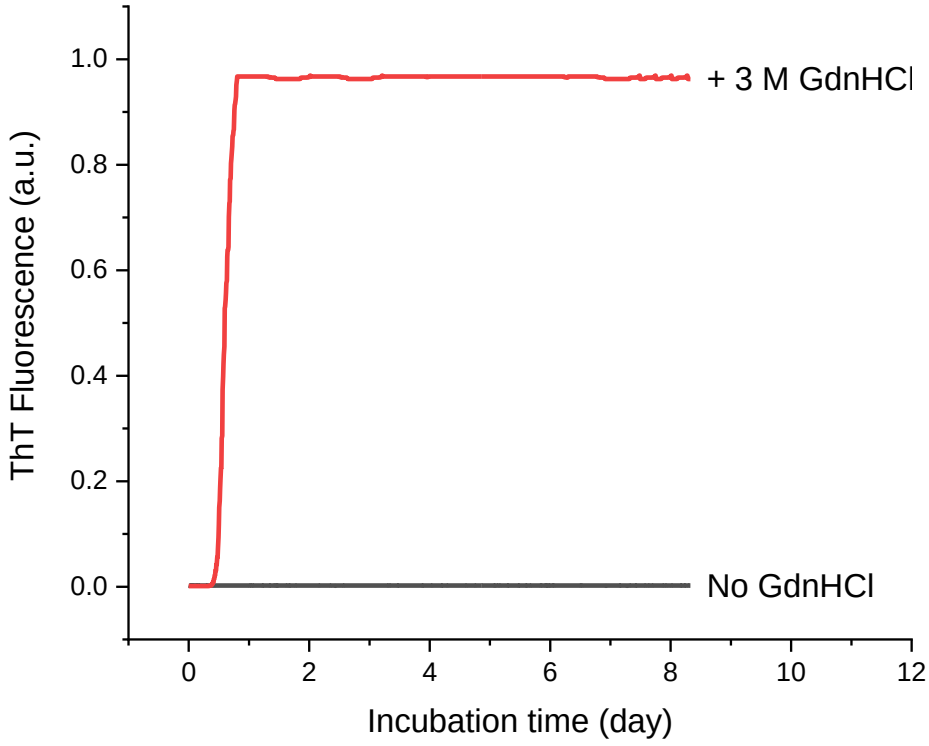


Figure 3.4 Effect of GdnHCl on HEWL amyloid formation.

In order to study effect of chemical denaturants in the solution. GdnHCl was added to the solution. Aggregation kinetics of HEWL in 20 mM potassium phosphate buffer of pH 6.3 with agitation (10s of shaking every 10 min) was followed by ThT fluorescence on a plate reader. Fluorescence was normalized to the value of the plateau phase in each reaction. The results suggested that the presence of GdnHCl accelerates the

HEWL fibrillation rate and reduces the lag phase, due to partially denaturing and unfolding the protein.

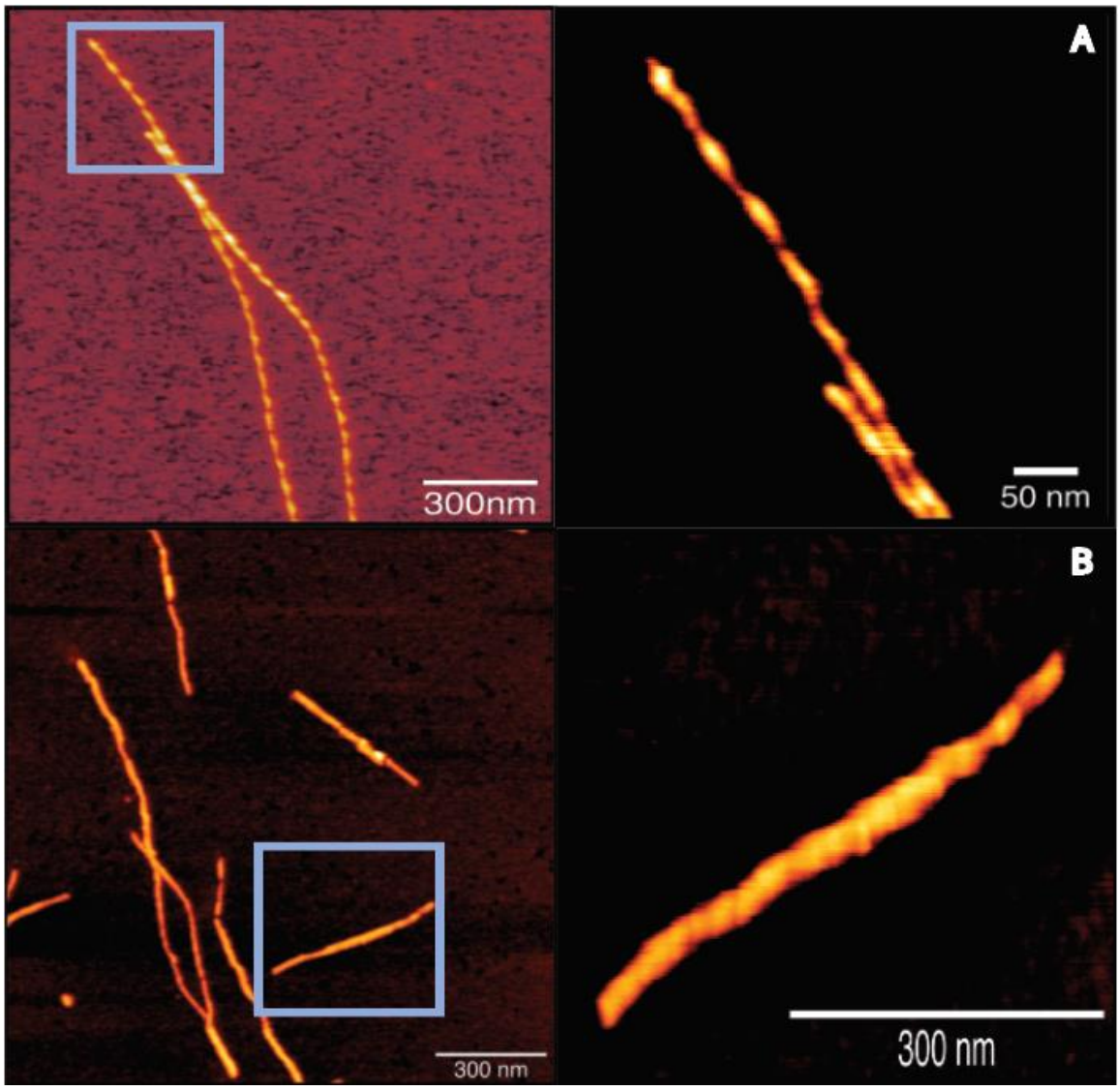


Figure 3.5 Effect of incubation temperature and shaking on the morphology of HEWL fibrils from the batch mode. HEWL incubated at pH 2.0, 45℃ with no agitation for seven days (A). HEWL incubated at pH 2.0, 65℃ with 300 rpm shaking for seven days (B). An Agilent 5500 Controller combined with an Agilent multipurpose AFM scanner was used to obtain the AFM images. The results suggested that different solutions and incubation

conditions can result in the formation of different polymorphs with different characteristics.

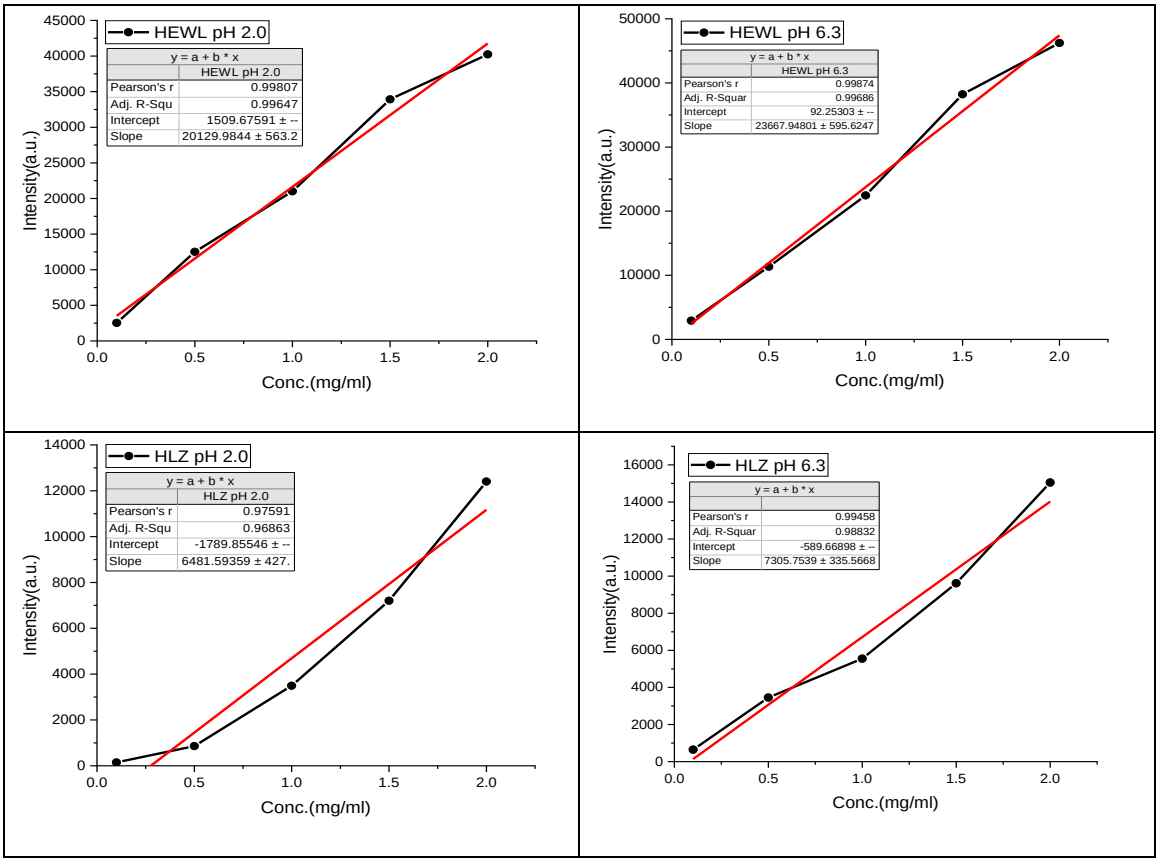

Figure 3.6 Effect of fibril concentration on ThT fluorescence intensity.

To compare fibril concentration and ThT fluorescence intensity, fibrils after formation were diluted based on their monomer concentration between 0.1 mg/ml and 1.5 mg/ml and confirmed using absorbance at 280 nm. The results (see Figure 3.6) suggested that there was a linear correlation between fibril concentration and ThT intensity, and there was a large species affect between HEWL and HLZ.

### 3.2 Formation of fibrils to be used as seeds and seed formation

HEWL and HLZ fibril formation was carried out as explained in (Section 2.2.1) at two different pH values: HEWL 2.0 and HLZ 2.0 in a buffer at pH 2.0, which represent the unfolding-fragmentation-fibrillation model (strongly destabilizing condition), and HEWL 6.3 and HLZ 6.3 at pH 6.3 buffer containing GdnHCl, which represents nucleation-elongation model (moderate, more physiological condition). In unfolding-fragmentation-fibrillation model the formation of fibrils was associated with at least partially unfolding, and acid hydrolysis at pH 2.0 and the fibrillization was carried out at a temperature close to midpoint of thermal denaturation at 65°C (Burova, Grinberg, Grinberg, Rariy, & Klibanov, 2000) in order to limit complete denaturation of the protein. In nucleation-elongation model the fibril formation is associated with the formation of partially unfolded species in the presence of 3 M GdnHCl which is a chemical denaturant, and the fibrillization was carried out at a temperature lower than the midpoint of thermal denaturation at 50°C to limit complete unfolding of the protein (Vernaglia, Huang, & Clark, 2004). ThT fluorescence was measured during incubation, and for characterization purposes, the fibrils were negatively stained with uranyl acetate and analyzed either by transmission electron microscopy (TEM), or fibrils placed on a fresh cleaved mica surface and analyzed by atomic force microscopy (AFM) (Section 2.2.5). ImageJ software was used for further analysis (http://rsb.info.nih.gov/ij/). Increase in the ThT fluorescence intensity, and electron microscopy confirmed the amyloid formation of the HEWL 2.0 (see Figure 3.7), HLZ 2.0 (see Figure 3.9), HEWL 6.3 (see Figure 3.8), and HLZ 6.3 (see Figure 3.10).

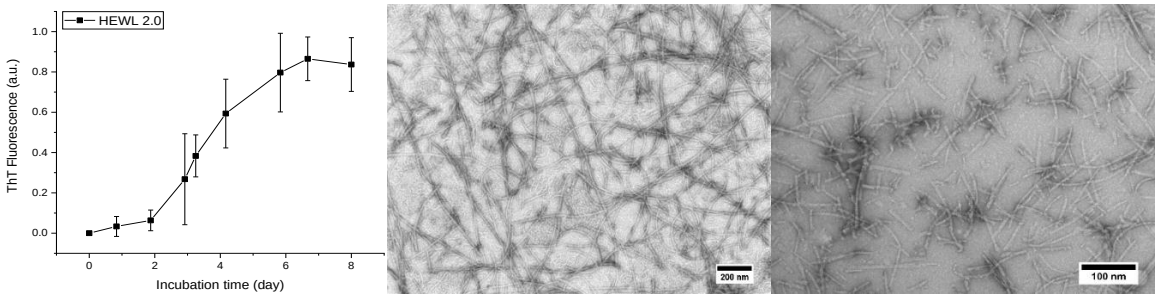


Figure 3.7 Kinetics and TEM images of HEWL 2.0 amyloid formation under conditions used to make seeds. Seeds were made from preformed fibrils. HEWL samples at 1μM concentration in 50 mM Glycine-HCl buffer of pH 2.0, were incubated at 65℃ with 300 rpm shaking for seven days. Fluorescence was normalized to the value of the plateau phase in each reaction. Data points correspond to the average ± standard deviation of three replicates. HEWL 2.0 fibrils before sonication (left). HEWL 2.0 fibrils after sonication of three pulses of 10 seconds followed by 5 seconds rest (right).

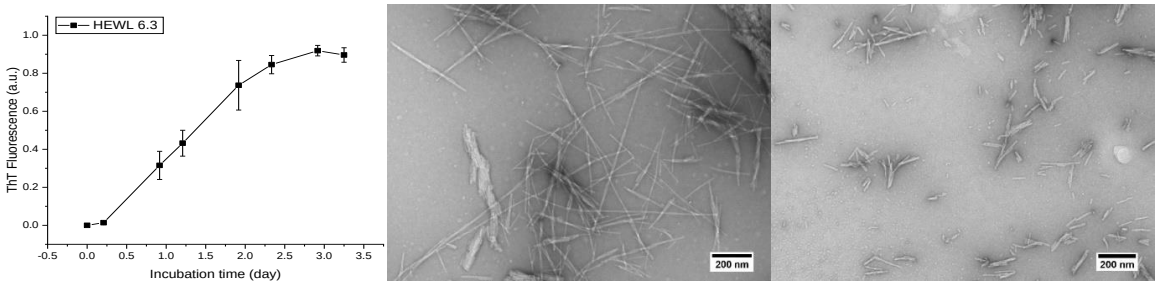


Figure 3.8 Kinetics and TEM images of HEWL 6.3 amyloid formation under conditions used to make seeds. Seeds were made from preformed fibrils. HEWL samples at 1 μM concentration in 20 mM potassium phosphate (K-Phos) pH 6.3 buffer with 3M Guanidine hydrochloride, were incubated at 50℃ with 300 rpm shaking for three days. Fluorescence was normalized to the value of the plateau phase in each reaction. Data points correspond

to the average ± standard deviation of three replicates. HEWL 6.3 fibrils before sonication (left). HEWL 6.3 fibrils after sonication of three pulses of 10 seconds followed by 5 seconds rest (right).

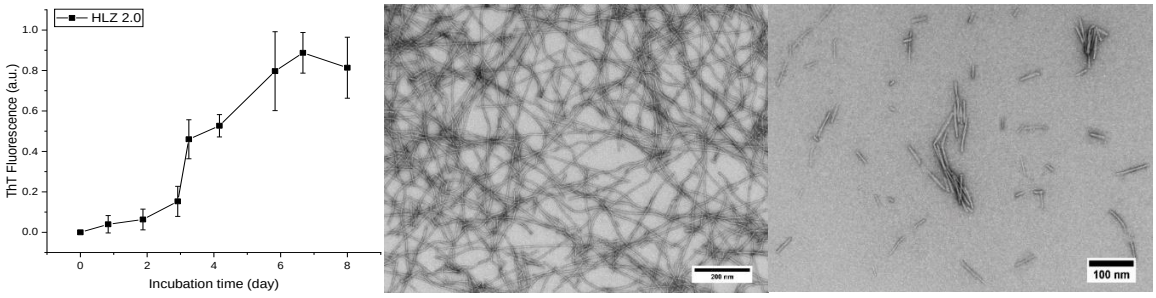


Figure 3.9 Kinetics and TEM images of HLZ 2.0 amyloid formation under conditions used to make seeds. Seeds were made from preformed fibrils. HLZ samples at 1 µM concentration in 50 mM Glycine-HCl pH 2.0 buffer, were incubated at 65°C with 300 rpm shaking for seven days. Fluorescence was normalized to the value of the plateau phase in each reaction. Data points correspond to the average ± standard deviation of three replicates. HLZ 2.0 fibrils before sonication (left). HLZ 2.0 fibrils after sonication for three pulses of 10 seconds followed by 5 seconds rest (right).

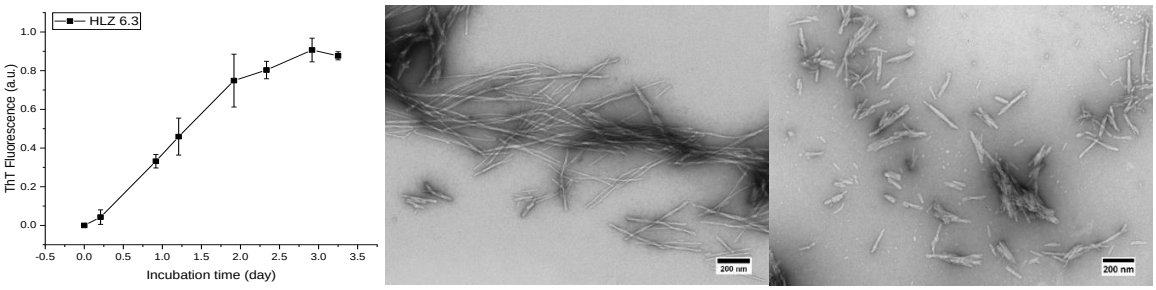


Figure 3.10 Kinetics and TEM images of HLZ 6.3 amyloid formation under conditions used to make seeds. Seeds were made from preformed fibrils. HLZ samples at 1 µM concentration in 20 mM potassium phosphate (K-Phos) pH 6.3 buffer with 3M Guanidine

hydrochloride, were incubated at 50°C with 300 rpm shaking for three days. Fluorescence was normalized to the value of the plateau phase in each reaction. Data points correspond to the average ± standard deviation of three replicates. HLZ 6.3 fibrils before sonication (left). HLZ 6.3 fibrils after sonication of three pulses of 10 seconds followed by 5 seconds rest (right).

### 3.3 Amyloid assembly kinetics of unseeded, self-seeded, cross-seeded, polymorph seeded, and cross-polymorph-seeded

The kinetics of fibril formation of unseeded, self-seeded, cross-seeded, polymorph seeded, and cross-polymorph-seeded (double seeded-species and polymorphs) were studied by utilizing ThT assay to monitor the process of amyloid polymerization in greater detail. The sigmoidal shape of the fibrillization curves collected for both fibril models from HEWL and HLZ have a classic lag phase which is eliminated by self-seeding, led to the nucleation-dependent polymerization in which the formation of nuclei is crucial for the process to begin. However, the representative traces presented in (see Figure 3.11) shows the differences in the duration of the lag phase, the slope of the growth phase and the plateau. HEWL 2.0 and HLZ 2.0 demonstrated a more extended lag phase, a less steep increase in fluorescence intensity in the growth phase, while HEWL 6.3 and HLZ 6.3 demonstrated a shorter lag phase and a steep rise in fluorescence intensity in the growth phase. These findings imply that under different pH conditions, various amyloid intermediates could form and that could result in variations in the morphologies of the amyloid fibrils.

All seeding experiments were examined by addition of 5% (m/v) pre-formed and sonicated HEWL 2.0, HEWL 6.3, HLZ 2.0, and HLZ 6.3 into the monomeric HEWL, or HLZ, solubilized in the aggregation buffers of pH 2.0, or pH 6.3 containing 3M GdnHCl at 45℃, with agitation (20s shaking every 10 min). In every experiment, the seed-free sample was used as a reference for comparison. Fitting was done on the kinetic curves of fibril formation to obtain the lag phase, half time, and growth rate using the following equation, $y= y_0+A/(1+\exp(-k*(t-t_{0.5})))$, where $y_0$ was the initial value, A was the amplitude of growth, k was the growth rate, and $t_{0.5}$ was the half time. Lag time was derived using the following equation, $t_{lag} = t_{0.5} - (1/2)\ k$. In some samples, lag time was measured by extrapolating the growth rate with pre-transition base-line (see Figure 3.12). ThT fluorescence intensity was normalized to the value of the plateau phase in each reaction.

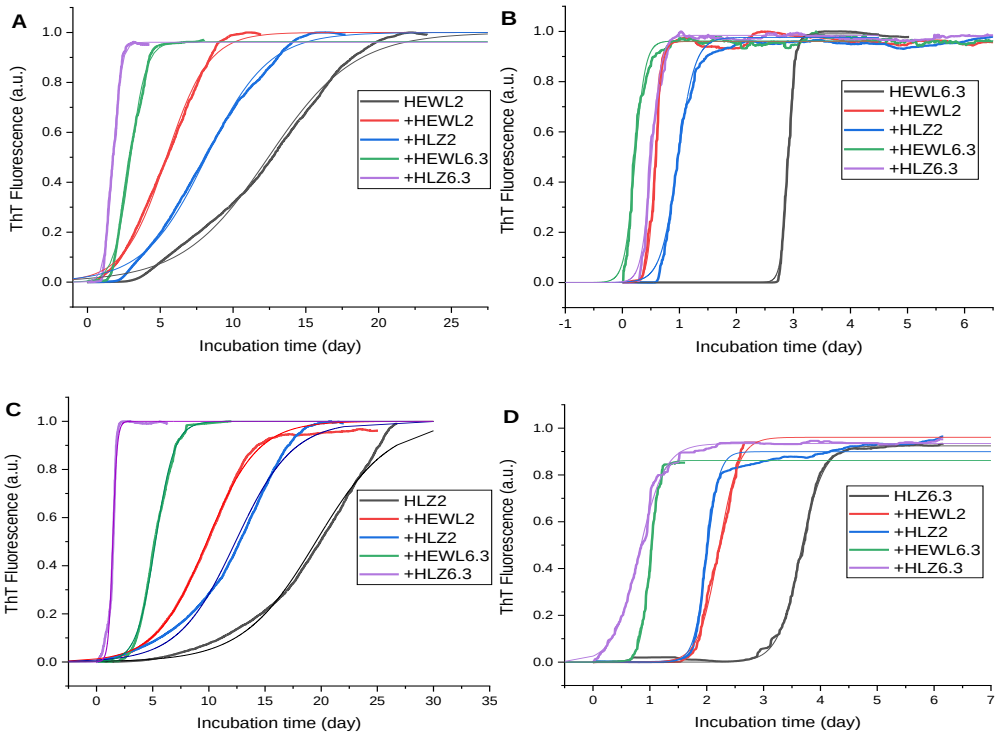

Figure 3.11 Fitted curves of representative traces of fibril formation. HEWL fibril seeds (5% w/w) cross-seeded HLZ, and conversely, HLZ fibril seeds (5% w/w) cross-seeded HEWL. In general fibrillation was faster in pH 6.3 condition in comparison to pH 2.0 condition.

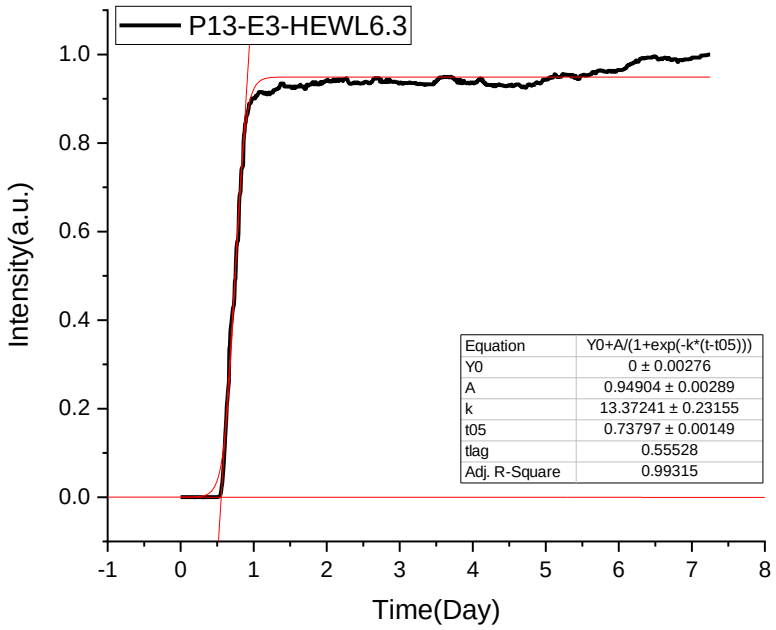


Figure 3.12 Determination of lag time ($t_{lag}$) by extrapolating the growth rate (k) with pre-transition base-line ($y_0$). The lag phase was determined by extrapolating the base line with growth rate in each kinetic curve in order to confirm accurate calculation.

Table 3.1 Fit parameters of seed free, seeded, cross-seeded, polymorph seeded, cross-polymorph seeded samples. The number of total replicates (N) was ranging from 11 and 25 depending on the different solution conditions. In general, unseeded reactions had larger lag time in comparison with seeded or cross-seeded reactions. pH 6.3 condition had shorter lag time and larger growth rate in comparison with pH 2.0 condition which was slower and had longer lag time.

| **Sample** | **N total** | **Lag time (day)** | **Half time (day)** | **Rate** |
|---|---|---|---|---|
| **HEWL 2.0** | 15 | 3.38 ± 0.38 | 12.16 ± 0.96 | 0.32 ± 0.03 |
| **HEWL 2.0 + HEWL 2.0** | 21 | 0.39 ± 0.54 | 2.90 ± 1.18 | 0.90 ± 0.45 |
| **HEWL 2.0 + HLZ 2.0** | 12 | 2.63 ± 0.71 | 6.87 ± 0.69 | 0.58 ± 0.14 |
| **HEWL 2.0 + HEWL 6.3** | 19 | 1.70 ± 0.41 | 2.85 ± 0.73 | 4.21 ±4.08 |
| **HEWL 2.0 + HLZ 6.3** | 18 | 1.32 ± 0.41 | 2.26 ± 0.43 | 3.41 ± 1.29 |
| **HLZ 2.0** | 11 | 11.81 ± 1.71 | 19.53 ± 0.58 | 0.27 ± 0.03 |
| **HLZ 2.0 + HEWL 2.0** | 12 | 2.90 ± 2.66 | 5.58 ± 4.58 | 1.08 ± 0.69 |
| **HLZ 2.0 + HLZ 2.0** | 14 | 9.57 ± 1.14 | 14.60 ± 1.45 | 0.37 ± 0.03 |
| **HLZ 2.0 + HEWL 6.3** | 17 | 2.64 ± 0.49 | 4.53 ± 0.86 | 1.45 ± 0.91 |
| **HLZ 2.0 + HLZ 6.3** | 17 | 2.30 ± 0.86 | 3.99± 1.81 | 2.37 ± 1.93 |

| | | | | |
|---|---|---|---|---|
| **HEWL 6.3** | 25 | 1.16 ± 0.85 | 1.29± 0.84 | 20.22 ± 4.85 |
| **HEWL 6.3 + HEWL 2.0** | 18 | 0.28 ± 0.11 | 0.46 ± 0.09 | 16.79 ± 4.45 |
| **HEWL 6.3 + HLZ 2.0** | 18 | 0.61 ± 0.28 | 0.79 ± 0.29 | 16.19 ± 6.17 |
| **HEWL 6.3 + HEWL 6.3** | 18 | 0.11 ± 0.05 | 0.35 ± 0.08 | 9.84 ± 3.44 |
| **HEWL 6.3 + HLZ 6.3** | 17 | 0.44 ± 0.25 | 0.68 ± 0.14 | 15.65 ± 9.27 |
| **HLZ 6.3** | 16 | 1.60 ± 0.81 | 1.96 ± 0.89 | 8.43 ± 3.12 |
| **HLZ 6.3 + HEWL 2.0** | 16 | 2.13 ± 0.94 | 2.60 ± 0.99 | 5.53 ± 1.79 |
| **HLZ 6.3 + HLZ 2.0** | 17 | 1.97 ± 0.89 | 2.30 ± 0.91 | 7.81 ± 2.07 |
| **HLZ 6.3 + HEWL 6.3** | 16 | 1.26 ± 0.38 | 1.67 ± 0.51 | 7.37 ± 4.29 |
| **HLZ 6.3 + HLZ 6.3** | 15 | 0.73 ± 0.92 | 1.35 ± 0.78 | 4.72 ± 2.06 |

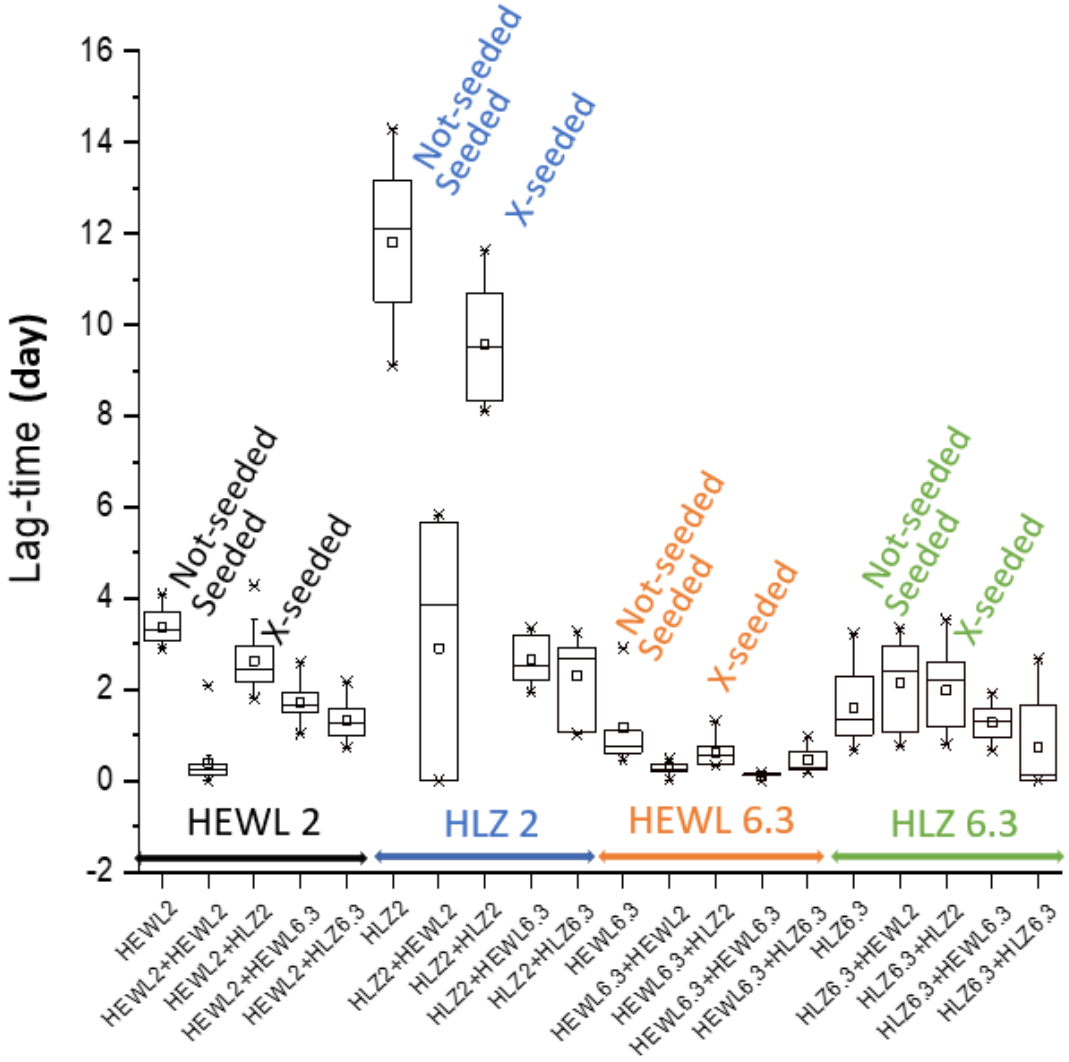


Figure 3.13 Boxplot of lag time. Lag time was ranging from hours to days depending on the solution conditions. HLZ 2.0 had the longest lag time. In general, seeded and cross-seeded reactions had shorter lag time in comparison with unseeded reactions.

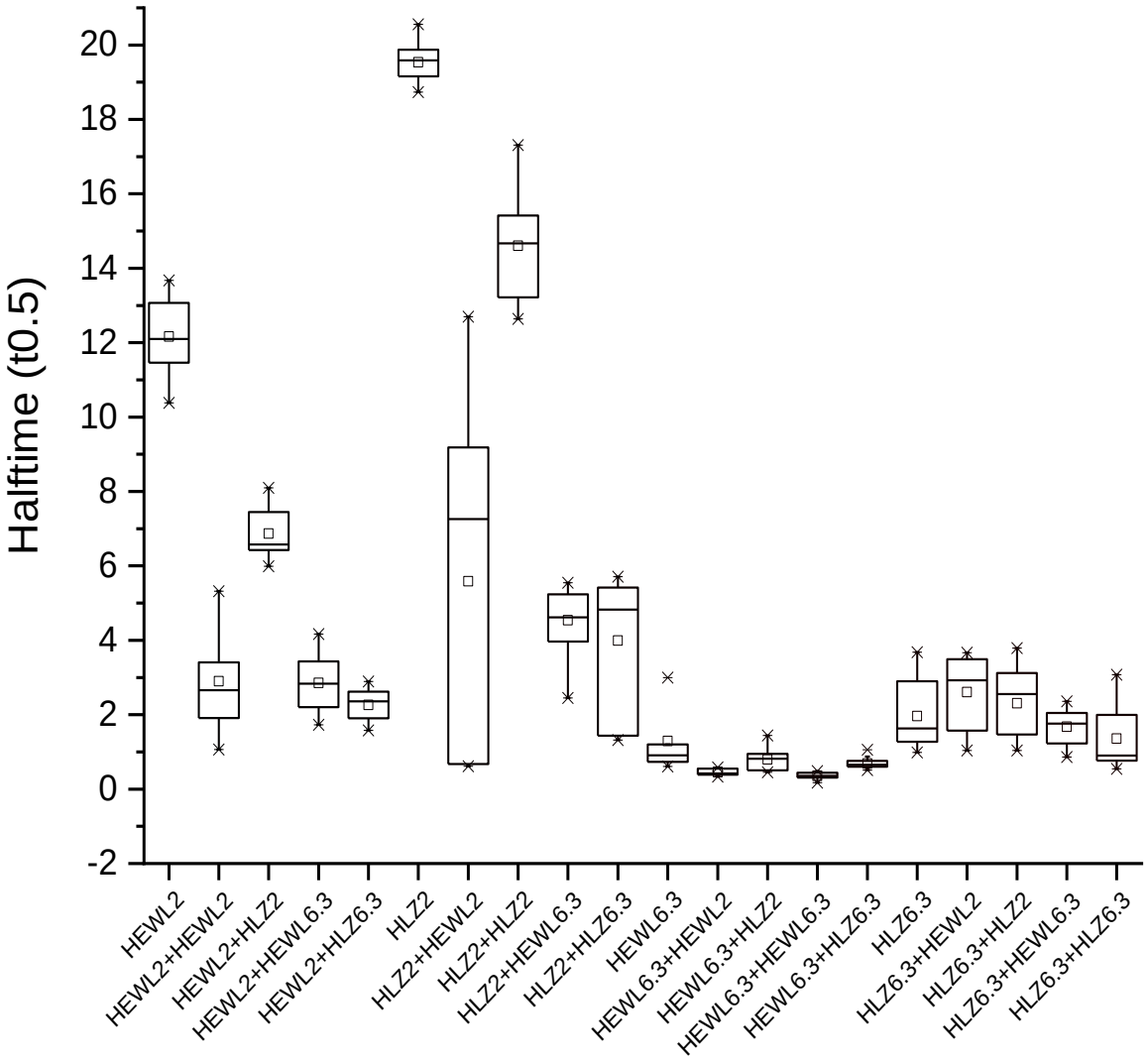


Figure 3.14 Boxplot of halftime (days). Half time results were similar to lag time, ranging from days to weeks depending on the solution condition of unseeded and seeded reactions. In general pH 6.3 conditions had shorter half time in comparison with pH 2.0 conditions.

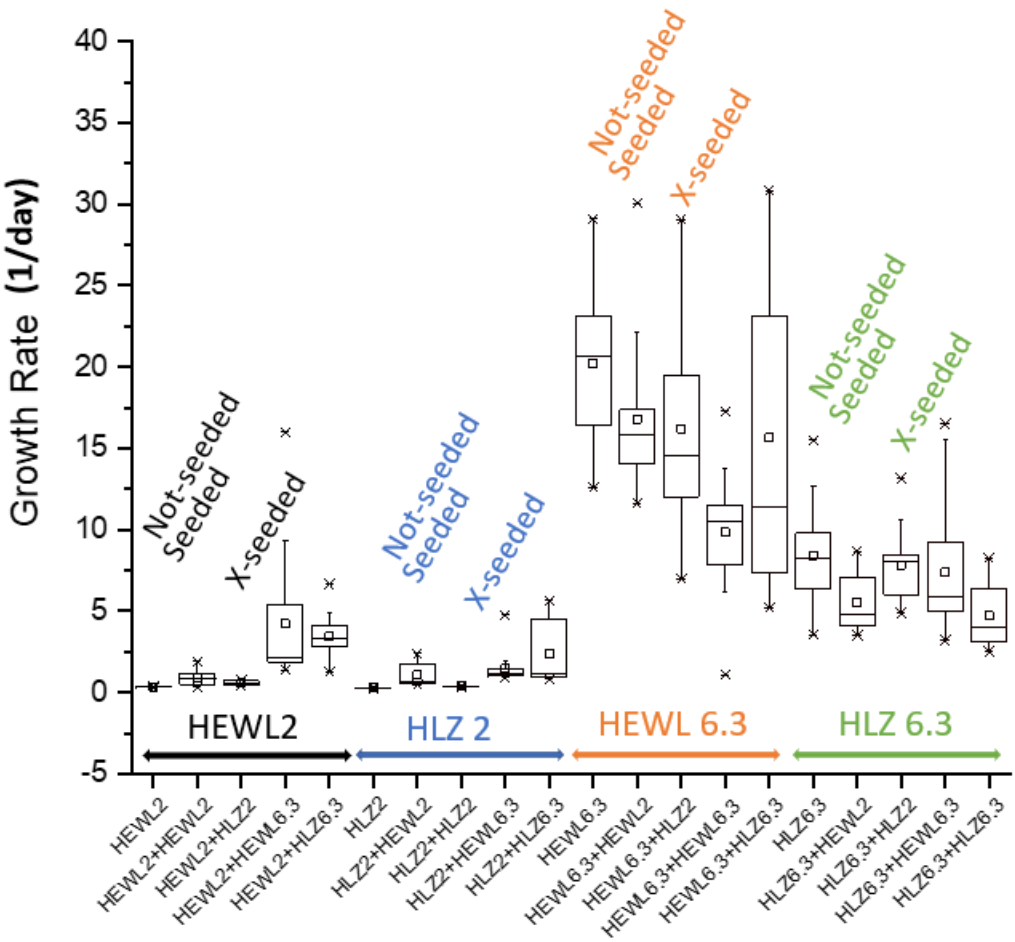


Figure 3.15 Boxplot of growth rate. pH 2.0 conditions growth rate was slower in comparison with pH 6.3 conditions. pH 6.3 showed much faster fibrillation in both unseeded and seeded reactions. Conversely pH 2.0 conditions were very slow even when seeded.

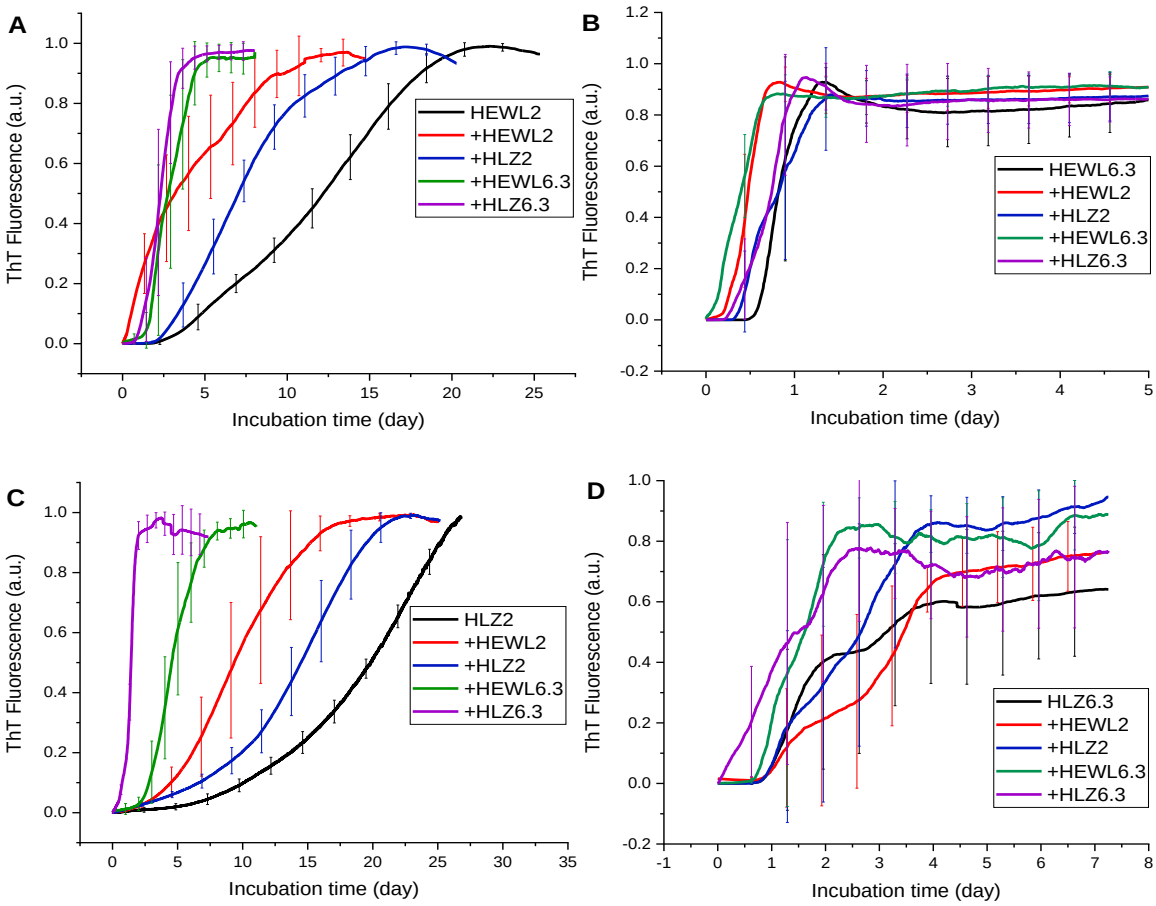


Figure 3.16 Effect of seeding on the kinetics of fibril formation.

The error bars represent the average deviation of multiple independent measurements (N between 11 and 25). Monomeric HEWL at a concentration of 2 mg/mL solubilized at 50 mM Gly-HCl buffer of pH 2.0, seed free, seeded with pre-formed HEWL 2.0, cross-seeded with HLZ 2.0, polymorph seeded with HEWL 6.3, and cross-polymorph seeded with HLZ 6.3 (A). Monomeric HEWL at a concentration of 2 mg/mL solubilized at 20 mM potassium phosphate buffer of pH 6.3 containing 3 M GdnHCl, seed free, seeded with pre-formed HEWL 6.3, cross-seeded with HLZ 6.3, polymorph seeded with HEWL 2.0, and cross-polymorph seeded with HLZ 2.0 (B). Monomeric HLZ at a concentration

of 2 mg/mL solubilized at 50 mM Gly-HCl buffer of pH 2.0, seed free, seeded with pre-formed HLZ 2.0, cross-seeded with HEWL 2.0, polymorph seeded with HLZ 6.3, and cross-polymorph seeded with HEWL (C). Monomeric HLZ at a concentration of 2 mg/mL solubilized at 20 mM potassium phosphate buffer of pH 6.3 containing 3 M GdnHCl, seed free, seeded with pre-formed HLZ 6.3, cross-seeded with HEWL 6.3, polymorph seeded with HLZ 2.0, and cross-polymorph seeded with HEWL 2.0. 6.3 (D). All reactions were incubated at 45℃ agitated by 20 seconds shaking every 10 minutes and monitored by ThT fluorescence. The results suggested that HEWL and HLZ pH 6.3 seeds accelerate the aggregation rate of HEWL and HLZ compared to pH 2.0 seeds. In aggregation buffer of pH 6.3 containing 3 M GdnHCl, all reactions were faster, and seeding had less effect on lag phase compared to pH 2.0 condition.

The plateau level of thioflavin-T fluorescence before normalization was higher in the pH 6.3 condition, compared to the pH 2.0 condition of human lysozyme and hen egg-white lysozyme. This indicated that a larger number of fibrils was formed in the pH 6.3 condition relative to the pH 2.0 condition. pH 6.3 condition showed a smaller lag phase, and a higher plateau level of ThT fluorescence, relative to pH 2.0, indicating that pH 6.3 condition was a better condition to form fibrils. pH 6.3 polymorph was the most efficient seed, even at pH 2.0 conditions, and HLZ pH 6.3 seed was the most potent seed.

### 3.4 Polymorphs

The TEM results suggested that morphological variability of lysozyme fibrils from hen egg-white (HEWL) monomer, and human (HLZ) monomer are evident. The electron microscopy and atomic force microscopy results showed that fibrils differ in

their length, width, and twist. Fibrils displayed, in both cases, a fibrillar and unbranched morphology. pH 2.0 polymorphs are long, curved, while pH 6.3 polymorph are short, rigid, and straight. The structural characteristics of amyloid fibrils produced under two different experimental conditions (acidic and neutral) were assessed by spectroscopic methods, electron microscopy, and image analysis. Results showed that the fluorescence intensity of ThT did not increase in the presence of monomeric lysozyme. This was consistent with the fact that ThT does not interact or bind with globular proteins in the native state (Nilsson et al., 2004). The results suggested that the pH 2.0 polymorph consists of intact and hydrolyzed protein, while the pH 6.3 polymorph contains only intact lysozyme (see Figure 3.18). Native lysozyme was used as a reference.

HEWL and HLZ have a molecular weight of 14.3 kDa and 14.7 kDa, respectively. No bands of larger protein aggregates were observed, suggesting that fibril formation does not require covalent bonds (*e.g.*, disulfide bonds), but contains hydrogen bonds, which were broken down by heating in the presence of SDS (Arnaudov & De Vries, 2005). MALDI-TOF results confirmed the SDS results, indicating that fibrils made at pH 2.0 and pH 6.3 differ in composition. The pH 2.0 polymorph consists of intact and hydrolyzed protein, while the pH 6.3 polymorph contains only intact lysozyme (see Figure 3.19). Native lysozyme was used as a reference.

Using hen egg-white lysozyme and human lysozyme, cross-seeding and cross-polymorph-seeding under various solution conditions were observed. Results suggested that the pH 6.3 polymorph was dominant for both species, even at pH 2, as it maintained

and self-propagated its unique fibril structure when used to seed lysozyme solutions at pH 2.0.

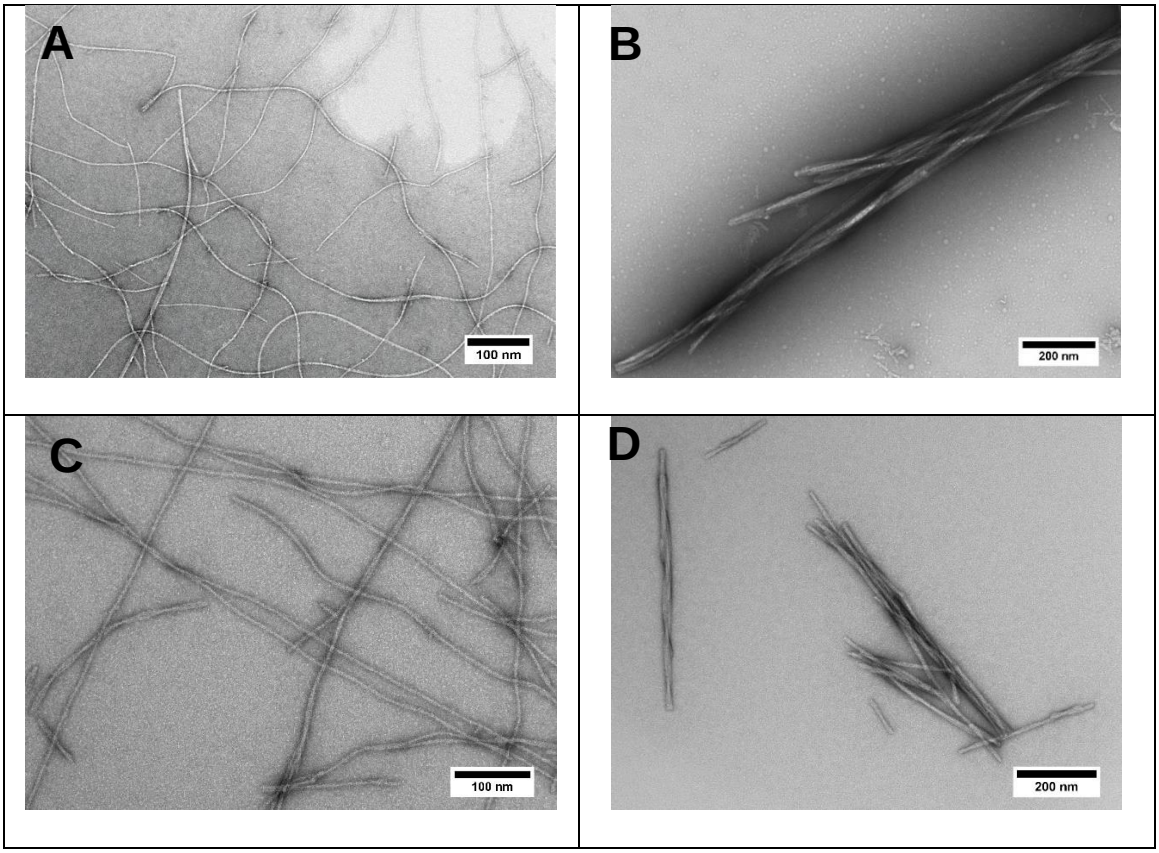


Figure 3.17 HEWL and HLZ polymorphs. Polymorphs exist, two amyloid-like fibril polymorphs of lysozyme were created at pH 2.0 and pH 6.3 from both HEWL and HLZ, and they look different under TEM. pH 2.0 Polymorph; HEWL (A), and HLZ (C). pH 6.3 Polymorph; HEWL (B), HLZ (D).

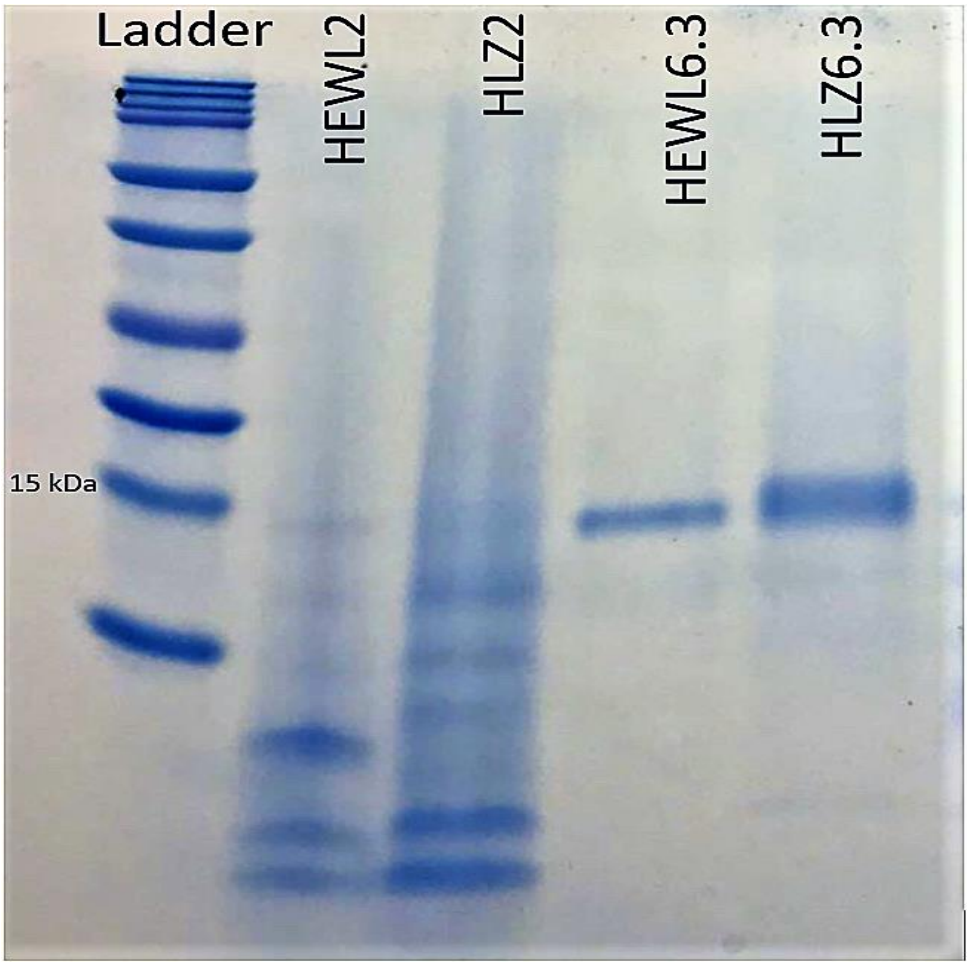


Figure 3.18 SDS-PAGE. HEWL and HLZ at pH 2.0,65℃, and pH 6.3, 50℃. Fibril samples were isolated using 50 kDa spin filter, then diluted with an equivalent volume of tricine sample buffer containing 2% β-mercaptoethanol, and finally heated at 95℃ for 5 minutes. These samples were run through 16.5% Tris-Tricine Precast Gels at 100 V for 100 minutes, or till the dye reached the bottom of the gel. pH 2.0 fibril polymorph was composed of intact and hydrolyzed protein, while pH 6.3 fibril polymorph was composed of only intact protein. Molecular weight of HEWL and HLZ were 14.3 kDa, and 14.7 kDa respectively. Larger protein bands than 14.7 kDa in the SDS gels were not visible.

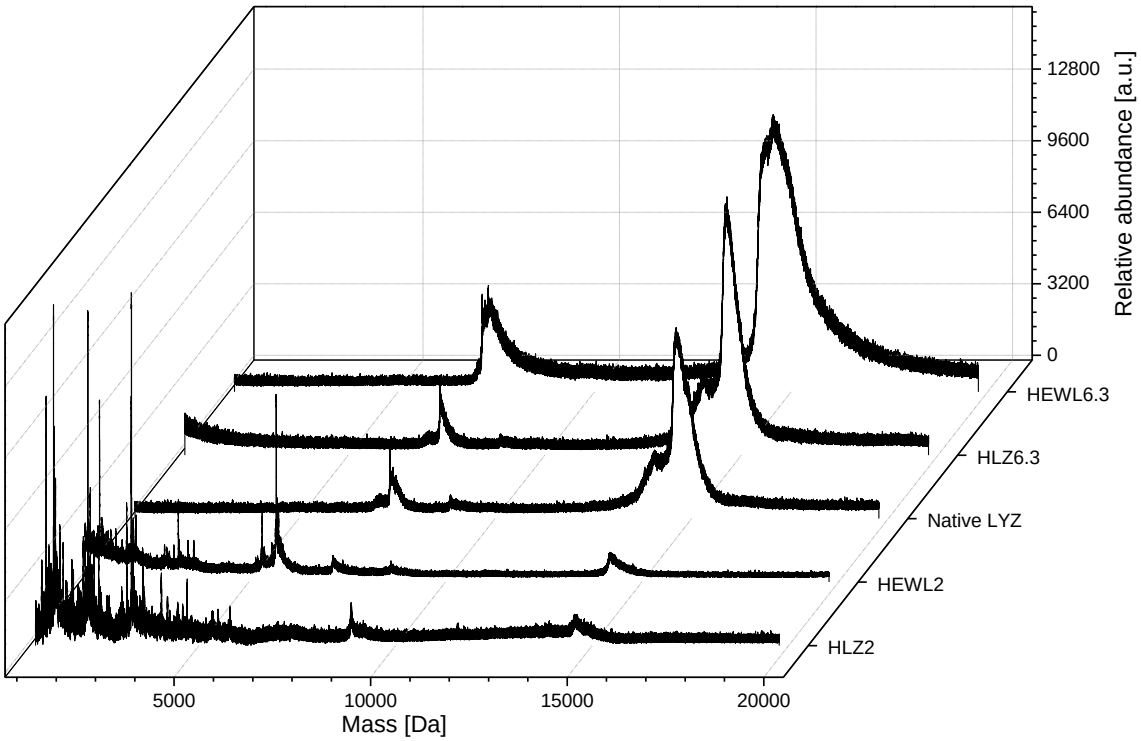


Figure 3.19 MALDI-TOF. Fibril samples were isolated via 50 kDa spin filter then sent to PAMS (Proteomics and Mass Spectrometry) Core Facility at the University of Georgia. pH 2.0 fibril polymorph was composed of intact and hydrolyzed protein, while pH 6.3 fibril polymorph was composed of only intact protein. Molecular weight of HEWL and HLZ were 14.3 kDa, and 14.7 kDa respectively. Native lysozyme was used as a reference.

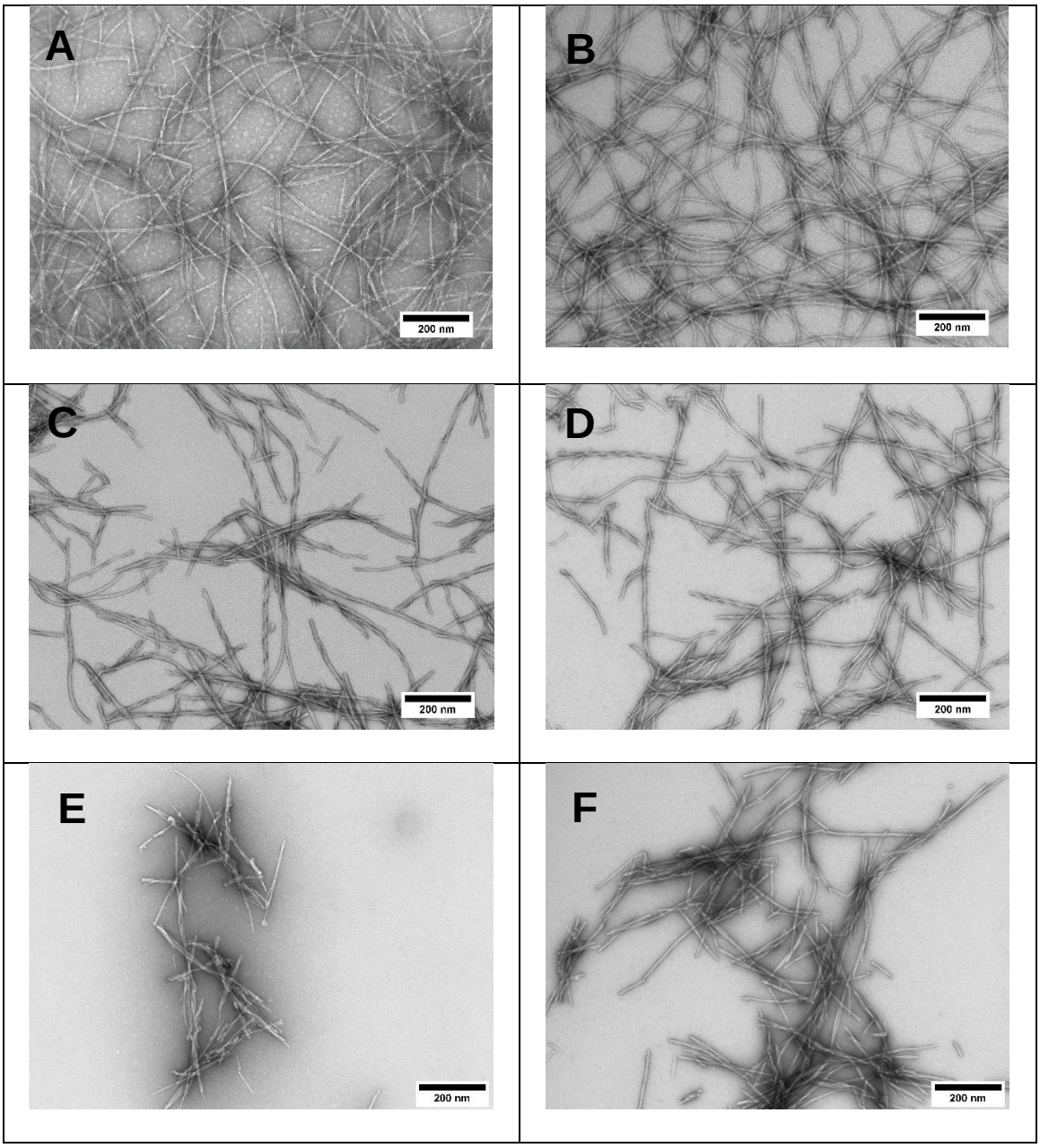


Figure 3.20 Seeded and cross-seeded samples of HLZ at pH 2.0 under TEM. (A) Monomeric HLZ seeded with HLZ 2.0 seed at pH 2.0 buffer (HLZ 2.0 + HLZ 2.0 seed). (B) monomeric HLZ cross-seeded with HEWL 2.0 seed at pH 2.0 buffer (HLZ 2.0 + HEWL 2.0 seed). (C) monomeric HLZ polymorph seeded with HLZ 6.3 seed at pH 2.0 buffer (HLZ 2.0 + HLZ 6.3 seed). (D) monomeric HLZ cross-polymorph seeded with

HEWL 6.3 seed at pH 2.0 buffer (HLZ 2.0 + HEWL 6.3 seed). (E) monomeric HLZ polymorph seeded with HLZ 2.0 seed at pH 6.3 buffer containing 3 M GdnHCl (HLZ 6.3 + HLz 2.0 seed). (F) monomeric HLZ cross-polymorph seeded with HEWL 2.0 seed at pH 6.3 buffer containing 3 M GdnHCl (HLZ 6.3 + HEWL 2.0 seed).

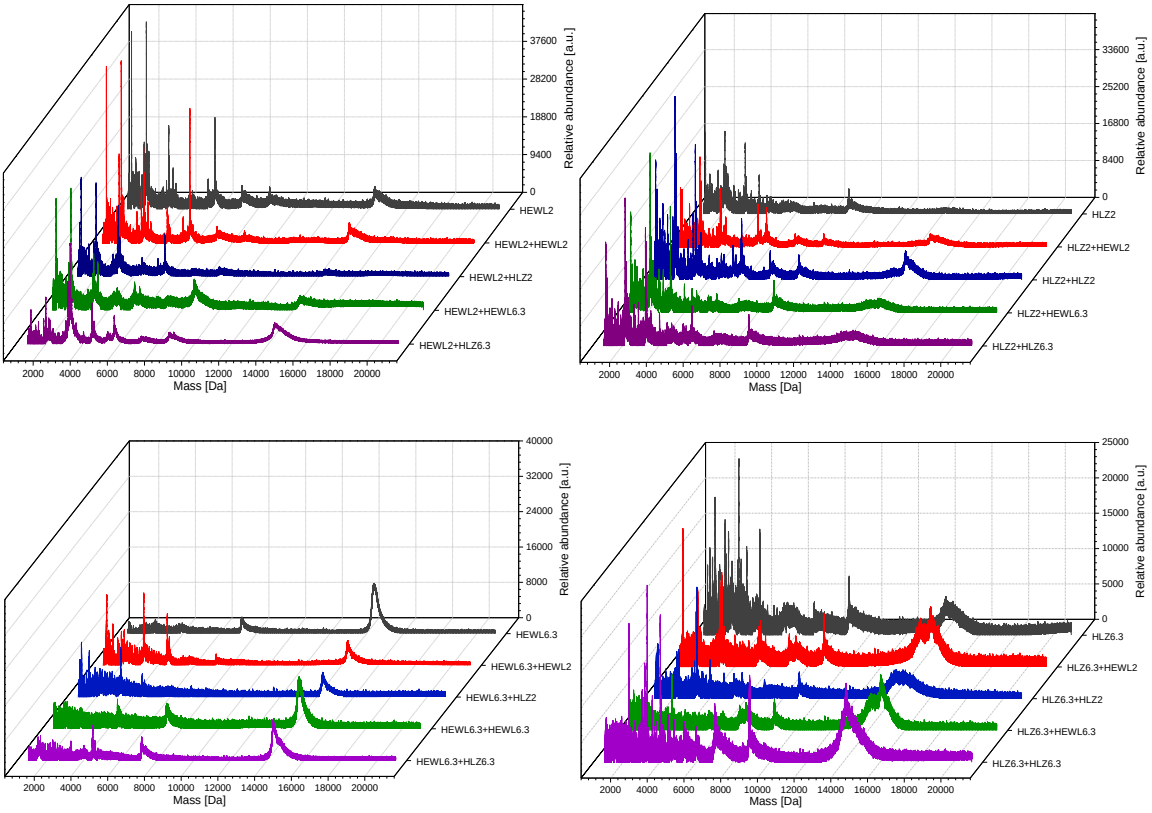


Figure 3.21 MALDI-TOF results of not seeded, seeded, and cross-seeded HEWL and HLZ. Fibril samples were isolated via 50 kDa spin filter then sent to PAMS (Proteomics and Mass Spectrometry) Core Facility at the University of Georgia. Molecular weight of HEWL and HLZ were 14.3 kDa, and 14.7 kDa respectively.

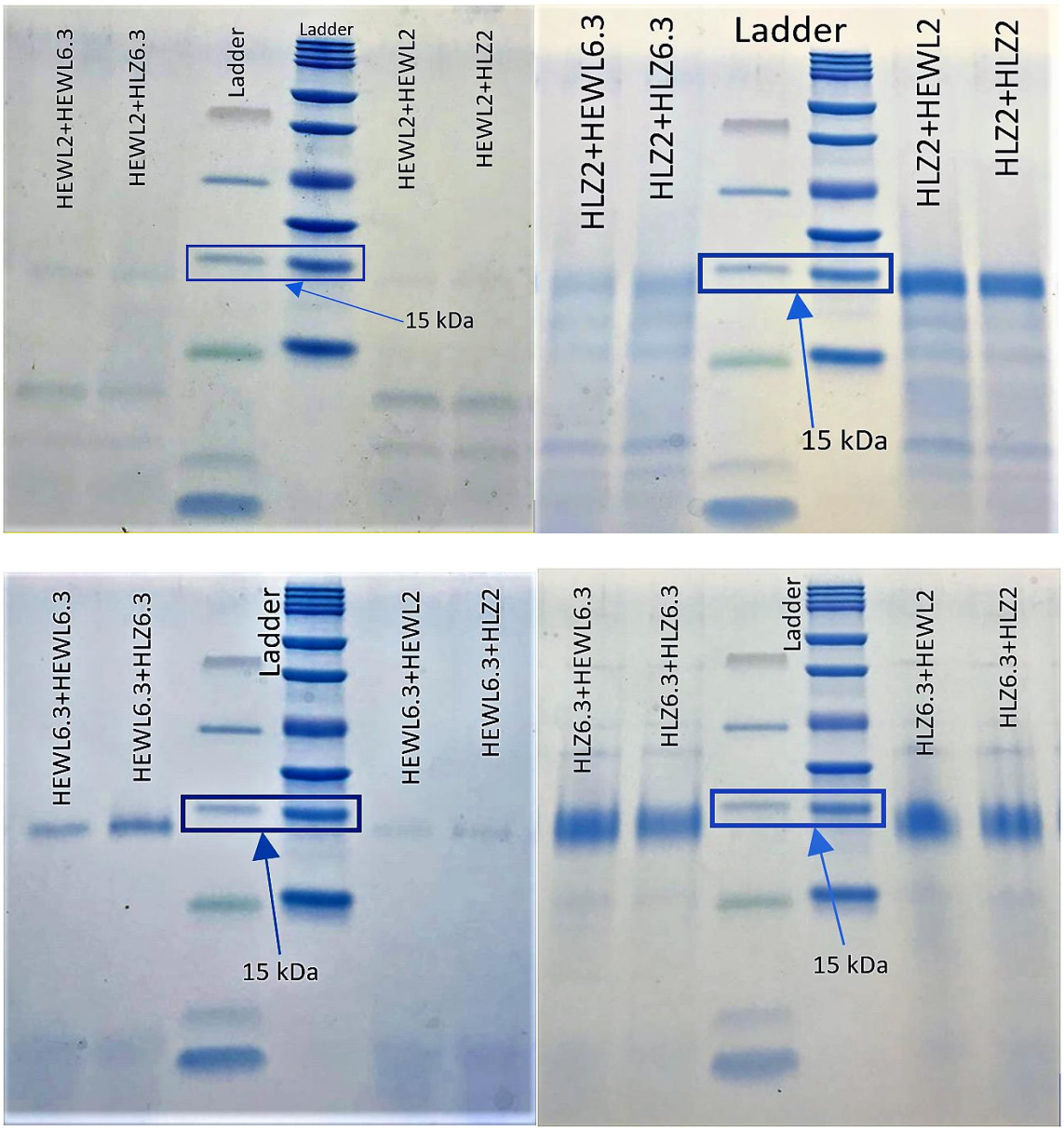


Figure 3.22 SDS-PAGE results of seeded and cross-seeded HEWL and HLZ. Fibril samples were isolated using 50 kDa spin filter, then diluted with an equivalent volume of tricine sample buffer containing 2% β-mercaptoethanol, and finally heated at 95℃ for 5 minutes. These samples were run through 16.5% Tris-Tricine Precast Gels at 100 V for 100 minutes. Molecular weight of HEWL and HLZ, 14.3, 14.7 kDa respectively.

### 3.5 Effect of pH 2.0 on fibrils formed at pH 6.3

In order to understand how pH 6.3 polymorphs are dominant even at pH 2.0 conditions, pH 6.3 fibrils were incubated at pH 2.0, 65℃ condition for a day, then analyzed under TEM and MALDI-TOF.

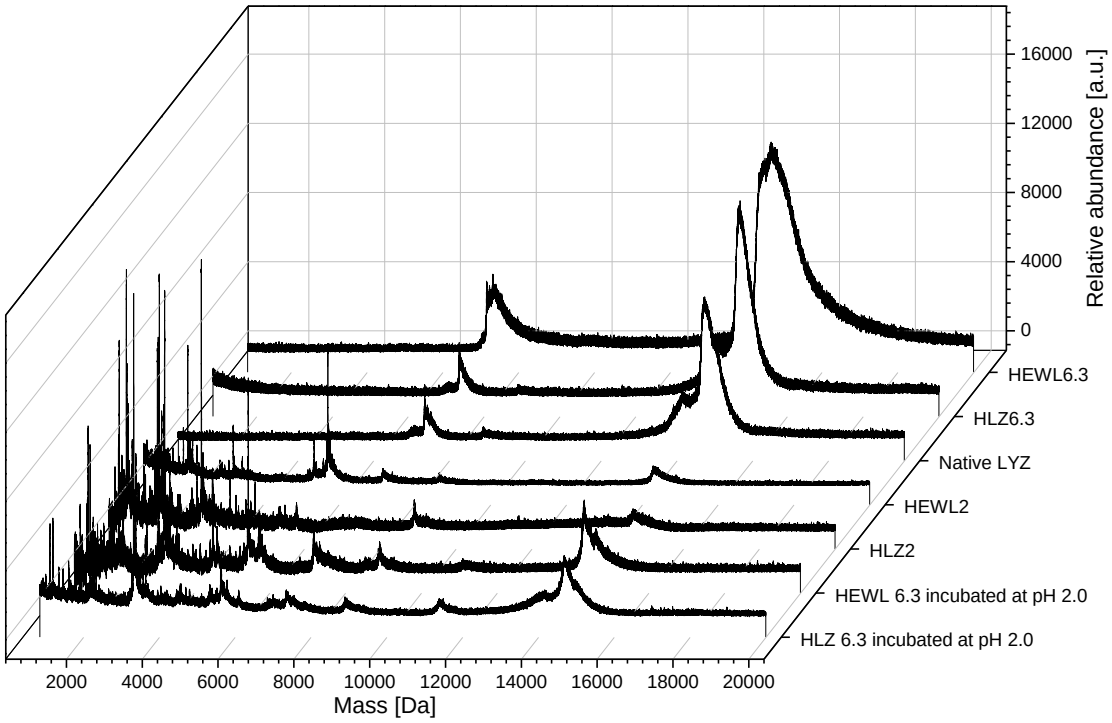


Figure 3.23 Effect of acidic pH on 6.3 fibrils. HEWL 6.3 and HLZ 6.3 fibrils were incubated in 50 mM Gly-HCl buffer of pH 2.0 at 65℃ while shaking at 300 rpm for one day. At 65℃, and pH 2.0 buffer, both HEWL 6.3 and HLZ 6.3 fibrils were partially hydrolyzed, but they maintained their fibrillar structure and morphology.

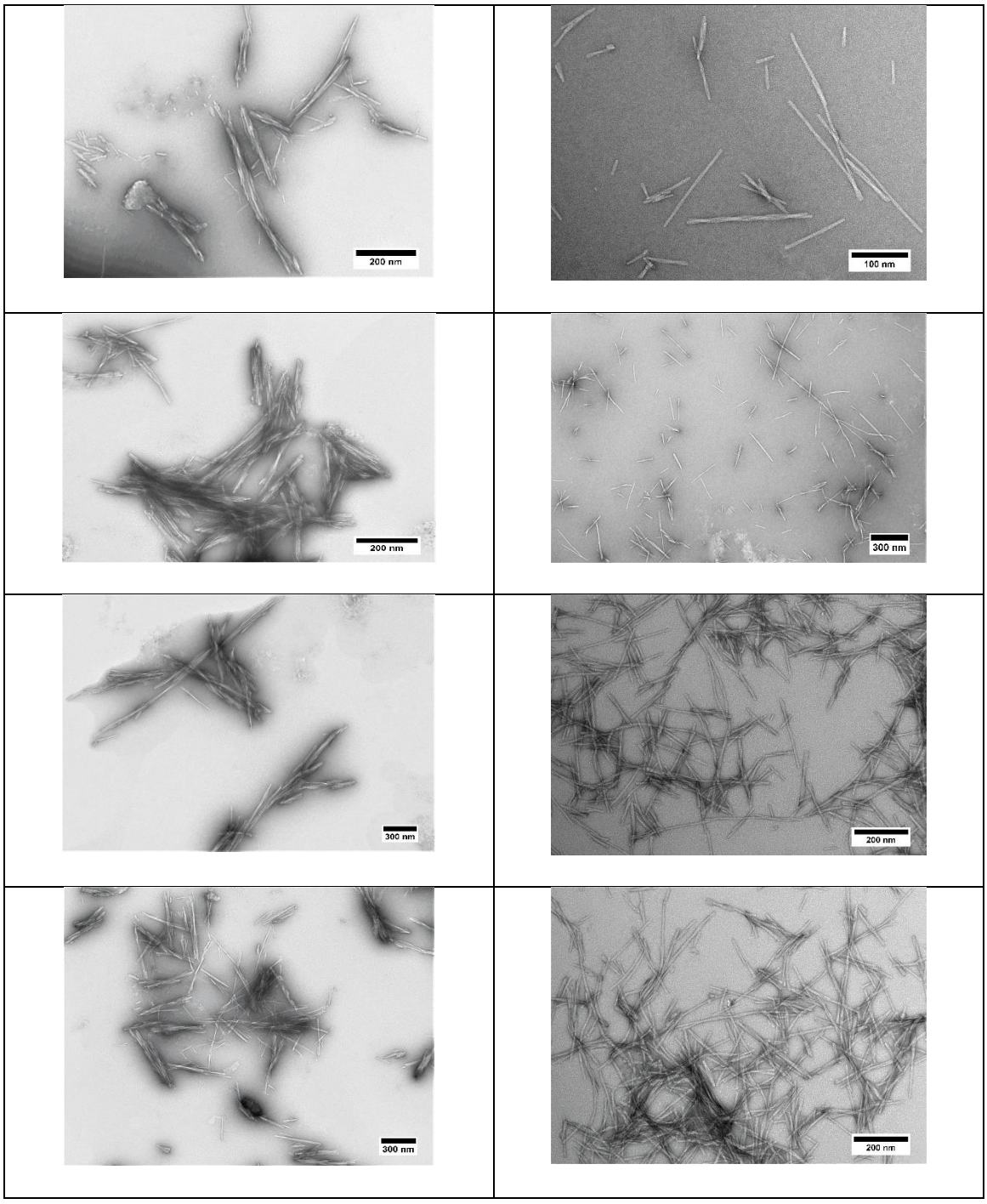


Figure 3.24 Effect of pH change on HEWL6.3 (left column) and HLZ6.3 (right column) fibrils. At 65℃, and pH 2.0 buffer, both HEWL 6.3 and HLZ 6.3 fibrils maintained their fibrillar structure and morphology.

### 3.6 Effect of protease treatment on fibril structure and formation kinetics

HEWL 6.3 fibrils were incubated overnight in simulated gastric fluid (SGF) buffer of pH 1.2, 37°C, with a pepsin:HEWL 6.3 fibril ratio of 1:20 w/w. Fluorescence emission spectra were recorded from 470 nm to 600 nm upon excitation at 440nm before and after pepsin digestion. The results suggested that at 37°C, HEWL 6.3 fibrils were resistant or only slightly sensitive to pepsin even at a 1:4 w/w pepsin:fibril ratio. The ThT fluorescence intensity did not decrease upon pepsin treatment (Fig. 3.25).

To assess the impact of pepsin treatment on fibril seeding ability, HLZ monomers were incubated with various HEWL fibrils (HEWL 6.3, and HEWL 6.3 and HEWL 2.0 sonicated fibrils) treated with pepsin in simulated gastric fluid (SGF), as shown in Figure 3.26. Within a period of four days, only one out of 36 samples formed fibrils under simulated gastric conditions, corresponding to one of 12 HLZ samples that was seeded with HEWL 6.3 fibrils pre-treated with 0.5 mg/mL pepsin.

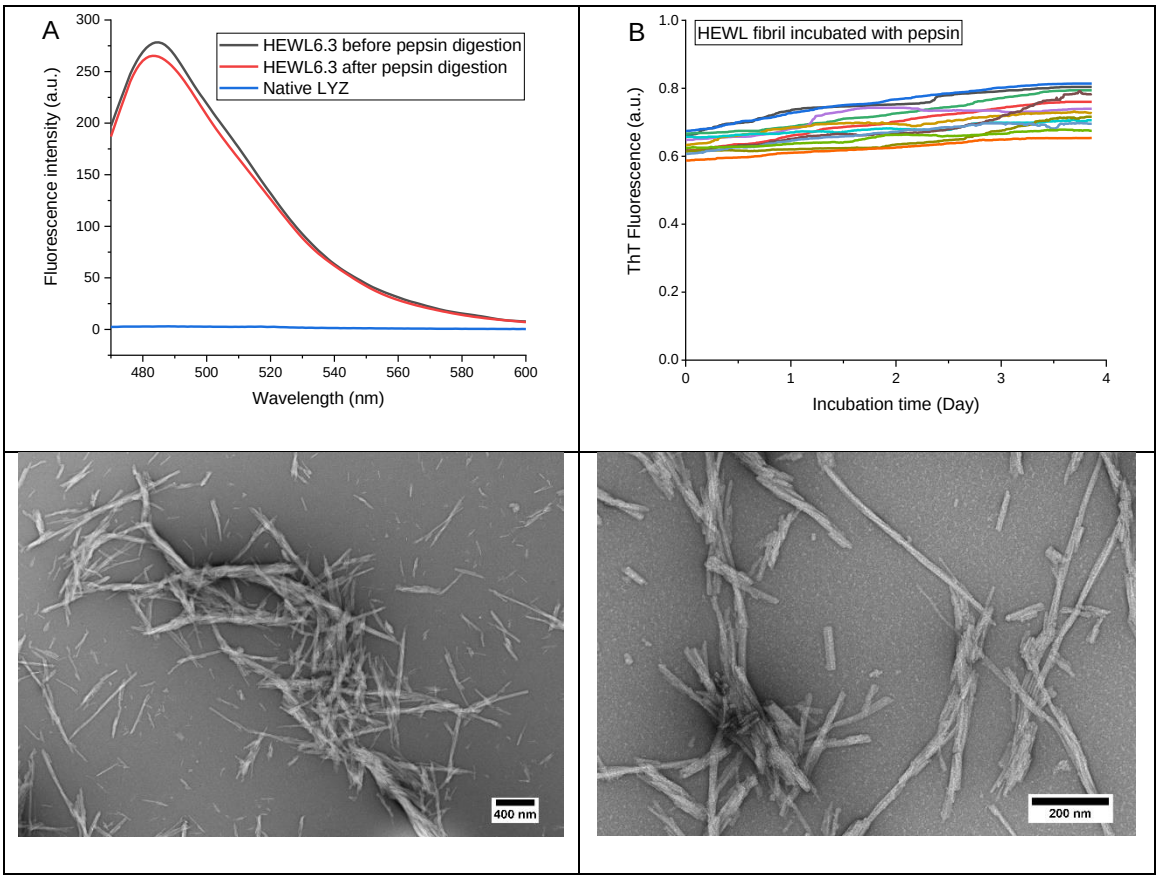


Figure 3.25 Effect of pepsin treatment on fibrils. (A). HEWL 6.3 fibrils incubated with and without pepsin at 37°C in SGF buffer of pH 1.2, at three different pepsin:HEWL ratios: 1:100, 1:20, and 1:4 w/w (B). Negatively stained TEM images of HEWL 6.3 fibrils after pepsin digestion support the results. Simulated Gastric Fluid (SGF-pH 1.2 buffer) with and without pepsin at 37°C with three different pepsin:HEWL ratio, 1:100, 1:20, 1:4 w/w. ThT absorbance spectrum and ThT fluorescence intensity were measured, and no major difference was observed before and after pepsin treatment (see Figure 3.25-top). Negatively stained TEM images of HEWL 6.3 fibrils after pepsin digestion are in agreement with ThT results (see Figure 3.25-bottom). The results suggested that at 37°C, HEWL 6.3 fibrils were resistant or slightly sensitive to pepsin even at 1:4 w/w

pepsin:fibril ratio. HLZ monomers were incubated and cross-seeded with HEWL 6.3 pepsin treated fibrils/seeds, HEWL 6.3 and HEWL 2.0 sonicated seeds at 37°C in simulated gastric fluid (SGF-pH 1.2) with two pepsin concentration (0.5mg/mL, and 0.1 mg/mL), at pepsin:HLZ ratio of 1:20 w/w, and 1:4 w/w (see Figure 3.26). Results reported no effect on ThT, and no effect on fibril morphology.

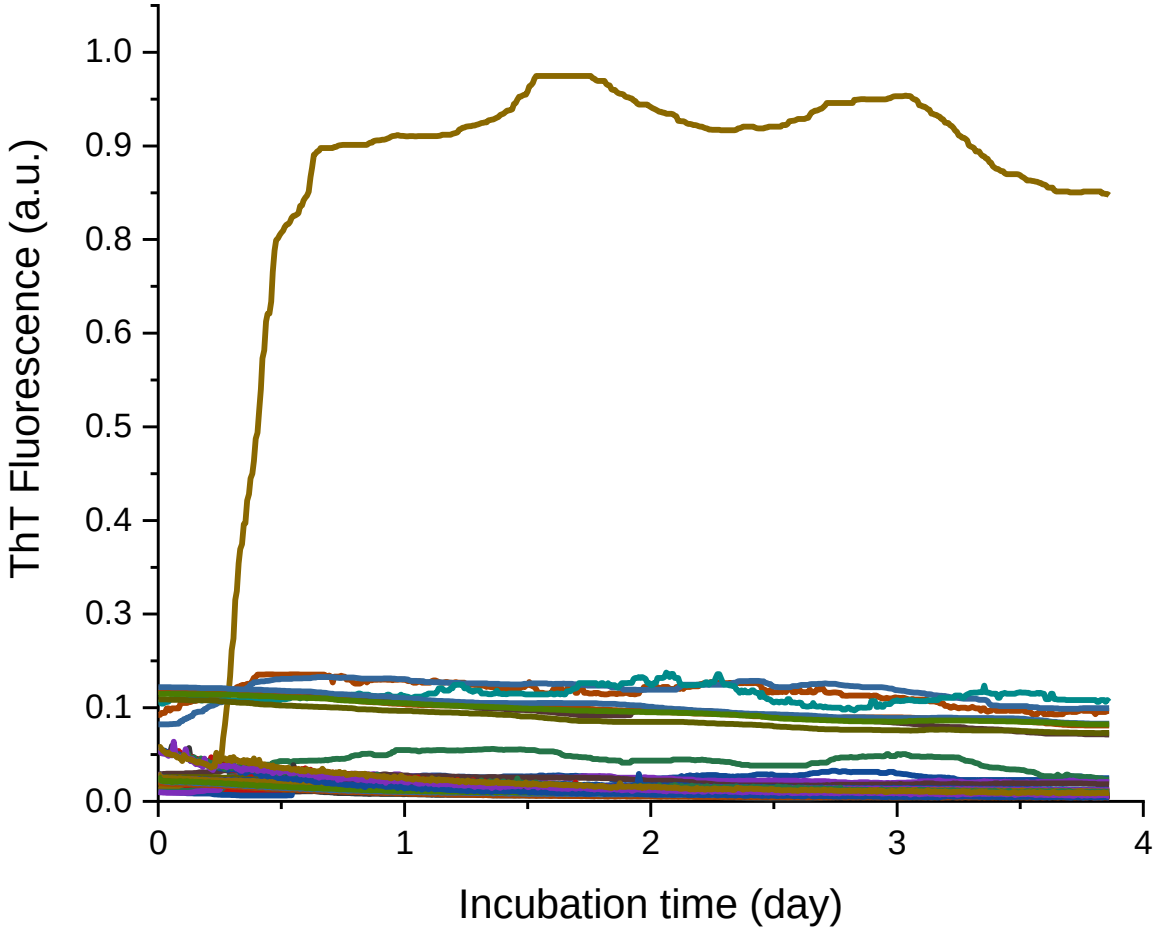


Figure 3.26 Cross-seeding under simulated gastric conditions. Native human lysozyme was incubated with HEWL fibrils in simulated gastric fluid (SGF), pH 1.2, 37°C, containing pepsin, over nearly four days. Different HEWL fibrils were used, where *n* = number of replicates shown: HEWL 6.3 pre-treated with pepsin (pepsin:fibril ratio of

1:20) ($n$ = 12), and HEWL 6.3 ($n$ = 12) and HEWL 2.0 ($n$ = 12) sonicated fibrils. Only one sample (HLZ with HEWL 6.3 fibrils pre-treated with pepsin) yielded a substantial increase in ThT fluorescence.

# CHAPTER 4

# 4 DISCUSSION

## 4.1 Summary

Nanofibrils made from food proteins are gaining interest as new food ingredients and nanomaterials. Before the use of nanofibrils directly in food or on food-contact surfaces, it would be crucial to investigate their consequences and impact on human health. Protein nanofibrils resemble amyloid fibrils, some of which are correlated with pathologies (*e.g.*, systemic amyloidosis, and neurodegenerative diseases) while others play a beneficial, functional role. Like amyloid, protein nanofibrils can self-propagate by 'seeding' and induce normally folded proteins to assemble into nanofibrils. Since amyloid fibrils are resistant to protease digestion, there is a chance that protein nanofibrils used in food, or cosmetics could *cross-seed* the amyloid formation of other proteins in the human body upon oral consumption, leading to systemic amyloidosis and toxicity. A given protein can form different amyloid fibrils that have unique structural properties, termed polymorphs. Different polymorphs of the same protein can have different properties (*e.g.*, seeding potential and efficiency) and toxicity behavior. Studies on cytotoxicity and cell viability assays were done on some nanofibrils made from food proteins, but to our understanding, few studies, if any, have examined cross-seeding between food protein nanofibrils and similar proteins endogenous to humans that are structurally related.

The objective of this research was to examine the cross-seeding ability of food protein nanofibrils at a mechanistic level and determine if they can cause their homologous human proteins to assemble into amyloid-like fibrils. For this study, hen egg-white lysozyme (HEWL) and human lysozyme (HLZ) were chosen as a model system for cross-seeding, for several reasons: lysozyme is one of the best characterized amyloid-forming proteins (Swaminathan, Ravi, Kumar, Kumar, & Chandra, 2011), HEWL is a common food-derived nanofibril source, HEWL and HLZ are highly similar in structure, and HLZ is readily available commercially. To our knowledge, this was the first study to explore cross-polymorph-seeding between HEWL and HLZ.

**4.2 Formation of amyloid fibrils by HEWL and HLZ**

It is generally accepted that a folded native protein needs to at least partially unfold and destabilize in order to form an assembly that is prone to aggregation and fibril formation (Christopher M Dobson, 2003; Kelly, 1998). Heating to a temperature close to the midpoint of the unfolding transition is not enough for destabilizing and fibril formation. Unfolding pathways are different under different solution conditions (*e.g.*, different pH values, the presence of chemical denaturants, and salts). The slow transition of lysozyme molecules to a partially unfolded state is crucial for fibril formation. (Arnaudov & De Vries, 2005). Fibril formation is much slower at pH 2.0 than at pH 6.3. Although protein hydrolysis does take place at pH 2.0, it is not crucial in the aggregation process (Mališauskas et al., 2003). In this case at pH 6.3 with 3 M GdnHCl, HEWL is partially unfolded with four disulfide bonds still remaining intact. GdnHCl is a chaotropic agent, and it can disrupt hydrogen bonding between water molecules, and this affects the

stability of other macromolecules in solution as well. Therefore, GdnHCl increases the entropy in the solution by disrupting the hydrophobic interactions and hydrogen bonding network. GdnHCl can cause denaturation by disrupting the water shell around hydrophobic surfaces (by weakening the hydrophobic effect) and exposing hydrophobic regions in the solution (Mason, Brady, Neilson, & Dempsey, 2007). Partial denaturation of HEWL is achieved by the addition of 3 M GdnHCl at pH 6.3 buffer, which is required to form amyloid-like fibrils from HEWL (Vernaglia et al., 2004).

The mechanism of fibril formation may depend strongly on the unfolding pathway of the protein under particular conditions (Arnaudov & De Vries, 2005), and increasing the temperature above the melting point of the protein is not sufficient for fibril formation. The difference in the behavior of HEWL at different pH values could be due to electrostatic interactions. HEWL is highly charged from pH 2.0-4.0, having between 17-11 positive charges in this pH range (Kuehner et al., 1999), and approximately eight positive charges at pH 6.3.

Amyloidogenicity is a natural property of human lysozyme and does not require the presence of specific mutations in its primary structure (Morozova-Roche et al., 2000).The ability to form amyloid-like fibrils is a generic property of almost all proteins. In this study, HEWL fibrils were formed under different pH values ranging from 1.2 to 7.0 (see Figure 3.1), with the kinetics being much faster at acidic pH. HEWL aggregated faster at pH 1.2 compared to pH 2.0, while the aggregation was delayed dramatically at pH 6.3, and 7.0. This could be due to the more rapid acid hydrolysis that occurs at low pH. Lysozyme fibril formation is concentration dependent, the higher the concentration, the

faster the aggregation rate with a shorter lag phase (see Figure 3.2). Addition of gyration beads into the solution during incubation accelerates the fibril formation. HEWL aggregates faster in the presence of glass beads compared to stainless steel beads (see Figure 3.3). Addition of chemical denaturants such as GdnHCl accelerates HEWL fibrillation and reduces the lag phase dramatically at higher pH, presumably by destabilizing the protein in a way that is prone to aggregate and form fibrils faster (see Figure 3.4).

Lysozyme amyloid fibrils were formed under acidic and near neutral pH conditions in order to obtain two distinct fibril polymorphs. In the acidic condition at pH 2.0 and the moderate condition at pH 6.3 with 3 M GdnHCl, all the samples developed a gel-like consistency after several days of incubation. Fibril formation was confirmed by an increase in the ThT fluorescence intensity and revealed many fibrils when examined by electron microscopy. The HEWL 2.0 fibril polymorph was formed at 65℃, in 50 mM Glycine-HCl pH 2.0 buffer while constantly shaking (300 rpm), with a lag phase of 2.5-3 days. HEWL 2.0 fibrils were long, thin, flexible, unbranched under TEM (see Figure 3.7). The morphology and lag time is consistent with other studies on HEWL fibril formation (Mocanu et al., 2014; Sivalingam et al., 2016; Sulatskaya et al., 2017). The HEWL 6.3 fibril polymorphs were formed at 50℃, in 20 mM potassium phosphate pH 6.3 buffer with 3 M GdnHCl while constantly shaking at 300 rpm. HEWL 6.3 fibrils formed very fast, with a lag time of several (~6 hours) hours. HEWL 6.3 fibrils were short, rigid and straight (see Figure 3.8). The morphology and lag phase was similar to the study by Vernaglia et al., however, they reported using stirring which resulted in a

shorter lag phase of half an hour (Vernaglia et al., 2004). Vernaglia et al. found that using a microplate reader at 45℃, pH 6.3 with 3 M GdnHCl, with agitation every 10 minutes for 20 seconds, HEWL fibrillation occurred only upon the addition of the seeds. In this project all the kinetic studies of fibrillation and seeding experiments were done in a microplate reader at 45℃ with agitation every 10 minutes for 20 seconds as well, however, according to our results, even unseeded HEWL formed fibrils under these conditions.

High fluorescence intensity results were confirmed by TEM images. HLZ 2.0 fibril polymorph was formed at 65℃ and pH 2.0 buffer while constantly shaking (300 rpm), with a lag phase of three days. HLZ 2.0 fibrils were long, thin, flexible, unbranched under TEM (see Figure 3.9). The morphology and lag phase was in agreement with other similar studies done on human lysozyme fibrillation (Felice et al., 2004; Swaminathan et al., 2011). HLZ 6.3 fibrils formed very fast, with a lag time of a couple hours. HLZ 6.3 fibrils were short, rigid, mostly stacked laterally beside each other (see Figure 3.10). The morphology and lag phase was similar to previous similar studies done on human lysozyme amyloid fibrillation (Mossuto et al., 2010). Seeds were formed by sonication, similar to previous work (Sivalingam et al., 2016). Pre-formed fibrils were sonicated for three pulses of 10 seconds followed by five seconds intervals. TEM images confirmed that sonication resulted in breaking the long mature fibrils into shorter fragments.

**4.3 Cross-seeding & polymorphism**

HEWL and HLZ fibrillation curves at pH 2.0 and pH 6.3 have a classic lag phase which is eliminated or shortened by addition of the different seeds (HEWL 2.0, HLZ 2.0,

HEWL 6.3, HLZ 6.3). Such behavior is typical of nucleation-dependent polymerization, in which the formation of nuclei is crucial for the process to begin, either by partial unfolding or fragmentation. The representative traces presented in Figure 3.11 show the differences in the duration of the lag phase, the slope of the growth phase and the plateau of the different conditions (total 20 different conditions). HEWL 2.0 and HLZ 2.0 demonstrated a more extended lag phase, a less steep increase in fluorescence intensity in the growth phase, while HEWL 6.3 and HLZ 6.3 demonstrated a shorter lag phase and a steep rise in fluorescence intensity in the growth phase. These findings imply that under different pH conditions, various amyloid intermediates can form and can result in variations in the structural morphologies of the amyloid fibrils (see Table 3.1).

Effects of seeding on the formation of lysozyme fibrils were examined in a microplate reader. All the seeding experiments were examined by addition of 5% (m/v) of pre-formed and sonicated HEWL 2.0, HEWL 6.3, HLZ 2.0, and HLZ 6.3 into the monomeric HEWL, or HLZ, solubilized in the aggregation buffers of pH 2.0, or pH 6.3 containing 3M GdnHCl at 45℃, with agitation (20s shaking every 10 min). Sonication causes mechanical damage and breaks fibrils into shorter fibrillar fragments, and these fragments act as nuclei (seeds) for subsequent protein fibrillation. According to the results at 45℃, HEWL could cross-seed the fibril formation of HLZ under all four conditions (HLZ 2.0 + HEWL 2.0 seed, HLZ 2.0 + HEWL 6.3 seed, HLZ 6.3 + HEWL 2.0 seed, HLZ 6.3 + HEWL 6.3 seed).

Some studies suggest that high sequence identity (>40%) is required for amyloid aggregates to be able to cross-seed one another (Clarke et al., 2005; Krebs et al., 2004).

In contrast, some studies reported cross-seeding between dissimilar protein sequences, for instance, cross-seeding of curli protein and prostate acid phosphatase (Hartman et al., 2013), and amyloid-β and human islet amyloid polypeptide with 25% sequence identity (M. Zhang et al., 2015). These findings indicate that if the two dissimilar amyloid proteins can adopt a highly similar fibrillar structure, they can cross-seed each other despite the sequence divergence (Wasmer et al., 2010). Therefore, fibril core can also play an essential role in cross-seeding between different proteins that are not similar in sequence.

In every kinetic experiment reported here, the seed-free sample was used as a reference. ThT kinetic traces were analyzed in order to characterize the lag phase, half time, and growth rate of fibril formation. The growth rate is much higher for the pH 6.3 conditions than pH 2.0 (see Figure 3.15). This indicates that pH 6.3 is a fast fibril forming condition, while pH 2.0 condition is a much slower condition, especially for HLZ. The lag phase for different conditions was ranging between a couple of hours and several days, depending on the solution condition and presence of seeds. The longest lag time belonged to unseeded HLZ. This indicates that pH 2.0, 45℃, with agitation every 10 minutes for 20 seconds, is not a good fibril formation condition for HLZ. According to work done by Crespo et al., it is difficult to get reproducible kinetic data for amyloid fibril formation, due to the formation of different intermediates and off-pathway species (*e.g.*, protein precipitates, and insoluble oligomers) during amyloid fibrillation of lysozyme (Crespo et al., 2016). Besides some experimental errors such as human error, or

systemic errors that could occur, the off-pathway phenomena can also justify the low reproducibility of the kinetic results.

HEWL and HLZ fibrils formed under pH 2.0 and pH 6.3 conditions show an evident polymorphism. The structural characteristics and morphology of the formed fibrils were evaluated using spectroscopic methods, electron microscopy, and image analysis, and fibril composition was analyzed using SDS-PAGE and MALDI-TOF. The plateau level of ThT fluorescence before normalization was higher for the pH 6.3 condition, compared to the pH 2.0 condition, for both HEWL and HLZ. This indicates either a greater extent of fibril formation occurs at pH 6.3 than at pH 2.0, or that ThT interacts with the pH 6.3 fibril polymorph differently than with the pH 2.0 polymorph. The pH 6.3 condition shows a smaller lag phase, and a higher plateau level of ThT fluorescence, relative to pH 2.0, indicating that pH 6.3 condition is a better condition to form fibrils. Results suggest that the pH 6.3 polymorph is dominant for both species, even at pH 2.0, as it maintains and self-propagates its unique fibril structure when used to seed lysozyme solutions at pH 2.0. The electron microscopy and atomic force microscopy results showed that pH 2.0 and pH 6.3 fibril polymorphs differ in their length, width, rigidity, and twist. Fibril polymorphs display, in both cases, an unbranched morphology. pH 2.0 fibril polymorphs are long, thin, semiflexible, and curved, while pH 6.3 fibril polymorphs are short, thicker, rigid, and twisted (see Figure 3.17). Our results are in agreement with previous studies of lysozyme fibril polymorphs (Mocanu et al., 2014; Mossuto et al., 2010; Sivalingam et al., 2016; Sulatskaya et al., 2017).

A major difference between the two polymorphs is that the pH 2.0 polymorph consists of intact and hydrolyzed protein, while the pH 6.3 polymorph contains only intact lysozyme (see Figure 3.18, and 3.19). The absence of larger protein bands than 14.7 kDa in the SDS gels (see Figure 3.18) suggests that fibril formation does not include disulfide bonds, but contains hydrogen bonds, which are broken down by heating in the presence of SDS. (Arnaudov & De Vries, 2005).

The seeded and cross-seeded samples of HLZ were analyzed under TEM. The HLZ 2.0 seeded with HEWL 2.0 and HLZ 2.0, both formed long, unbranched, flexible fibrils, however, HLZ 2.0 seeded with HEWL 6.3 and HLZ 6.3, formed shorter, more twisted, more rigid fibrils, resembling pH 6.3 polymorph. In contrast, when HLZ 6.3 was seeded with HEWL 2.0 or HLZ 2.0 seeds, the new formed fibrils were short, straight, and rigid and this indicates that 6.3 polymorphs were dominant even at pH 2.0, and the newly formed fibrils preserved the pH 6.3 polymorph seed structure and morphology.

In order to better understand why pH 6.3 polymorphs are dominant even at pH 2.0 conditions, pH 6.3 fibrils were incubated at pH 2.0, 65℃ condition over a day, then analyzed under TEM and MALDI-TOF. The TEM and MALDI-TOF results suggest that pH 6.3 polymorphs of HEWL and HLZ are resistant to low pH and higher temperature. Although acid hydrolysis occurs at pH 2.0 and 65℃, the 6.3 fibrils remain intact, meaning that the fibril core is resistant while the other residues that are not involved in the fibril core can get hydrolyzed. The results suggest that, even though the monomeric form is hydrolyzed, fibrils maintain their morphology (see Figure 3.23, and 3.24). Thus, the pH 6.3 polymorph retains its morphology even at pH 2.0, meaning that pH 6.3 fibril

seeds can act as nuclei, and elongate by addition of lysozyme monomers to the nucleation sites at the fibril ends. Although protein hydrolysis can take place at pH 2.0, 65℃, it is not crucial in the aggregation process (Mališauskas et al., 2003).

**4.4 Nanofibrils digestibility and food safety**

Cross-seeding is more likely the more similar in sequence and structure two proteins are, and the milk and egg proteins most commonly used to form nanofibrils are structurally similar (60-90% similarity) to several human proteins. Amyloid fibrils can survive digestion and spread to other parts of the body, as evidenced by prions (Colby & Prusiner, 2011) and amyloid A (AA) protein from foie gras (Solomon et al., 2007). These findings indicate that protein nanofibrils may induce the amyloid formation of other structurally similar human proteins upon oral consumption, in a susceptible population under certain conditions.

In order to mimic stomach and physiological conditions, the effect of protease treatment on fibril structures and formation kinetics were investigated. Pepsin is a digestive enzyme which is found in the natural gastric juice in the stomach. Pepsin is only able to break peptide bonds, which has a broad specificity, where the cleavage sites are not directed by the amino acid sequence but by the conformational and dynamical characteristics of the polypeptide chain (Fruton, 1970). Polverino de Laureto et al. reported that native HEWL and bovine α-lactalbumin appear to be fully resistant to proteolysis with pepsin at pH 2.0 in an enzyme-to-substrate ratio of 1:500 (by weight) at ~20°C, while horse, pigeon, and dog lysozyme are partially digested under these conditions (Polverino de Laureto, Frare, Gottardo, van Dael, & Fontana, 2002). Frare et

al. reported that because HEWL is very stable and resistant to proteases in its native state (*e.g.*, to proteinase K, thermolysin at neutral pH and pepsin at pH 2.0), they conducted proteolysis of HEWL with pepsin at pH 0.9 containing 2 M GdnHCl with an E:S ratio of 1:300 by weight. This unusual proteolysis resulted in two protein fragments (Frare, de Laureto, Zurdo, Dobson, & Fontana, 2004). Another study by Frare et al. reported that pepsin digestion of HLZ fibrils and native HLZ occurred under harsh conditions at pH 2.0 and 57℃ for several hours with an E:S ratio of 1:30 by weight. Native HLZ, almost completely degraded, while fragment 32-108 from fibrils was resistant to pepsin digestion (Frare et al., 2006).

Since pepsin is responsible for initiating protein digestion in the body, fibrils were incubated in Simulated Gastric Fluid (SGF) at 37℃. Results suggest that only one out of 36 cross-seeded samples formed fibrils under simulated gastric conditions (HEWL 6.3 pepsin treated fibrils with 0.5 mg/mL pepsin). This indicates a very low probability of cross-seeding between HEWL and HLZ under physiological conditions *in vitro*. Since *in vitro* experiments fail to replicate the cellular, and *in vivo* conditions, it is not reasonable to conclude the safety or toxicity of the nanofibrils based on these results alone.

**4.5 Future research**

The results of this project suggest that there is a low probability of cross-seeding between HEWL and HLZ under physiological conditions *in vitro*. Since *in vitro* experiments fail to replicate the cellular, and *in vivo* conditions, it is not reasonable to conclude the safety or toxicity of the nanofibrils from *in vitro* studies. *In vitro* is an exaggerated pure condition conducted in a test tube, while in the body other elements and

factors are involved which are not replicable *in vitro*. In this project lysozyme was used as a model system since there is a chance that protein nanofibrils can survive digestion and the GI tract, it is prudent to investigate other nanofibrils that could be used as a food ingredient or enter the body as a nanotechnology device. Therefore, further investigation is required to investigate the fate of nanofibrils after consumption *in vivo*, in order to ensure safe food supply.

Different fibril polymorphs from the same protein could have different morphology, toxicity, cross-seeding propensity, and characteristics, therefore studying polymorphism is crucial. Since the food nanofibrils can be made under various conditions and that can result in the formation of different fibril polymorphs (variants), it is prudent to study the cross-seeding and cross-polymorph-seeding among other food protein nanofibrils with their similar human proteins. As some studies reported cross-seeding between dissimilar proteins, it is also crucial to study cross-seeding between plant proteins and human proteins as well.

# CHAPTER 5

# 5 CONCLUSIONS

This study examined cross-seeding between two homologous variants under two different conditions, using hen egg white lysozyme (HEWL) and human lysozyme (HLZ) as a model system. Nanofibrils of HEWL and HLZ formed at both pH 2.0, 65℃ and pH 6.3 with 3 M GdnHCl, 50℃, agitated (300 rpm shaking). Under these solution conditions, two distinct polymorphs were formed from both species (HEWL and HLZ). The fibril polymorphs that formed under acidic pH (pH 2.0 polymorphs) were shown to be composed of intact and hydrolyzed protein while fibril polymorphs that were formed under mild conditions (pH 6.3 polymorphs) were composed only of intact lysozyme, as determined using MALDI-TOF and SDS-PAGE. These polymorphs showed different morphologies under AFM and TEM. pH 2.0 polymorphs are long, and flexible, while pH 6.3 polymorphs are short and rigid.

Seeding and cross-seeding under swapped incubation conditions were examined *in vitro* at 45℃, and under physiological conditions (SGF) in the presence of pepsin at 37℃. Seeded reactions were conducted in the presence of 5% w/w sonicated or pepsin digested seeds. Seeding and cross-seeding occurred between HEWL and HLZ at the 45℃ condition, and at the physiological condition, only one out of 36 samples aggregated and showed >10-fold increase in ThT fluorescence intensity. Cross-seeded samples were

examined under TEM, and the results suggest that the pH 6.3 polymorphs are dominant at both pH conditions. The addition of 6.3 polymorph seeds into pH 2.0 condition resulted in rapid elongation and the new fibrils preserved the properties of the 6.3 polymorphs. However, the same observation was not true for pH 2.0 polymorphs. Limited proteolytic digestion by pepsin was indicated for both polymorphs examined by ThT fluorescence intensity kinetics, and TEM.

Major conclusions from this study:

1) HEWL can cross-seed HLZ
    - Fibrillation kinetics are strongly determined by solution conditions – physiological conditions (especially temperature) may mitigate cross-seeding
    - Supports that further work is needed to establish the safety of food-derived nanofibrils
2) Seeding/cross-seeding ability can depend on the polymorph
    - Supports that different polymorphs from the same protein should be treated as having distinct functionality (including safety/risk)
3) HEWL and HLZ fibrils were resistant to pepsin digestion at a pepsin:fibril ratio of 1:20 at 37℃.

REFERENCES

Abdolvahabi, A., Shi, Y., Rasouli, S., Croom, C. M., Chuprin, A., & Shaw, B. F. (2017). How do gyrating beads accelerate amyloid fibrillization? *Biophysical Journal*, *112*(2), 250–264.

Acheson, D. W. K. (2002). Bovine spongiform encephalopathy (mad cow disease). *Nutrition Today*, *37*(1), 19–25.

Adamcik, J., & Mezzenga, R. (2012). Proteins Fibrils from a Polymer Physics Perspective. *Macromolecules*, *45*(3), 1137–1150. https://doi.org/10.1021/ma202157h

Akkermans, C., Goot A.J, van der, Venema, P., Gruppen, H., Vereijken, J. M., Linden E, van der, … Boom, R. M. (2007). Micrometer-Sized Fibrillar Protein Aggregates from Soy Glycinin and Soy Protein Isolate. *Journal of Agricultural and Food Chemistry*, *55*(24), 9877–9882. https://doi.org/10.1021/jf0718897

Alam, P., Siddiqi, K., Chturvedi, S. K., & Khan, R. H. (2017). Protein aggregation: From background to inhibition strategies. *International Journal of Biological Macromolecules*, *103*, 208–219. https://doi.org/10.1016/j.ijbiomac.2017.05.048

Alavez, S., Vantipalli, M. C., Zucker, D. J. S., Klang, I. M., & Lithgow, G. J. (2011). Amyloid-binding compounds maintain protein homeostasis during ageing and extend lifespan. *Nature*, *472*(7342), 226.

Annamalai, K., Gührs, K., Koehler, R., Schmidt, M., Michel, H., Loos, C., … Schönland,

S. (2016). Polymorphism of amyloid fibrils in vivo. *Angewandte Chemie International Edition*, *55*(15), 4822–4825.

Antimonova, O. I., Grudinina, N. A., Egorov, V. V., Polyakov, D. S., Il'in, V., Shavlovskii, M., … Shavlovsky, M. M. (2016). Interaction of the dye Congo red with fibrils of lysozyme, beta2-microglobulin, and transthyretin. *Cell and Tissue Biology*, *10*(6), 468–475. https://doi.org/10.1134/S1990519X1606002X

Arnaudov, L. N., & De Vries, R. (2005). Thermally induced fibrillar aggregation of hen egg white lysozyme. *Biophysical Journal*, *88*(1), 515–526. https://doi.org/10.1529/biophysj.104.048819

Arosio, P., Knowles, T. P. J., & Linse, S. (2015). On the lag phase in amyloid fibril formation. *Physical Chemistry Chemical Physics : PCCP*, *17*(12), 766–7618. https://doi.org/10.1039/c4cp05563b

Auer, S. (2015). Nucleation of Polymorphic Amyloid Fibrils. *Biophysical Journal*, *108*(5), 1176–1186. https://doi.org/10.1016/j.bpj.2015.01.013

Auer, S., Ricchiuto, P., & Kashchiev, D. (2012). Two-step nucleation of amyloid fibrils: omnipresent or not? *Journal of Molecular Biology*, *422*(5), 723–730.

Balguerie, A., Dos Reis, S., Ritter, C., Chaignepain, S., Coulary-Salin, B., Forge, V., … Riek, R. (2003). Domain organization and structure–function relationship of the HET-s prion protein of Podospora anserina. *The EMBO Journal*, *22*(9), 2071–2081.

Barnhart, M. M., & Chapman, M. R. (2006). Curli biogenesis and function. *Annu.Rev.Microbiol.*, *60*, 131–147.

Bateman, L., Ye, A., & Singh, H. (2010). In vitro digestion of beta-lactoglobulin fibrils

formed by heat treatment at low pH. *Journal of Agricultural and Food Chemistry*, *58*(17), 9800–9808. https://doi.org/10.1021/jf101722t

Bateman, L., Ye, A., & Singh, H. (2011). Re-formation of fibrils from hydrolysates of β-lactoglobulin fibrils during in vitro gastric digestion. *Journal of Agricultural and Food Chemistry*, *59*(17), 9605–9611.

Bekard, I., & Dunstan, D. E. (2014). Electric field induced changes in protein conformation. *Soft Matter*, *10*(3), 431–437.

Berchowitz, L. E. E., Kabachinski, G., Walker, M. R. R., Carlile, T. M. M., Gilbert, W. V. V., Schwartz, T. U. U., & Amon, A. (2015). Regulated Formation of an Amyloid-like Translational Repressor Governs Gametogenesis. *Cell*, *163*(2), 406–418. https://doi.org/10.1016/j.cell.2015.08.060

Biancalana, M., & Koide, S. (2010). Molecular mechanism of Thioflavin-T binding to amyloid fibrils. *Biochimica et Biophysica Acta - Proteins and Proteomics*, *1804*(7), 1405. https://doi.org/10.1016/j.bbapap.2010.04.001

Bolisetty, S., & Mezzenga, R. (2016). Amyloid–carbon hybrid membranes for universal water purification. *Nature Nanotechnology*, *11*(4), 365.

Bousset, L., Pieri, L., Ruiz-Arlandis, G., Gath, J., Jensen, P. H., Habenstein, B., … Meier, B. H. (2013). Structural and functional characterization of two alpha-synuclein strains. *Nature Communications*, *4*, 2575.

Burova, T. V, Grinberg, N. V, Grinberg, V. Y., Rariy, R. V, & Klibanov, A. M. (2000). Calorimetric evidence for a native-like conformation of hen egg-white lysozyme dissolved in glycerol. *Biochimica et Biophysica Acta (BBA)-Protein Structure and*

*Molecular Enzymology*, *1478*(2), 309–317.

Byrne, R. A., Kastrati, A., Massberg, S., Wieczorek, A., Laugwitz, K.-L., Hadamitzky, M., … Hausleiter, J. (2011). Biodegradable polymer versus permanent polymer drug-eluting stents and everolimus-versus sirolimus-eluting stents in patients with coronary artery disease: 3-year outcomes from a randomized clinical trial. *Journal of the American College of Cardiology*, *58*(13), 1325–1331.

Celej, M. S., Caarls, W., Demchenko, A. P., & Jovin, T. M. (2009). A triple-emission fluorescent probe reveals distinctive amyloid fibrillar polymorphism of wild-type α-synuclein and its familial Parkinson's disease mutants. *Biochemistry*, *48*(31), 7465–7472.

Chapman, M. R., Robinson, L. S., Pinkner, J. S., Roth, R., Heuser, J., Hammar, M., … Hultgren, S. J. (2002). Role of Escherichia coli curli operons in directing amyloid fiber formation. *Science*, *295*(5556), 851–855.

Cheon, M., Kang, M., & Chang, I. (2016). Polymorphism of fibrillar structures depending on the size of assembled Aβ 17-42 peptides. *Scientific Reports*, *6*, 38196.

Chernoff, Y. O., Galkin, A. P., Lewitin, E., Chernova, T. A., Newnam, G. P., & Belenkiy, S. M. (2000). Evolutionary conservation of prion-forming abilities of the yeast Sup35 protein. *Molecular Microbiology*, *35*(4), 865–876.

Cherny, I., Rockah, L., Levy-Nissenbaum, O., Gophna, U., Ron, E. Z., & Gazit, E. (2005). The formation of Escherichia coli curli amyloid fibrils is mediated by prion-like peptide repeats. *Journal of Molecular Biology*, *352*(2), 245–252.

Chiti, F., & Dobson, C. M. (2006). Protein Misfolding, Functional Amyloid, and Human

Disease. *Annual Review of Biochemistry*, *75*(1), 333–366. https://doi.org/10.1146/annurev.biochem.75.101304.123901

Chiti, F., Webster, P., Taddei, N., Clark, A., Stefani, M., Ramponi, G., & Dobson, C. M. (1999). Designing conditions for in vitro formation of amyloid protofilaments and fibrils. *Proceedings of the National Academy of Sciences of the United States of America*, *96*(7), 3590–3594. Retrieved from http://www.pnas.org/content/96/7/3590.abstract

Chung, S. Y., & Subbiah, S. (1996). A structural explanation for the twilight zone of protein sequence homology. *Structure*, *4*(10), 1123–1127.

Claessen, D., Rink, R., de Jong, W., Siebring, J., de Vreugd, P., Boersma, F. G. H., … Wösten, H. A. B. (2003). A novel class of secreted hydrophobic proteins is involved in aerial hyphae formation in Streptomyces coelicolor by forming amyloid-like fibrils. *Genes & Development*, *17*(14), 1714–1726.

Clarke, J., Wright, C. F., Dobson, C. M., Teichmann, S. A., Clarke, J., & Dobson, C. M. (2005). The importance of sequence diversity in the aggregation and evolution of proteins. *Nature*, *438*(7069), 878–881. https://doi.org/10.1038/nature04195

Cobb, N. J., Apostol, M. I., Chen, S., Smirnovas, V., & Surewicz, W. K. (2014). Conformational stability of mammalian prion protein amyloid fibrils is dictated by a packing polymorphism within the core region. *Journal of Biological Chemistry*, *289*(5), 2643–2650.

Cobb, N. J., & Surewicz, W. K. (2009). Prion diseases and their biochemical mechanisms. *Biochemistry*, *48*(12), 2574–2585.

Colby, D. W., & Prusiner, S. B. (2011). Prions. *Cold Spring Harbor Perspectives in Biology*, *3*(1), a006833.

Conway, K. A., Harper, J. D., & Lansbury, P. T. (2000). Fibrils formed in vitro from α-synuclein and two mutant forms linked to Parkinson's disease are typical amyloid. *Biochemistry*, *39*(10), 2552–2563.

Crespo, R., Villar-Alvarez, E., Taboada, P., Rocha, F. A., Damas, A. M., & Martins, P. M. (2016). What Can the Kinetics of Amyloid Fibril Formation Tell about Off-pathway Aggregation? *The Journal of Biological Chemistry*, *291*(4), 2018–2032. https://doi.org/10.1074/jbc.M115.699348

Cui, D., Kawano, H., Hoshii, Y., Liu, Y., & Ishihara, T. (2008). Acceleration of murine AA amyloid deposition by bovine amyloid fibrils and tissue homogenates. *Amyloid*, *15*(2), 77–83.

Cui, D., Kawano, H., Takahashi, M., Hoshii, Y., Setoguchi, M., Gondo, T., & Ishihara, T. (2002). Acceleration of murine AA amyloidosis by oral administration of amyloid fibrils extracted from different species. *Pathology International*, *52*(1), 40–45.

Dobson, C. M. (2003). Protein folding and misfolding. *Nature*, *426*(6968), 884.

Dobson, C. M. (2004). Principles of protein folding, misfolding and aggregation. *Seminars in Cell & Developmental Biology*, *15*(1), 3–16. https://doi.org/10.1016/j.semcdb.2003.12.008

Dovidchenko, N. V, & Galzitskaya, O. V. (2015). Computational approaches to identification of aggregation sites and the mechanism of amyloid growth. In *Lipids in Protein Misfolding* (pp. 213–239). Springer.

Dueholm, M. S., Petersen, S. V., Sønderkaer, M., Larsen, P., Christiansen, G., Hein, K. L., … Otzen, D. E. (2010). Functional amyloid in Pseudomonas. *Molecular Microbiology*, *77*(4), no. https://doi.org/10.1111/j.1365-2958.2010.07269.x

Eichner, T., & Radford, S. E. E. (2011). A Diversity of Assembly Mechanisms of a Generic Amyloid Fold. *Molecular Cell*, *43*(1), 8–18. https://doi.org/10.1016/j.molcel.2011.05.012

Elfwing, A., Bäcklund, F. G., Musumeci, C., Inganäs, O., & Solin, N. (2015). Protein nanowires with conductive properties. *Journal of Materials Chemistry C*, *3*(25), 6499–6504. https://doi.org/10.1039/C5TC00896D

Erskine, E., Morris, R., Schor, M., Earl, C., Gillespie, R. M. C., Bromley, K., … Serpell, L. (2018). Formation of functional, non-amyloidogenic fibres by recombinant Bacillus subtilis TasA. *BioRxiv*, 188995.

Falabella, P., Riviello, L., Pascale, M., Di Lelio, I., Tettamanti, G., Grimaldi, A., … Pennacchio, F. (2012). Functional amyloids in insect immune response. *Insect Biochemistry and Molecular Biology*, *42*(3), 203–211. https://doi.org///doi.org/10.1016/j.ibmb.2011.11.011

Farjami, T., Madadlou, A., & Labbafi, M. (2015). Characteristics of the bulk hydrogels made of the citric acid cross-linked whey protein microgels. *Food Hydrocolloids*, *50*, 159–165.

Farjami, T., Madadlou, A., & Labbafi, M. (2016). Modulating the textural characteristics of whey protein nanofibril gels with different concentrations of calcium chloride. *The Journal of Dairy Research*, *83*(1), 109–114.

https://doi.org/10.1017/S0022029915000667

Felice, F. G. De, Vieira, M. N. N., Meirelles, M. N. L., Morozova-Roche, L. A., Dobson, C. M., Ferreira, S. T., … Ferreira, S. T. (2004). Formation of amyloid aggregates from human lysozyme and its disease-associated variants using hydrostatic pressure. *FASEB Journal : Official Publication of the Federation of American Societies for Experimental Biology*, *18*(10), 1099–1101. https://doi.org/10.1096/fj.03-1072fje

Foegeding, E. A. (2007). Rheology and sensory texture of biopolymer gels. *Current Opinion in Colloid & Interface Science*, *12*(4), 242–250. https://doi.org/10.1016/j.cocis.2007.07.001

Foegeding, E. A., & Davis, J. P. (2011). Food protein functionality: A comprehensive approach. *Food Hydrocolloids*, *25*(8), 1853–1864. https://doi.org/10.1016/j.foodhyd.2011.05.008

Fowler, D. M., Koulov, A. V., Balch, W. E., & Kelly, J. W. (2007). Functional amyloid - from bacteria to humans. *Trends in Biochemical Sciences*, *32*(5), 217–224. https://doi.org/10.1016/j.tibs.2007.03.003

Frare, E., de Laureto, P. P., Zurdo, J., Dobson, C. M., & Fontana, A. (2004). A highly amyloidogenic region of hen lysozyme. *Journal of Molecular Biology*, *340*(5), 1153–1165.

Frare, E., Mossuto, M. F., Polverino de Laureto, P., Dumoulin, M., Dobson, C. M., & Fontana, A. (2006). Identification of the Core Structure of Lysozyme Amyloid Fibrils by Proteolysis. *Journal of Molecular Biology*. https://doi.org/10.1016/j.jmb.2006.06.055

Fruton, J. S. (1970). Specificity and mechanism of pepsin action. In *Structure–Function Relationships of Proteolytic Enzymes* (pp. 222–236). Elsevier.

Fuciños, C., Fuciños, P., Míguez, M., Pastrana, L. M., Rúa, M. L., Vicente, A. A., … Vicente, A. A. (2017). Creating functional nanostructures: Encapsulation of caffeine into α-lactalbumin nanotubes. *Innovative Food Science and Emerging Technologies*, *40*, 10–17. https://doi.org/10.1016/j.ifset.2016.07.030

Gao, Z., Zhao, J., Huang, Y., Yao, X., Zhang, K., Fang, Y., … Yang, H. (2017). Edible Pickering emulsion stabilized by protein fibrils. Part 1: Effects of pH and fibrils concentration. *LWT - Food Science and Technology*, *76*, 1–8. https://doi.org/10.1016/j.lwt.2016.10.038

Gebbink, M. F. B. G., Claessen, D., Bouma, B., Dijkhuizen, L., & Wösten, H. A. B. (2005). Amyloids—a functional coat for microorganisms. *Nature Reviews Microbiology*, *3*(4), 333.

Gharibyan, A. L., Zamotin, V., Yanamandra, K., Moskaleva, O. S., Margulis, B. A., Kostanyan, I. A., & Morozova-Roche, L. A. (2007). Lysozyme Amyloid Oligomers and Fibrils Induce Cellular Death via Different Apoptotic/Necrotic Pathways. *Journal of Molecular Biology*. https://doi.org/10.1016/j.jmb.2006.10.101

Glabe, C. G. (2008). Structural classification of toxic amyloid oligomers. *Journal of Biological Chemistry*, *283*(44), 29639–29643.

Glabe, C. G., & Kayed, R. (2006). Common structure and toxic function of amyloid oligomers implies a common mechanism of pathogenesis. *Neurology*, *66*(1 suppl 1), S78.

Glasse, R. (1967). Cannibalism in the kuru region of New Guinea. *Transactions of the New York Academy of Sciences*, *29*(6 Series II), 748–754.

Gonzalez-Jordan, A., Nicolai, T., & Benyahia, L. (2016). Influence of the protein particle morphology and partitioning on the behavior of particle-stabilized water-in-water emulsions. *Langmuir*, *32*(28), 7189–7197.

Gras, S. L. (2007). Amyloid Fibrils: From Disease to Design. New Biomaterial Applications for Self-Assembling Cross-β Fibrils. *Australian Journal of Chemistry*, *60*(5), 333–342. https://doi.org/10.1071/CH06485

Graveland-Bikker, J. F., & de Kruif, C. G. (2006). Unique milk protein based nanotubes: Food and nanotechnology meet. *Trends in Food Science & Technology*, *17*(5), 196–203. https://doi.org/10.1016/j.tifs.2005.12.009

Greger, M. (2008). Amyloid fibrils: potential food safety implications. *International Journal of Food Safety, Nutrition and Public Health*, *1*(2), 103–115.

Grigolato, F., Colombo, C., Ferrari, R., Rezabkova, L., & Arosio, P. (2017). Mechanistic Origin of the Combined Effect of Surfaces and Mechanical Agitation on Amyloid Formation. *ACS Nano*, *11*(11), 11358–11367.

Groenning, M. (2010). Binding mode of Thioflavin T and other molecular probes in the context of amyloid fibrils—current status. *Journal of Chemical Biology*, *3*(1), 1–18. https://doi.org/10.1007/s12154-009-0027-5

Groenning, M., Olsen, L., van de Weert, M., Flink, J. M., Frokjaer, S., & Jørgensen, F. S. (2007). Study on the binding of Thioflavin T to β-sheet-rich and non-β-sheet cavities. *Journal of Structural Biology*, *158*(3), 358–369.

https://doi.org/10.1016/j.jsb.2006.12.010

Haass, C., & Selkoe, D. J. (2007). Soluble protein oligomers in neurodegeneration: lessons from the Alzheimer's amyloid β-peptide. *Nature Reviews Molecular Cell Biology*, *8*(2), 101.

Haezebrouck, P., Joniau, M., Van Dael, H., Hooke, S. D., Woodruff, N. D., & Dobson, C. M. (1995). An equilibrium partially folded state of human lysozyme at low pH.<br>. *An Equilibrium Partially Folded State of Human Lysozyme at Low PH*.

Harrison, R. S., Sharpe, P. C., Singh, Y., & Fairlie, D. P. (2007). Amyloid peptides and proteins in review. In *Reviews of physiology, biochemistry and pharmacology* (pp. 1–77). Springer.

Hartman, K., Brender, J. R., Monde, K., Ono, A., Evans, M. L., Popovych, N., … Ramamoorthy, A. (2013). Bacterial curli protein promotes the conversion of PAP248-286 into the amyloid SEVI: cross-seeding of dissimilar amyloid sequences. *PeerJ*, *1*, e5.

Iconomidou, V. A., Vriend, G., & Hamodrakas, S. J. (2000). Amyloids protect the silkmoth oocyte and embryo. *FEBS Letters*, *479*(3), 141–145.

Invernizzi, G., Papaleo, E., Sabate, R., & Ventura, S. (2012). Protein aggregation: mechanisms and functional consequences. *The International Journal of Biochemistry & Cell Biology*, *44*(9), 1541–1554.

Jahn, T. R., & Radford, S. E. (2005). The Yin and Yang of protein folding. *The FEBS Journal*, *272*(23), 5962–5970.

Jeong, J. S., Ansaloni, A., Mezzenga, R., Lashuel, H. A., & Dietler, G. (2013). Novel

Mechanistic Insight into the Molecular Basis of Amyloid Polymorphism and Secondary Nucleation during Amyloid Formation. *Journal of Molecular Biology*, *425*(10), 1765–1781. https://doi.org/10.1016/j.jmb.2013.02.005

Kashchiev, D. (2015). Protein Polymerization into Fibrils from the Viewpoint of Nucleation Theory. *Biophysical Journal*, *109*(10), 2126–2136. https://doi.org/10.1016/j.bpj.2015.10.010

Kaur, M., Healy, J., Vasudevamurthy, M., Lassé, M., Puskar, L., Tobin, M. J., … Sasso, L. (2014). Stability and cytotoxicity of crystallin amyloid nanofibrils. *Nanoscale*, *6*(21), 13169–13178.

Kavanagh, G. M., Clark, A. H., Gosal, W. S., & Ross-Murphy, S. B. (2000). Heat-induced gelation of β-lactoglobulin/α-lactalbumin blends at pH 3 and pH 7. *Macromolecules*, *33*(19), 7029–7037.

Kayed, R., Head, E., Thompson, J. L., McIntire, T. M., Milton, S. C., Cotman, C. W., & Glabe, C. G. (2003). Common structure of soluble amyloid oligomers implies common mechanism of pathogenesis. *Science*, *300*(5618), 486–489.

Kelly, J. W. (1998). The alternative conformations of amyloidogenic proteins and their multi-step assembly pathways. *Current Opinion in Structural Biology*, *8*(1), 101–106.

Kenney, J. M., Knight, D., Wise, M. J., & Vollrath, F. (2002). Amyloidogenic nature of spider silk. *European Journal of Biochemistry*, *269*(16), 4159–4163.

Knowles, T. P. J., & Mezzenga, R. (2016). Amyloid fibrils as building blocks for natural and artificial functional materials. *Advanced Materials*, *28*(31), 6546–6561.

Knowles, T. P. J., Oppenheim, T. W., Buell, A. K., Chirgadze, D. Y., & Welland, M. E. (2010). Nanostructured films from hierarchical self-assembly of amyloidogenic proteins. *Nature Nanotechnology*, *5*(3), 204.

Krebs, M. R. H. H., Morozova-Roche, L. A., Daniel, K., Robinson, C. V., Dobson, C. M., Morozova-Roche, L. A., … Dobson, C. M. (2004). Observation of sequence specificity in the seeding of protein amyloid fibrils. *Protein Science*, *13*(7), 1933–1938. https://doi.org/10.1110/ps.04707004

Kuehner, D. E., Engmann, J., Fergg, F., Wernick, M., Blanch, H. W., & Prausnitz, J. M. (1999). Lysozyme net charge and ion binding in concentrated aqueous electrolyte solutions. *The Journal of Physical Chemistry B*, *103*(8), 1368–1374.

Kumar, E. K., Haque, N., & Prabhu, N. P. (2017). Kinetics of protein fibril formation: Methods and mechanisms. *International Journal of Biological Macromolecules*, *100*, 3–10. https://doi.org/10.1016/j.ijbiomac.2016.06.052

Kumar, S., & Udgaonkar, J. B. (2010). Mechanisms of amyloid fibril formation by proteins. *Current Science*, *98*(5), 639–656. https://doi.org/10.1134/S0006297914130057

Kumita, J. R., Johnson, R. J. K., Alcocer, M. J. C., Dumoulin, M., Holmqvist, F., McCammon, M. G., … Dobson, C. M. (2006). Impact of the native-state stability of human lysozyme variants on protein secretion by Pichia pastoris. *The FEBS Journal*, *273*(4), 711–720.

Lara, C., Adamcik, J., Jordens, S., & Mezzenga, R. (2011). General self-assembly mechanism converting hydrolyzed globular proteins into giant multistranded

amyloid ribbons. *Biomacromolecules*, *12*(5), 1868. https://doi.org/10.1021/bm200216u

Lara, C., Gourdin-Bertin, S., Adamcik, J., Bolisetty, S., & Mezzenga, R. (2012). Self-Assembly of Ovalbumin into Amyloid and Non-Amyloid Fibrils. *Biomacromolecules*, *13*(12), 4213–4221. https://doi.org/10.1021/bm301481v

Lassé, M., Ulluwishewa, D., Healy, J., Thompson, D., Miller, A., Roy, N., … Gerrard, J. A. (2016). Evaluation of protease resistance and toxicity of amyloid-like food fibrils from whey, soy, kidney bean, and egg white. *Food Chemistry*, *192*, 491–498. https://doi.org/10.1016/j.foodchem.2015.07.044

Legname, G., Baskakov, I. V, Nguyen, H.-O. B., Riesner, D., Cohen, F. E., DeArmond, S. J., & Prusiner, S. B. (2004). Synthetic mammalian prions. *Science*, *305*(5684), 673–676.

Li, C., Adamcik, J., & Mezzenga, R. (2012). Biodegradable nanocomposites of amyloid fibrils and graphene with shape-memory and enzyme-sensing properties. *Nature Nanotechnology*, *7*(7), 421.

Li, X., Wang, L., Fan, Y., Feng, Q., Cui, F., & Watari, F. (2013). Nanostructured scaffolds for bone tissue engineering. *Journal of Biomedical Materials Research Part A*, *101*(8), 2424–2435.

Lian, H.-Y., Jiang, Y., Zhang, H., Jones, G. W., & Perrett, S. (2006). The yeast prion protein Ure2: structure, function and folding. *Biochimica et Biophysica Acta (BBA)-Proteins and Proteomics*, *1764*(3), 535–545.

Litvinovich, S. V, Brew, S. A., Aota, S., Akiyama, S. K., Haudenschild, C., & Ingham,

K. C. (1998). Formation of amyloid-like fibrils by self-association of a partially unfolded fibronectin type III module1. *Journal of Molecular Biology*, *280*(2), 245–258.

Loveday, S. M., Su, J., Rao, M. A., Anema, S. G., & Singh, H. (2012). Whey protein nanofibrils: Kinetic, rheological and morphological effects of group IA and IIA cations. *International Dairy Journal*, *26*(2), 133–140. https://doi.org/10.1016/j.idairyj.2012.03.001

Loveday, S. M., Su, J., Rao, M. A., Anema, S. G., & Singh, H. (2012). Whey Protein Nanofibrils: The Environment–Morphology–Functionality Relationship in Lyophilization, Rehydration, and Seeding. *Journal of Agricultural and Food Chemistry*, *60*(20), 5229–5236. https://doi.org/10.1021/jf300367k

Loveday, S. M., Wang, X. L., Rao, M. A., Anema, S. G., & Singh, H. (2011). Effect of pH, NaCl, CaCl2and Temperature on Self-Assembly of β-Lactoglobulin into Nanofibrils: A Central Composite Design Study. *Journal of Agricultural and Food Chemistry*, *59*(15), 8467–8474. https://doi.org/10.1021/jf201870z

Lundmark, K., Westermark, G. T., Nyström, S., Murphy, C. L., Solomon, A., & Westermark, P. (2002). Transmissibility of systemic amyloidosis by a prion-like mechanism. *Proceedings of the National Academy of Sciences*, *99*(10), 6979–6984.

Majumdar, A., Cesario, W. C. C., White-Grindley, E., Jiang, H., Ren, F., Khan, M. "Repon" R., … Si, K. (2012). Critical Role of Amyloid-like Oligomers of Drosophila Orb2 in the Persistence of Memory. *Cell*, *148*(3), 515–529. https://doi.org/10.1016/j.cell.2012.01.004

Makin, O. S., & Serpell, L. C. (2005). Structures for amyloid fibrils. *FEBS Journal*, *272*(23), 5950–5961. https://doi.org/10.1111/j.1742-4658.2005.05025.x

Mališauskas, M., Zamotin, V., Jass, J., Noppe, W., Dobson, C. M., & Morozova-Roche, L. A. (2003). Amyloid protofilaments from the calcium-binding protein equine lysozyme: formation of ring and linear structures depends on pH and metal ion concentration. *Journal of Molecular Biology*, *330*(4), 879–890.

Marcon, G., Plakoutsi, G., & Chiti, F. (2006). Protein Aggregation Starting From The Native Globular State1. *Methods in Enzymology*, *413*, 75–91.

Mason, P. E., Brady, J. W., Neilson, G. W., & Dempsey, C. E. (2007). The interaction of guanidinium ions with a model peptide. *Biophysical Journal*, *93*(1), L06.

McGlinchey, R. P., & Lee, J. C. (2018). Why Study Functional Amyloids? Lessons from the Repeat Domain of Pmel17. *Journal of Molecular Biology*.

Melrose, J., Ghosh, P., & Taylor, T. K. F. (1989). Lysozyme, a major low-molecular-weight cationic protein of the intervertebral disc, which increases with ageing and degeneration. *Gerontology*, *35*(4), 173–180.

Ménsua, C., Carrasco, L., Bautista, M. J., Biescas, E., Fernandez, A., Murphy, C. L., … Lujan, L. (2003). Pathology of AA amyloidosis in domestic sheep and goats. *Veterinary Pathology*, *40*(1), 71–80.

Mishra, R., Sörgjerd, K., Nyström, S., Nordigården, A., Yu, Y.-C. C., & Hammarström, P. (2007). Lysozyme Amyloidogenesis Is Accelerated by Specific Nicking and Fragmentation but Decelerated by Intact Protein Binding and Conversion. *Journal of Molecular Biology*, *366*(3), 1029–1044. https://doi.org/10.1016/j.jmb.2006.11.084

Moayedzadeh, S., Madadlou, A., & Khosrowshahi asl, A. (2015). Formation mechanisms, handling and digestibility of food protein nanofibrils. *Trends in Food Science & Technology*, *45*(1), 50–59. https://doi.org/10.1016/j.tifs.2015.05.005

Mocanu, M.-M. M., Ganea, C., Siposova, K., Filippi, A., Demjen, E., Marek, J., … Gazova, Z. (2014). Polymorphism of hen egg white lysozyme amyloid fibrils influences the cytotoxicity in LLC-PK1 epithelial kidney cells. *International Journal of Biological Macromolecules*, *65*, 176–187. https://doi.org/10.1016/j.ijbiomac.2014.01.030

Mohammadian, M., & Madadlou, A. (2018). Technological functionality and biological properties of food protein nanofibrils formed by heating at acidic condition. *Trends in Food Science and Technology*, *75*(July 2017), 115–128. https://doi.org/10.1016/j.tifs.2018.03.013

Morales, R., Moreno-Gonzalez, I., & Soto, C. (2013). Cross-seeding of misfolded proteins: implications for etiology and pathogenesis of protein misfolding diseases. *PLoS Pathogens*, *9*(9), e1003537. https://doi.org/10.1371/journal.ppat.1003537

Morozova-Roche, L. A., Zurdo, J., Spencer, A., Noppe, W., Receveur, V., Archer, D. B., … Dobson, C. M. (2000). Amyloid Fibril Formation and Seeding by Wild-Type Human Lysozyme and Its Disease-Related Mutational Variants. *Journal of Structural Biology*, *130*(2–3), 339–351. https://doi.org/10.1006/jsbi.2000.4264

Mossuto, M. F., Dhulesia, A., Devlin, G., Frare, E., Kumita, J. R., de Laureto, P. P., … Salvatella, X. (2010). The Non-Core Regions of Human Lysozyme Amyloid Fibrils Influence Cytotoxicity. *Journal of Molecular Biology*, *402*(5), 783–796.

https://doi.org/10.1016/j.jmb.2010.07.005

Mostaert, A. S., Crockett, R., Kearn, G., Cherny, I., Gazit, E., Serpell, L. C., … Jarvis, S. P. (2009). Mechanically functional amyloid fibrils in the adhesive of a marine invertebrate as revealed by Raman spectroscopy and atomic force microscopy. *Archives of Histology and Cytology*, *72*(4/5), 199–207. https://doi.org/10.1679/aohc.72.199

Munialo, C. D., Martin, A. H., van der Linden, E., & de Jongh, H. H. J. J. (2014). Fibril Formation from Pea Protein and Subsequent Gel Formation. *Journal of Agricultural and Food Chemistry*, *62*(11), 2418–2427. https://doi.org/10.1021/jf4055215

Nelson, R., & Eisenberg, D. (2006). Recent atomic models of amyloid fibril structure. *Current Opinion in Structural Biology*, *16*(2), 260–265. https://doi.org/10.1016/j.sbi.2006.03.007

Nelson, R., Sawaya, M. R., Balbirnie, M., Madsen, A. Ø., Grothe, R., & Eisenberg, D. (2006). Structure of the cross-β spine of amyloid-like fibrils, *435*(7043), 773–778.

Ng, W. S., Lee, C. S., Chuah, C. H., & Cheng, S.-F. (2017). Preparation and modification of water-blown porous biodegradable polyurethane foams with palm oil-based polyester polyol. *Industrial Crops and Products*, *97*, 65–78.

Nicolai, T., Britten, M., & Schmitt, C. (2011). β-Lactoglobulin and WPI aggregates: formation, structure and applications. *Food Hydrocolloids*, *25*(8), 1945–1962.

Nielsen, S. B., Macchi, F., Raccosta, S., Langkilde, A. E., Giehm, L., Kyrsting, A., … Nielsen, N. C. (2013). Wildtype and A30P mutant alpha-synuclein form different fibril structures. *PloS One*, *8*(7), e67713.

Nilsson, M. R., & Dobson, C. M. (2003). In vitro characterization of lactoferrin aggregation and amyloid formation. *Biochemistry*, *42*(2), 375. Retrieved from https://www.ncbi.nlm.nih.gov/pubmed/12525164

Nyström, G., Fernández-Ronco, M. P., Bolisetty, S., Mazzotti, M., & Mezzenga, R. (2016). Amyloid templated gold aerogels. *Advanced Materials*, *28*(3), 472–478.

Oboroceanu, D. (2011). Characterization of β-lactoglobulin fibrillar assemblies.

Oboroceanu, D., Wang, L., Magner, E., & Auty, M. A. E. E. (2014). Fibrillization of whey proteins improves foaming capacity and foam stability at low protein concentrations. *Journal of Food Engineering*, *121*(1), 102–111. https://doi.org///doi.org/10.1016/j.jfoodeng.2013.08.023

Ohkuma, S., & Poole, B. (1978). Fluorescence probe measurement of the intralysosomal pH in living cells and the perturbation of pH by various agents. *Proceedings of the National Academy of Sciences*, *75*(7), 3327–3331.

Otte, J., Ipsen, R., Bauer, R., Bjerrum, M. J., & Waninge, R. (2005). Formation of amyloid-like fibrils upon limited proteolysis of bovine α-lactalbumin. *International Dairy Journal*, *15*(3), 219–229. https://doi.org/10.1016/j.idairyj.2004.07.004

Ow, S.-Y., & Dunstan, D. E. (2013). The effect of concentration, temperature and stirring on hen egg white lysozyme amyloid formation. *Soft Matter*, *9*(40), 9692–9701.

Pearce, F. G., Mackintosh, S. H., & Gerrard, J. A. (2007). Formation of amyloid-like fibrils by ovalbumin and related proteins under conditions relevant to food processing. *Journal of Agricultural and Food Chemistry*, *55*(2), 318–322. https://doi.org/10.1021/jf062154p

Pellarin, R., Schuetz, P., Guarnera, E., & Caflisch, A. (2010). Amyloid fibril polymorphism is under kinetic control. *Journal of the American Chemical Society*, *132*(42), 14960–14970.

Pepys, M. B., Hawkins, P. N., Booth, D. R., Vigushin, D. M., Tennent, G. A., Soutar, A. K., … Terry, C. J. (1993). Human lysozyme gene mutations cause hereditary systemic amyloidosis. *Nature*, *362*(6420), 553.

Pilkington, S. M., Roberts, S. J., Meade, S. J., & Gerrard, J. A. (2010). Amyloid fibrils as a nanoscaffold for enzyme immobilization. *Biotechnology Progress*, *26*(1), 93–100. https://doi.org/10.1002/btpr.309

Podrabsky, J. E., Carpenter, J. F., & Hand, S. C. (2001). Survival of water stress in annual fish embryos: dehydration avoidance and egg envelope amyloid fibers. *American Journal of Physiology-Regulatory, Integrative and Comparative Physiology*, *280*(1), R131.

Polverino de Laureto, P., Frare, E., Gottardo, R., van Dael, H., & Fontana, A. (2002). Partly folded states of members of the lysozyme/lactalbumin superfamily: a comparative study by circular dichroism spectroscopy and limited proteolysis. *Protein Science*, *11*(12), 2932–2946.

Rambaran, R. N., & Serpell, L. C. (2008). Amyloid fibrils: abnormal protein assembly. *Prion*, *2*(3), 112–117.

Raynes, J. K., Carver, J. A., Gras, S. L., & Gerrard, J. A. (2014). Protein nanostructures in food - Should we be worried? *Trends in Food Science and Technology*, *37*(1), 42–50. https://doi.org/10.1016/j.tifs.2014.02.003

Riek, R., & Eisenberg, D. S. (2016). The activities of amyloids from a structural perspective. *Nature*, *539*(7628), 227.

Romero, D., Vlamakis, H., Losick, R., & Kolter, R. (2014). Functional analysis of the accessory protein TapA in Bacillus subtilis amyloid fiber assembly. *Journal of Bacteriology*, 13.

Rouse, S. L., Hawthorne, W. J., Berry, J.-L., Chorev, D. S., Ionescu, S. A., Lambert, S., … Morgan, R. M. L. (2017). A new class of hybrid secretion system is employed in Pseudomonas amyloid biogenesis. *Nature Communications*, *8*(1), 263.

Sander, C., & Schneider, R. (1991). Database of homology-derived protein structures and the structural meaning of sequence alignment. *Proteins: Structure, Function, and Bioinformatics*, *9*(1), 56–68.

Sattianayagam, P. T., Gibbs, S. D. J., Rowczenio, D., Pinney, J. H., Wechalekar, A. D., Gilbertson, J. A., … Gillmore, J. D. (2012). Hereditary lysozyme amyloidosis–phenotypic heterogeneity and the role of solid organ transplantation. *Journal of Internal Medicine*, *272*(1), 36–44.

Sawaya, M. R., Sambashivan, S., Nelson, R., Ivanova, M. I., Sievers, S. A., Apostol, M. I., … Eisenberg, D. (2007). Atomic structures of amyloid cross-β spines reveal varied steric zippers. *Nature*, *447*(7143), 453–457. https://doi.org/10.1038/nature05695

Schleeger, M., Vandenakker, C. C., Deckert-Gaudig, T., Deckert, V., Velikov, K. P., Koenderink, G., & Bonn, M. (2013). Amyloids: From molecular structure to mechanical properties. *Polymer*, *54*(10), 2473–2488.

https://doi.org/10.1016/j.polymer.2013.02.029

Schmit, J. D., Ghosh, K., & Dill, K. (2011). What drives amyloid molecules to assemble into oligomers and fibrils? *Biophysical Journal*, *100*(2), 450–458. https://doi.org/10.1016/j.bpj.2010.11.041

Schmuck, B., Sandgren, M., & Härd, T. (2017). A fine-tuned composition of protein nanofibrils yields an upgraded functionality of displayed antibody binding domains. *Biotechnology Journal*, *12*(6), n/a. https://doi.org/10.1002/biot.201600672

Sebastiao, M., Quittot, N., & Bourgault, S. (2017). Thioflavin T fluorescence to analyse amyloid formation kinetics: Measurement frequency as a factor explaining irreproducibility. *Analytical Biochemistry*, *532*, 83–86. https://doi.org/10.1016/j.ab.2017.06.007

Serfert, Y., Lamprecht, C., Tan, C.-P. P., Keppler, J. K., Appel, E., Rossier-Miranda, F. J., … Schwarz, K. (2014). Characterisation and use of β-lactoglobulin fibrils for microencapsulation of lipophilic ingredients and oxidative stability thereof. *Journal of Food Engineering*, *143*, 53–61. https://doi.org///doi.org/10.1016/j.jfoodeng.2014.06.026

Shamsi, T. N., Athar, T., Parveen, R., & Fatima, S. (2017). A review on protein misfolding aggregation and strategies to prevent. *International Journal of Biological Macromolecules*, *105*, 993–1000. https://doi.org/10.1016/j.ijbiomac.2017.07.116

Shen, Y., Posavec, L., Bolisetty, S., Hilty, F. M., Nyström, G., Kohlbrecher, J., … Mezzenga, R. (2017). Amyloid fibril systems reduce, stabilize and deliver bioavailable nanosized iron. *Nature Nanotechnology*, *12*(7), 642–647.

https://doi.org/10.1038/nnano.2017.58

Shewmaker, F., McGlinchey, R. P., & Wickner, R. B. (2011). Structural insights into functional and pathological amyloid. *Journal of Biological Chemistry*, jbc. R111. 227108.

Siddiqi, M. K., Alam, P., Chaturvedi, S. K., Shahein, Y. E., & Khan, R. H. (2017). Mechanisms of protein aggregation and inhibition. *Front Biosci (Elite Ed)*, *9*, 1–20. https://doi.org/10.2741/781

Sivalingam, V., Prasanna, N. L., Sharma, N., Prasad, A., & Patel, B. K. (2016). Wild-type hen egg white lysozyme aggregation in vitro can form self-seeding amyloid conformational variants. *Biophysical Chemistry*, *219*, 28–37. https://doi.org/10.1016/j.bpc.2016.09.009

Sneideris, T., Darguzis, D., Botyriute, A., Grigaliunas, M., Winter, R., & Smirnovas, V. (2015). pH-Driven Polymorphism of Insulin Amyloid-Like Fibrils. *PLoS One*, *10*(8), e0136602. https://doi.org/10.1371/journal.pone.0136602

Šneideris, T., Kulicka, E., & Smirnovas, V. (2018). Polymorphism of Prion Protein Amyloid-Like Fibrils. *Biophysical Journal*, *114*(3), 429a.

Sneideris, T., Milto, K., & Smirnovas, V. (2015). Polymorphism of amyloid-like fibrils can be defined by the concentration of seeds. *PeerJ*, *3*, e1207. https://doi.org/10.7717/peerj.1207

Solomon, A., Richey, T., Murphy, C. L., Weiss, D. T., Wall, J. S., Westermark, G. T., & Westermark, P. (2007). Amyloidogenic potential of foie gras. *Proceedings of the National Academy of Sciences of the United States of America*, *104*(26), 10998–

11001. https://doi.org/10.1073/pnas.0700848104

Steadman, L. B., & Merbs, C. F. (1982). Kuru and cannibalism? *American Anthropologist*, *84*(3), 611–627.

Stefani, M. (2010). Biochemical and biophysical features of both oligomer/fibril and cell membrane in amyloid cytotoxicity. *The FEBS Journal*, *277*(22), 4602–4613.

Stefani, M., & Dobson, C. M. (2003). Protein aggregation and aggregate toxicity: new insights into protein folding, misfolding diseases and biological evolution. *Journal of Molecular Medicine*, *81*(11), 678–699. https://doi.org/10.1007/s00109-003-0464-5

Stępkowski, D., & Bieniaś, J. (2012). Nature of cross-seeding barriers of amyloidogenesis. *Acta Biochimica Polonica*, *59*(2), 307. Retrieved from https://www.ncbi.nlm.nih.gov/pubmed/22577625

Stroud, J. C., Liu, C., Teng, P. K., & Eisenberg, D. (2012). Toxic fibrillar oligomers of amyloid-β have cross-β structure. *Proceedings of the National Academy of Sciences*, *109*(20), 7717–7722.

Sugimoto, Y., Kamada, Y., Tokunaga, Y., Shinohara, H., Matsumoto, M., Kusakabe, T., … Ueda, T. (2011). Aggregates with lysozyme and ovalbumin show features of amyloid-like fibrils. *Biochemistry and Cell Biology*, *89*(6), 533–544.

Sulatskaya, A. I., Kuznetsova, I. M., & Turoverov, K. K. (2011). Interaction of thioflavin T with amyloid fibrils: stoichiometry and affinity of dye binding, absorption spectra of bound dye. *The Journal of Physical Chemistry B*, *115*(39), 11519–11524.

Sulatskaya, A. I., Rodina, N. P., Povarova, O. I., Kuznetsova, I. M., & Turoverov, K. K.

(2017). Different conditions of fibrillogenesis cause polymorphism of lysozyme amyloid fibrils. *Journal of Molecular Structure*, *1140*, 52–58. https://doi.org/10.1016/j.molstruc.2016.10.037

Sunde, M., Serpell, L. C., Bartlam, M., Fraser, P. E., Pepys, M. B., & Blake, C. C. F. (1997). Common core structure of amyloid fibrils by synchrotron X-ray diffraction1. *Journal of Molecular Biology*, *273*(3), 729–739.

Swaminathan, R., Ravi, V. K., Kumar, S., Kumar, M. V. S., & Chandra, N. (2011). Lysozyme: A model protein for amyloid research. *Advances in Protein Chemistry and Structural Biology*, *84*, 63–111. https://doi.org/10.1016/B978-0-12-386483-3.00003-3

Taglialegna, A., Lasa, I., & Valle, J. (2016). Amyloid structures as biofilm matrix scaffolds. *Journal of Bacteriology*, *198*(19), 2579–2588. https://doi.org/10.1128/JB.00122-16

Thirumalai, D., Reddy, G., & Straub, J. E. (2011). Role of water in protein aggregation and amyloid polymorphism. *Accounts of Chemical Research*, *45*(1), 83–92.

Thorn, D. C., Meehan, S., Sunde, M., Rekas, A., Gras, S. L., MacPhee, C. E., … Carver, J. A. (2005). Amyloid Fibril Formation by Bovine Milk κ-Casein and Its Inhibition by the Molecular Chaperones αS- and β-Casein. *Biochemistry*, *44*(51), 17027–17036. https://doi.org/10.1021/bi051352r

Tipping, K. W., Karamanos, T. K., Jakhria, T., Iadanza, M. G., Goodchild, S. C., Tuma, R., … Radford, S. E. (2015). pH-induced molecular shedding drives the formation of amyloid fibril-derived oligomers. *Proceedings of the National Academy of*

*Sciences*, *112*(18), 5691–5696. https://doi.org/10.1073/pnas.1423174112

Tjernberg, L. O., Rising, A., Johansson, J., Jaudzems, K., & Westermark, P. (2016). Transmissible amyloid. *Journal of Internal Medicine*, *280*(2), 153–163.

Toyama, B. H., & Weissman, J. S. (2011). Amyloid Structure: Conformational Diversity and Consequences. *Annual Review of Biochemistry*, *80*(1), 557–585. https://doi.org/10.1146/annurev-biochem-090908-120656

Ulleberg, E. K., Comi, I., Holm, H., Herud, E. B., Jacobsen, M., & Vegarud, G. E. (2011). Human gastrointestinal juices intended for use in in vitro digestion models. *Food Digestion*, *2*(1–3), 52–61.

Usov, I., Adamcik, J., & Mezzenga, R. (2013). Polymorphism complexity and handedness inversion in serum albumin amyloid fibrils. *ACS Nano*, *7*(12), 10465–10474. https://doi.org/10.1021/nn404886k

van den Akker, C. C., Schleeger, M., Bonn, M., & Koenderink, G. H. (2014). Structural Basis for the Polymorphism of β-Lactoglobulin Amyloid-Like Fibrils. In *Bio-nanoimaging* (pp. 333–343). Elsevier.

Van Gerven, N., Van der Verren, S. E., Reiter, D. M., & Remaut, H. (2018). The role of functional amyloids in bacterial virulence. *Journal of Molecular Biology*.

Veerman, C., de Schiffart, G., Sagis, L. M. C., & van der Linden, E. (2003). Irreversible self-assembly of ovalbumin into fibrils and the resulting network rheology. *International Journal of Biological Macromolecules*, *33*(1–3), 121–127.

Veerman, C., Sagis, L. M. C. C., & Van der Linden, E. (2003). Gels at extremely low weight fractions formed by irreversible self-assembly of proteins. *Macromolecular*

*Bioscience*, *3*(5), 243–247. https://doi.org/10.1002/mabi.200390035

Vernaglia, B. A., Huang, J., & Clark, E. D. (2004). Guanidine hydrochloride can induce amyloid fibril formation from hen egg-white lysozyme. *Biomacromolecules*, *5*(4), 1362–1370. https://doi.org/10.1021/bm0498979

Vetri, V., D'Amico, M., Foderà, V., Leone, M., Ponzoni, A., Sberveglieri, G., … Militello, V. (2011). Bovine Serum Albumin protofibril-like aggregates formation: Solo but not simple mechanism. *Archives of Biochemistry and Biophysics*, *508*(1), 13–24. https://doi.org/10.1016/j.abb.2011.01.024

Viguier, B., Zór, K., Kasotakis, E., Mitraki, A., Clausen, C. H., Svendsen, W. E., & Castillo-León, J. (2011). Development of an electrochemical metal-ion biosensor using self-assembled peptide nanofibrils. *ACS Applied Materials & Interfaces*, *3*(5), 1594–1600.

Wasmer, C., Zimmer, A., Sabaté, R., Soragni, A., Saupe, S. J., Ritter, C., & Meier, B. H. (2010). Structural similarity between the prion domain of HET-s and a homologue can explain amyloid cross-seeding in spite of limited sequence identity. *Journal of Molecular Biology*, *402*(2), 311–325.

Westermark, P., Lundmark, K., & Westermark, G. T. (2009). Fibrils from designed non-amyloid-related synthetic peptides induce AA-amyloidosis during inflammation in an animal model. *PLoS One*, *4*(6), e6041.

Xue, W.-F., Homans, S. W., & Radford, S. E. (2009). Amyloid fibril length distribution quantified by atomic force microscopy single-particle image analysis. *Protein Engineering, Design & Selection*, *22*(8), 489–496.

Zaidi, S., Hassan, M. I., Islam, A., & Ahmad, F. (2014). The role of key residues in structure, function, and stability of cytochrome-c. *Cellular and Molecular Life Sciences*, *71*(2), 229–255. https://doi.org/10.1007/s00018-013-1341-1

Zako, T., Sakono, M., Hashimoto, N., Ihara, M., & Maeda, M. (2009). Bovine insulin filaments induced by reducing disulfide bonds show a different morphology, secondary structure, and cell toxicity from intact insulin amyloid fibrils. *Biophysical Journal*, *96*(8), 3331–3340.

Zeng, G., Vad, B. S., Dueholm, M. S., Christiansen, G., Nilsson, M., Tolker-Nielsen, T., … Otzen, D. E. (2015). Functional bacterial amyloid increases Pseudomonas biofilm hydrophobicity and stiffness. *Frontiers in Microbiology*, *6*(OCT), 1099. https://doi.org/10.3389/fmicb.2015.01099

Zhang, B., Une, Y., Fu, X., Yan, J., Ge, F., Yao, J., … Kametani, F. (2008). Fecal transmission of AA amyloidosis in the cheetah contributes to high incidence of disease. *Proceedings of the National Academy of Sciences*, *105*(20), 7263–7268.

Zhang, J., Huang, M., Guan, S., Bi, H.-C., Pan, Y., Duan, W., … Bian, J.-S. (2006). A mechanistic study of the intestinal absorption of cryptotanshinone, the major active constituent of Salvia miltiorrhiza. *Journal of Pharmacology and Experimental Therapeutics*, *317*(3), 1285–1294.

Zhang, M., Hu, R., Chen, H., Chang, Y., Ma, J., Liang, G., … Zheng, J. (2015). Polymorphic cross-seeding amyloid assemblies of amyloid-β and human islet amyloid polypeptide. *Physical Chemistry Chemical Physics*, *17*(35), 23245–23256.

Zhang, Y.-H. H., & Huang, L.-H. H. (2014). Effect of heat-induced formation of rice

bran protein fibrils on morphological structure and physicochemical properties in solutions and gels. *Food Science and Biotechnology*, *23*(5), 1417–1423. https://doi.org/10.1007/s10068-014-0194-1

Zhou, J., Zhang, H., Yang, H., Wang, L., & Qian, H. (2014). Formation of heat-induced cottonseed congossypin (7S) fibrils at pH 2.0. *Journal of the Science of Food and Agriculture*, *94*(10), 2009–2015.